UNIVERSITY OF PADUA

DEPARTMENT OF CIVIL, ENVIRONMENTAL AND ARCHITECTURAL ENGINEERING

Master Thesis in Environmental Engineering

THERMAL DEGRADATION OF POLYETHYLENE IN A TUBULAR REACTOR FOR THE PRODUCTION OF VALUABLE OILS

Supervisor: Professor Paolo Canu

Student: Serena Frasson

ACADEMIC YEAR 2013-2014

Summary

INTRODUCTION 5

CHAPTER 1 7

1.1. Reactors 8
- **1.1.1. Rotary kilns** 8
- **1.1.2. Fluidized bed** 8
- **1.1.3. Fixed bed** 9
- **1.1.4. Spouted bed** 9

1.2. Products and processes 10

1.3. Inputs 12
- **1.3.1. Single component** 12
- **1.3.2. Mixtures** 12
- **1.3.3. Real waste** 13

1.4. Process parameters 15
- **1.4.1. Temperature** 15
- **1.4.2. Residence time** 17
- **1.4.3. Heating rate** 19

1.5. Economic viability 20

1.6. Feedstock recycling 21

CHAPTER 2 23

2.1. Measurements 25
- 2.1.1. Fusion transition 26
  - 2.1.1.1. Specific heat 28
- 2.1.2. Glass and crystalline transition 28
- 2.1.3. Oxydation reaction 29
- 2.1.4. Volatilization 30
- 2.1.5. Sample weight 31
- 2.1.6. Reproducibility 32

CHAPTER 3 35

3.1. Thermal conductivity 36

3.2. Fluidity 37

3.3. Morphological characterization 40

3.4. Summary **44**

CHAPTER 4 45

4.1. Properties **45**
4.1.1. Dew point 45
4.1.2. Boiling point 47
4.1.3. Calorific value 47
4.1.4. Viscosity 48

4.2. Analysis **49**
4.2.1. The European Protocol 49
4.2.2. Other methods 50

CHAPTER 5 53

5.1. Gas chromatography **53**

5.2. Mass spectrometry **55**

CHAPTER 6 57

6.1. Reactor **57**
6.1.1. Kettle-type reactor 57
6.1.2. Tubular reactor 60

6.2. Condenser **62**

6.3. Thermal profiles **64**
6.3.1. Initial pliers and resistance configuration 64
6.3.2. Second pliers and resistance configuration 68
6.3.3. Inner control thermocouple 69
6.3.4. Sic 70

6.4. Standard method development **72**
6.4.1. Reactor 72
6.4.2. Condenser 73

CHAPTER 7 75

7.1. Inert gas flow rate **75**

7.2. Reproducibility **76**

7.3. Isothermal time **77**

7.4. End temperature **77**

7.5. Heating rate **78**

7.6. Sample amount **79**

7.7. Error estimation **79**

CHAPTER 8 **81**

8.1. Residue analysis **81**

8.2. Gas analysis **82**
8.2.1. Gas identification 82
8.2.2. Gas production 86

8.3. Oil analysis **88**
8.3.1. Differential scanning calorimetry 88
8.3.2. Mass spectrometry 88

CONCLUSIONS **95**

APPENDIX A **97**

REFERENCES **103**

Introduction

In the last few decades, plastic consumption has increased. Annual consumption of plastic in occidental Europe is about 60 million tons, which results in about 23 million tons of plastic waste, distributed in all major Municipal Solid Waste (MSW) categories: containers and packaging plastics (bags, sacks, wraps, soft drink, milk, and water containers), durable goods, appliances, furniture, casings of lead-acid batteries, and other products (Adrados et al., 2011). Considering that the 90% of plastics used today are synthesized exploiting non-renewable fossil resources, re-processing plastics would allow preserving fossil fuels, but also decreasing of carbon-dioxide (CO_2) emissions.

Approximately 63 wt% of the whole Plastic Solid Waste (PSW) comes from packing and packaging (Adrados et al., 2011); the European Directive on packing and packaging (94/62/CE, with subsequent amendments) compelled member states to take into account life-cycle assessments and cost-benefit analysis, to prevent the formation of packaging waste, to set up return, collection and recovery systems, and eventually to recover energy, in order to reduce their impact on the environment. This directive set the objective to recycle between 55 wt% and 85 wt% and to incinerate (with coupled energy recovery) at least 60 wt% of packaging waste; it was duly transposed by all Member States and the level of enforcement was satisfactory overall.

Further improvement of these result are difficult to achieve with the common separation techniques, because it is not technically possible or economically viable to get a complete separation of the whole waste of a Multi-material Recovery Facility (MRF). The most widespread separation method is density sorting; since most plastics are very close in density (ρ_{HDPE} = 0.941, ρ_{MDPE} = 0.926–0.940, ρ_{LDPE} =0.915–0.925, ρ_{LLDPE} = 0.91–0.94, ρ_{PP} = 0.96 g/cc), it is coupled with hydro-cyclones, which use centrifugal force, air classifier, sieves, and electrostatics. In addition there are several physical treatments, such as: shredding, milling, washing, drying, agglutination, extrusion, quenching and paint or contaminants removal through abrasion or solvent stripping.

Pyrolysis may be an alternative for the reclamation of MRFs rejected streams, which amount on 20-30% of their total waste input and consist of many different materials (e.g., polyethylene, polypropylene, polystyrene, polyvinyl chloride, polyethylene terephthalate, aluminium and tetra-brick), reducing the load to landfills or incinerators (Adrados et al., 2001).

The various recycling methods of PSW are classified in three categories, in order of raw material decreasing quality: primary (mechanical), secondary (chemical) and tertiary (energy recovery).

Mechanical recycling is the ideal way to reuse plastic, because is the re-introduction of scrap, industrial single-polymer (PE, PP, PS, etc.) plastic edges to the extrusion cycle in order to gain products of comparable quality. It maintains polymers' molecular structure but it is applicable only to semi-clean scrap, therefore it is preceded by an accurate identification and separation of comingled plastic with manual or automated sorting.

Chemical recycling converts plastic materials into liquids or gases, which are suitable as feedstock for the production of new petrochemicals and plastics (Mastellone et al., 1999) or as fuels. The term chemical underlines the alteration in the chemical structure of the polymer, which is bound to occur during depolymerisation (thermolysis) processes. Its main advantage is the possibility to treat heterogeneous and contaminated polymers with limited use of pre-treatment; so it is becoming a viable solution compared to recycling, which has to deal with treatments and a large amount of discards.

Chemical recycling allows to obtain a clean, high calorific value gas (22–30 MJ/m^3) from a wide variety of waste streams; i.e. condensation polymers such as polyethylene terephthalate (PET) and nylon give back monomer units (feedstock recycling), while vinyl polymers such as polyolefins produce a mixture containing numerous components to be used as a fuel.

There are several technologies in this category, such as hydrogenation, gasification, pyrolysis and cracking. The first means the addition of hydrogen by chemical reaction, employing a depolymerisation and eventually a de-chlorination section, where the agglomerated plastic is kept between 350 and 400°C.

Gasification gives gases with high calorific value using O_2 or air in a sub- stoichiometric ratio; in order to obtain gases with lower heating value (LHV) of 10000 kJ/N the process shall take place at temperatures higher than 500°C; it generates a significant amount of char, which needs to be further processed (Al-Salem et al., 2009).

Pyrolysis and cracking indicate the thermolysis in an inert atmosphere; throughout literature these two terms are used indifferently, but it seems more precise to distinguish them on a temperature basis. Pyrolysis is the process, which gains oils at low temperatures (400-450°C) in absence of oxygen (Adrados et al., 2011); cracking is the degradation at higher temperatures, with the consequent production of mainly gases. Both can be solely thermic or catalytic, if a catalyst is exploited to speed up reaction times.

Energy recovery involves complete or partial oxidation of the material, producing heat, power and/or gaseous fuels, oils and chars besides by-products that must be disposed of, such as ash. Incineration is considered when the previous processes have failed due to economical constrains. Plastic materials possess a very high calorific value and this makes it a convenient energy source, as shown in table 1.

Table 1. Calorific value of plastics compared with common fuels (Mastellone et al., 1999).

Item	Calorific value (MJ kg^{-1})
Polyethylene	43.3–46.5
Polypropylene	46.50
Polystyrene	41.90
Kerosene	46.50
Gas oil	45.20
Heavy oil	42.50
Petroleum	42.3
Household PSW mixture	31.8

Waste combustion generally ensures a volume reduction of 90-99%, but the combustion of synthetic polymers such as PVC, PET, PS and PE is known to generate volatile organic compounds (VOCs), smoke (particulate matter), particulate-bound heavy metals, polycyclic aromatic hydrocarbons (PAHs), polychlorinated dibenzofurans (PCDFs) and overall dioxins (Buekens et al., 1998). Hence the capture and cleaning of flue gases is a great issue that heavily affects the cost-effectiveness of the whole process. It can be dealt alternatively with ammonia addition to the combustion chamber, flue gas cooling, acid neutralization, activated carbon addition and/or filtration (Yassin et al., 2005).

Chapter 1
Pyrolysis of plastic material

Pyrolysis is a thermal degradation process, which takes place in an oxygen free atmosphere.

It can be considered a waste treatment technology, because it has the ability to produce clean high-calorific gases and valuable oils from a wide variety of natural or anthropogenic sources. It is also a way to pursue the chemical recycling of feedstock and plastic waste lends itself to this type of recovery, because of its high market value, the progressive raw material scarcity, not to mention its characteristic polymeric structure, which can be shortened up to the generating monomer.

At the present state of fact, pyrolysis is not yet a fully developed industrial technique, but efforts shall be made to render it a viable solution, because it provides a number of operational, environmental advantages, and financial benefits.

Operational advantages could be described by the handling of heterogeneous and contaminated material with little need for pre-treatments, the utilisation of residual output (char) as a fuel or as a feedstock, and the absence of the flue gas cleaning process. Furthermore it lowers the gaseous volumes from 5 to 20 times with respect to combustion (Al Salem et al., 2009).

Environmentally, pyrolysis reduces at once, the waste volume to be landfilled and the need for raw materials, concentrating pollutants in a stabilized inert matrix and recovering valuable hydrocarbons.

Moreover pyrolysis allows to manage properly hazardous waste (i.e. used tyres), because, on the contrary of combustion, avoids the problem of dioxin formation and the resulting oils are relatively free from chlorinated compounds.

Financially, pyrolysis is becoming viable, because products could be conveniently sold on the markets, due to the continuous raising of the petrol price. The high calorific value fuel could be easily used in gas engines to produce electricity and heat.

The main obstacles, which hinder the development of this process are the placing of the solid residue, where most pollutants concentrate, the high investment costs related to the large amounts of energy needed, because plastic is a poor thermal conductor and the treatment of the final fuel produced if specific target are required (i.e. for oils low volatility and high octane number).

Unfortunately there is not sufficient understanding of the underlying reaction pathways, preventing a quantitative prediction of the full product distribution, which are heavily affected not only by the feeding materials, but also by the process parameters.

Despite this, pyrolysis can result in a very profitable and sustainable industrial scheme, providing a high product yield and a minimal waste.

1.1. Reactors

Different kinds of reactors are used for pyrolysis; they have evolved with the degree of knowledge related to this process. The type of reactor used determines mainly the quality of heat transfer, mixing, gas and liquid phase residence times and the quality of products.

1.1.1. Rotary kilns

The first pyrolysis experiences were drawn with rotary kilns (Kaminsky et al., 1991). They are marked by long residence times (20 minutes) and lead to a various product spectrum, due to the large temperature gradient through the reactor; thus oil and gases generated likewise are only used for combustion and energy production. Considering the scarce performance of these kilns, the research upon them had been abandoned in the first 2000, switching to more convenient configurations, such as fluidized bed.

1.1.2. Fluidized bed

This reactor is characterized by an excellent heat and mass transfer, as well as a relatively constant temperature throughout the reactor. The fluidized bed is generated by a flow of inert gas, at a rate sufficient to maintain the bed fluid; basically the bed shall behave like a liquid. The product spectra is far more uniform than the rotary kilns, but this process, if it is not well controlled, can undergo defluidization. This happens when the melted material sticks to the bed and renders it no more fluid; a solution could be providing more heat, when needed, maintaining constant the feeding rate and favouring the separation of the packed substance.

The Hamburg University researched in this sense, developing a process, for 30 kg/h plastics, called the Hamburg process which it is illustrated in figure 1.1. The plant has its core in a reactor with an inner diameter of 450 mm. It is fluidized by exhaust gases, preheated at 400 °C and heated by radiant-heat tubes. Pyrolysis gas, after leaving the reactor is cleaned of fine dust in a cyclone and passes through two quenching columns, which are filled with glass bodies, to condense oils. Finally the remaining gas is purified in an electrostatic precipitator and reused or flared.

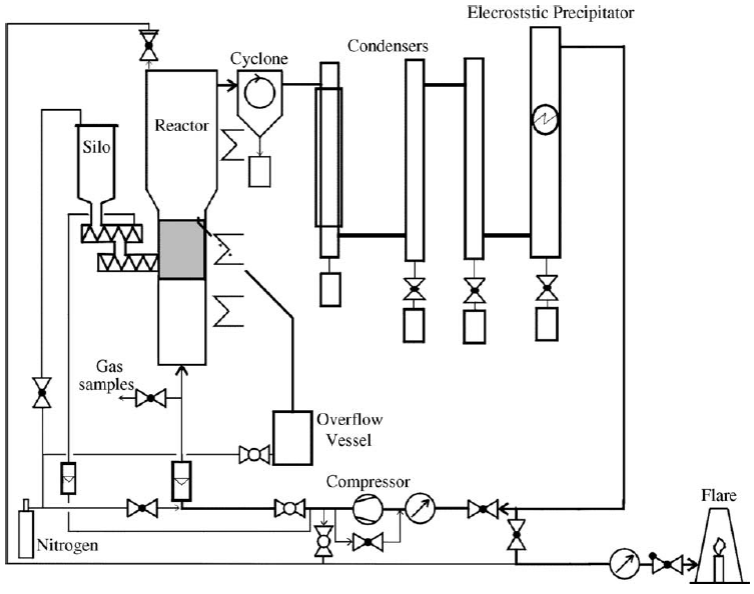

Figure 1.1 Hamburg pyrolysis pilot plant (Kaminsky et al., 2003).

1.1.3. Fixed bed

Fixed bed is the easiest large scale configuration for a reactor, it does not allow a heat distribution as good as the fluidized bed, but McCaffrey developed an interesting arrangement in nitrogen atmosphere, which is showed in figure 1.2. Any products which are volatile at the off-take temperature leave the reactor and enter the condenser. However, higher boiling point products return to the reactor, where they are mixed with the melt and further degraded.

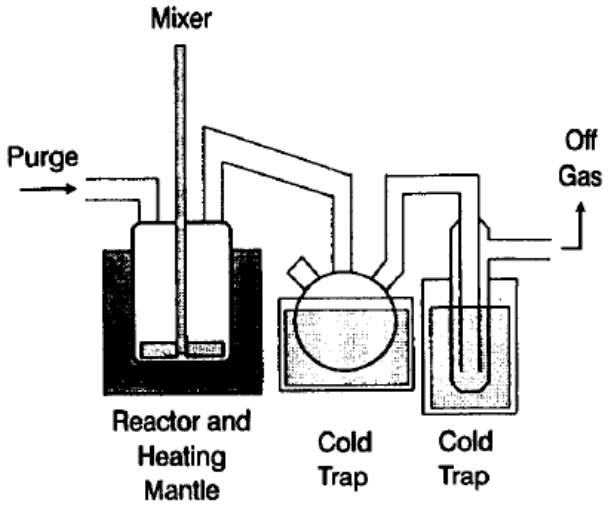

Figure 1.2 Kettle-type reactor (McCaffrey et al., 1994)

1.1.4. Spouted bed

This particular configuration gives to the reactor a conical form in the lower part and it is illustrated in figure 1.3. The Arabiourrutia's hydrodynamic studies proved that so particles with a wide size or density distribution can be handled without segregation or defluidization problems. The vigorous contact between phases and the collision between particles in the spout avoids the agglomeration of solid particles (sand) with melted plastic.

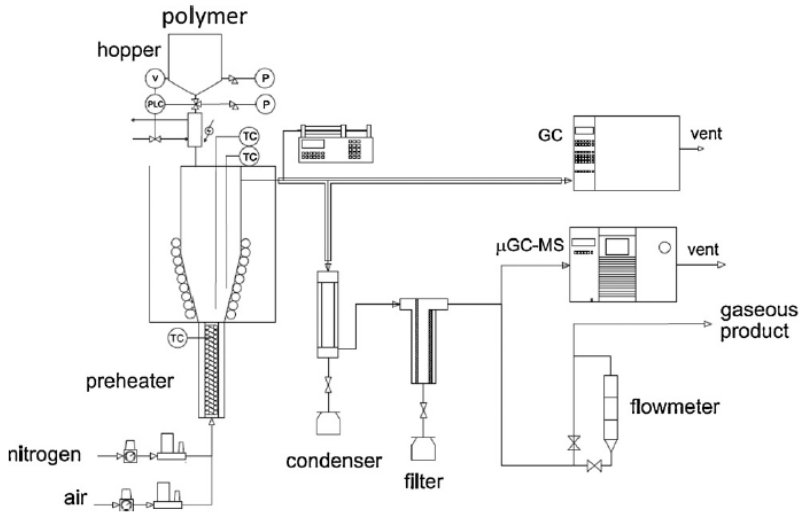

Figure 1.3 Pyrolysis unit with spouted bed reactor (Arabiourrutia et al., 2011)

1.2. Products and processes

Pyrolysis produces three different phases: a gas phase (20-90 wt. %), a liquid phase (tars, 5–50 wt. %) and a solid phase (char 0. 2–10 wt. %).

Gases are characterized by compounds with less than 4 carbon atoms and a boiling point lower than 300°C. They have an important calorific value (50 MJ/m^3), so they can be employed as fluidizing agents in the reactor or provide the energy and heat requirements for the pyrolysis process and consequently off-set the costs of recycling. The process shall optimize their content of ethene, propene, butadiene and other olefins.

Char has a high calorific value and many possible applications as activated carbon, as material for a fluidized bed or as a catalyst. These depend on its degree of purity, because, as said before, the major part of pollutants concentrates in this phase. In fact all kind of fillers like carbon black, metal oxides, silica and metals are found in the residue (Kaminsky et al., 2000).

Liquid products consist of oils, light and heavy waxes, which are distinguished on the bases of boiling points and carbon number, as shown in table1.1. Waxes show an increased viscosity with respect to oils and are made by non-aromatic chains of alkenes and alkanes. This fraction seems the most valuable on the markets, because lend itself to be recycled back into the production process.

Table 1.1 Tars' boiling points and carbon numbers (Predel et al., 2000).

TARS	Boling Point °C	Carbon n°
Oils	BP<300	5<C<20
Light waxes	300<BP<500	18<C<50
Heavy waxes	BP>500	C>37

It is clear that products strongly depend in their quantity and quality on process parameters, configuration and feeding material. Currently four processes had been identified throughout literature:

- **Pyrolysis at low-temperatures** (400-550°C) to produce aliphatic waxes and oils, that may serve as feedstock for a steam cracker;
- **Cracking** in an inert-gas stream (600-800°C) to achieve mainly high heat-content gaseous olefins (ethene, propene, butadiene and other) and aromatic oils, rich in benzene, toluene and xylene (BTX) that can serve to refineries or other petrochemical processing plants;
- **Monomer recovery** at low temperatures (450°C-550°C) from single polymer such as PMMA, PS, PTFE, PET. Carrier can vary from inert gases (He or N_2), pyrolysis gases and steam. This is commercially very convenient, but it does not always behave like an inert gas. In contact with chlorinated compounds it can reduce the Cl content in oils and tar, but it can also lead to carbon oxides.

The Hamburg process, illustrated in paragraph § 1.1.2, which uses an indirectly heated fluidized bed, was varied for different purposes: production of high heating value gases and aromatic oils (benzene, toluene and xylene) or mainly aliphatic oils and extraction of the simple monomer from complex plastic chains. In table 1.2 are investigated various feedstock and their product fractions at different temperatures.

Table 1.2 Products characterization of various polymeric waste and oil-containing raw materials (Kaminsky et al., 2003).

Feedstocks	Pyrolysis temperature (°C)	Gas (wt.%)	Oil (wt.%)	Residue (wt.%)	Other products (wt.%)
Polyethylene PE	760	55.8	42.4	1.8 C	
Polyethylene PE	530	7.6	50.3	0.1	42 waxes
Polypropylene PP	740	49.6	48.8	1.6 C	
Polystyrene PS	580	9.9	24.6	0.6	64.9 styrene
Mixtures of PE/PP/PS	750	52.0	46.6	1.4	
Polyester	768	50.8	40.0	7.1	2.1 H_2O
Polyurethane	760	37.9	56.3	0.5	5.0 H_2O 0.3 HCN
ABS copolymer	740	6.9	90.8	1.1	1.2 HCN
Polyamide PA	760	39.2	56.8	0.6	3.4 HCN
Polycarbonate	710	26.5	46.4	24.6	2.5 H_2O
Phenolformaldehyde resins	780	14.4	28.1	49.5	8.0 H_2O
Poly(methyl methacrylate) PMMA	450	1.25	1.4	0.15 C	97.2 MMA
Poly(vinyl chloride) PVC	740	6.8	28.1	8.8	56.3 HCl
Polytetrafluoroethylene PTFE	555	18.8	5.2	0.3	76 TFE
Disposable syringes	720	56.3	36.4	5.8	1.5 steel
Plastic from sorted domestic waste	787	43.6	26.4	25.4	4.6 H_2O
Shredder waste (heavy)	733	29.9	26.7	27.6	14.0 metals 1.8 H_2O
Shredder waste (light)	700	26.8	21.4	51.8	
EPDM elastomer	700	32.3	19.2	47.5	1.0 H_2O
SB rubber	740	25.1	31.9	42.8	0.2 H_2S
Tyre parts	750	35.3	22.4	40.6	1.6 steel 0.1 H_2O
Whole scrap tyres	700	22.4	22.0	39.0	11.5 steel 5.1 H_2O

Experiments show that pyrolysis and cracking proceed smoothly for polyolefins, polystyrene, rubber, styrene thermo-polymers (ABS), polyesters, and mixtures thereof. It is also possible to gain waxes from polyethylene, to recover back the monomers styrene and mono-methyl methacrylate (MMA) in liquid from and the tetrafluoroethylene (TFE) in gaseous form. Furthermore polyolefins, polyesters and rubber give similar amount of gas and oils while polystyrene, PMMA, PVC yield more oils than gas (Kaminsky 2000). PCV and real waste can create problems, due to the high chloride content and the undesirable sub-products (steel and metals), respectively.

The great part of the literature deals with single stage processes, which are easy to manage and simple to build up. However, in more recent times, two different reactors have been developed in order to separate the initial melting phase from the real conversion phase (Della Zassa et al., 2010). The first phase is called pyrolysis due to the low temperature; the second is defined as cracking, because it happens at a higher temperature, as illustrated in figure 1.4.

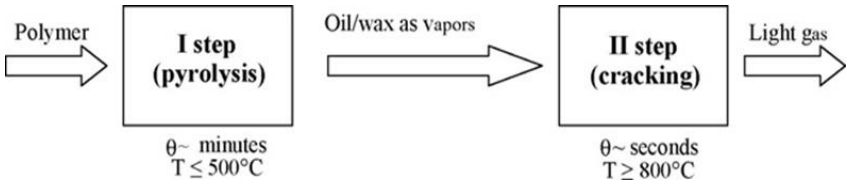

Figure 1.4 Double stage process (Della Zassa et al., 2010)

This configuration allows a better control of the polymer conversion, because decouples the homogeneous gas phase from the physical transformation of melting phase. Process parameters can be optimized in the two reactors; a long retention time in the melting reactor will allow treating a homogeneous material in the second, where the optimization of gaseous product requires high temperatures and short residence times. The first step at mild conditions (low temperature, slow heating rate and long residence time) gives mostly linear saturated and unsaturated hydrocarbons, which are suitable to be cracked to ethene. Separating the two reactors and adapt parameters to their different aims, will allow improve yields, sample conversion and product quality.

1.3. Inputs

The main variable that affects products composition is the feeding material, which can be constituted by one or more components and it is the key for the process choice.

1.3.1. Single component

Only in case of a pure single-component plastic it is possible to recover monomer as the predominant product. Examples are the pyrolysis of PMMA, polytetrafluoroethylene (PTFE), and polystyrene (PS). Yields had been improved in ten years research, becoming very high, as shown in table 1.3.

Table 1.3 Yields of monomer recovery (Kaminsky et al., 1991 and 2003).

Kaminsky	1991	2003	T (°C)
PS	64%	76,8%	550-580
PMMA	97%	98%	450-500
PTFE	-	76%	555

As reported in paragraph §1.2, PVC pyrolysis is hindered by its chloride content. In order to process its products in existing plants, chlorine content should not exceed 10 ppm. By addition of lime, HCl can be bound chemically, but the $CaCl_2$ form in the process can cause particle agglomeration and clog the bed. Hence gaseous HCl needs to be removed in a preliminary step at 300-400°C, before more extensive cracking reactions take place and it will be available for further use (Kaminsky et al., 1991).

1.3.2. Mixtures

Pyrolysis of mixtures composed by polyolefins in different weight fractions was investigated by Predel et al., in a fluidized bed reactor. In table 1.4 are drawn mass balances on different inputs composed by various percentages of polyethylene and polypropylene. Decomposition was run at 510°C, with pyrolysis gases as fluidizing medium and ensuring a residence time of about 5 seconds.

Table 1.4 Mass balances of four PE/PP mixtures (Predel et al., 2000)

Input (%) / Output (%)	PE	100	60	40	0
	PP	0	40	60	100
Gases		2.6	4.5	5.1	6.9
Oils		13.2	19.4	23.2	35.4
Light waxes		24	23.2	22.4	20.2
Heavy waxes		60	52.8	49.1	37.3
Soot		0.17	0.11	0.18	0.078

Gas and oil production of pure PE-feed is only about one third of that evolved by PP-feed and also the amount of heavy waxes is nearly cut down to half. On the contrary, light waxes decreases only slightly when changing from PE to PP. Yields of mixtures stay between these percentages depending on their composition: the presence of PP increases the oils and decreases the wax presence in products.

Polyethylene and polypropylene don't show any remarkable interaction: the mixture products are nearly the sum of the single component pyrolysis. On the other hand, simultaneous pyrolysis of polystyrene and polyolefins is not so advantageous, because it was found that the polystyrene present in mixed plastic is the main responsible for aromatic species in pyrolysis tars. LDPE gives, instead waxes with a negligible concentration of aromatic species (Williams et al., 1998).

It is also proven that PS has mixing effects on PE or PP or their mixtures; whenever 10% of PS is added to PE and/or PP, the amount of gases and oils increases on the expense of the heavy waxes, which become richer in unsaturated compounds with more than 30 carbons (Predel et al., 2000). The easiest way to gain high yields of monomers from a mixture is the fractionated pyrolysis; so polystyrene is recycled at low temperatures (500-550°C) and polyolefins are cracked to olefins at 700 or 750°C (Kaminsky et al., 1998).

Conversion depends also on ratios and it was found that the higher yield in term of oils is given by a ratio of 1:1 between PS and polyolefins (PE; PP, LDPE, HDPE) or PET (Siddiqui et al., 2009). Under single-component thermal pyrolysis at 440°C, PS is the only one that shows a complete conversion; the other plastics shown moderate (LDPE and HDPE) to high (PP and PET) yields. PS's reactivity depends on the amount of feed, but increasing the amount of PS with respect to the other plastics decreases the conversion percent.

Also the branching degree has its influence on pyrolysis yields; it was observed that at low temperatures (450-500 °C) decomposition happens firstly for PP, which is more branched than PE. Furthermore LDPE, which is casually polymerized, gives lighter waxes than HDPE, which has oriented molecules (Arabiourrutia et al., 2011).

1.3.3. Real waste

A real waste, even if made up only by a single component can contain pollutants (Cl and metals) and fillers or additives, which hinder decomposition. For example the MMA can be recovered from pure PMMA up to 97 wt. % in a fluidised bed at 450°C. If PMMA is filled with silica, this yield slightly decreases to 90%, but when dealing with aluminium tri-hydroxide (ATH), it drops to 58%. ATH is a flame retardant, because at high temperatures produces water that kills the flame and has no catalytic inclination (Kaminsky et al., 2003). On the other hand, glass and metals have shown to play a catalytic role in a real waste, increasing the gas/liquid ratio and modifying liquid composition leading to more aromatic species (Adrados et al., 2011).

A real waste from municipal sorting plant is composed by 60% of packaging plastic (PE, PP, PS, PET, PVC) and the rest are other packaging materials (i.e. aluminium and poly-laminates, 5.4%) or inappropriate materials (34.6%), that should not have been placed in the plastic container. Inappropriate materials primarily consist of paper, glass, clothing waste, wood waste and other types of plastic waste. The precise characterization is reported in table 1.5.

Results of the pyrolysis of this real waste sample at 500°C with a 30 minutes retention time are listed in table 1.6. The solid char yield is quite high and depends on the presence of –OH and =O groups that reacts with hydrogen atoms of the polymeric structure; they are typical in paper, wood and gardening,

and sum to 11.29 wt% in the real sample. A real sample has relatively low moisture content, but high ash content, due to the presence of inorganic components, including metals and inappropriate materials (see table 1.7). The high heating value (HHV) is lowered by the CO_2 content, which stems from the cellulosic material and it is about 30 MJ/kg.

Table 1.5 Composition of a real sample (wt %) from a material recovery facility (Adrados et al., 2011).

Material	Real sample
Plastic packaging waste	
Polyethylene (PE)	18.77
Polypropylene (PP)	21.94
Polystyrene (PS)	8.36
Expanded PS	3.02
Polyethylene terephthalate (PET)	3.23
Polyvinyl chloride (PVC)	0.79
PE film	2.14
PP film	1.73
Subtotal	59.98
Other packaging waste materials	
Complex materials	0.22
Aluminum film	2.50
Non-ferrous metal (Al)	1.35
Ferrous metal (Fe)	1.27
Subtotal	5.34
Inappropriate materials	
Acrylonitrile butadiene styrene (ABS)	2.39
Polymethyl methacrylate (PMMA)	0.55
Polyurethane (PUR)	0.18
Polyamide (PA)	0.25
Polycarbonate (PC) (compact disk)	0.83
Elastomer	2.42
Latex	0.97
Medical waste	0.98
Paper	4.19
Clothing waste	0.08
Gardening waste	0.56
Wood waste	3.32
Glass	16.18
Inert	1.78
Subtotal	34.68

Table 1.6 Pyrolysis products (%wt.) from a real waste sample (Adrados et al., 2011).

Fraction	Real sample
Liquids	40.9
Gases	25.6
Solids (inorganic + char)	28.2 + 5.3
Ratio liquid/gas	1.6

Table 1.7 Elemental composition of a real waste pyrolized sample (%wt.) (Adrados et al., 2011).

Sample	Real sample
Moisture	1.0
Ash	28.2
C	58.7
H	8.7
N	0.5
S	<0.1
Cl	1.0
Others[a]	1.8
H/C rate	1.8

1.4. Process parameters

The main process parameters are temperature, residence time and heating rate; in this paragraph their influence over qualitative and quantitative products' characteristics will be investigated.

1.4.1. Temperature

It is quite obvious that the amount of gas increases rising the temperature; on the contrary, in order to enhance oil production, low temperatures and slow heating rates shall be maintained, as it is shown in table 1.8, where test on PE were run at different temperatures (Williams et al., 1998).

Table 1.8 Product yields (%wt.) from the fluidized bed pyrolysis of LDPE with respect to temperature (Williams et al., 1998).

Product	Temperature (°C)				
	500	550	600	650	700
Gas	10.8	21.4	24.2	40.1	71.4
Oil	43.9	43.2	51.0	47.8	24.6
Wax	45.3	35.4	24.8	12.1	4.0
Oil + Wax	89.2	78.6	75.8	59.9	28.6

Also the proportions of oil to wax changes as temperature increases with less wax and more oil fraction, enhancing wax cracking to oil and further to gas. Waxes didn't show any qualitative change with temperature, they are a high viscosity, cream colored material. Oils, instead, show a decrease in viscosity above 600°C. Finally, char fraction increased from 0.2% at 500°C to 5.9% at 700°C, because more extended gas-phase tar-cracking reactions takes place.

The main gases produced from PE pyrolysis are alkene gases, ethene, propene and butene, in addition to the alkane gases and hydrogen. As the temperature increases, concentration of some gases raises (see Table 1.9); ethene and propene showed a marked increase, between 650 to 700°C.

Table 1.9 Gas composition (%wt.) from the fluidized bed pyrolysis of LDPE with respect to temperature (Williams et al., 1998).

Gas	Temperature (°C)				
	500	550	600	650	700
Hydrogen	1.05	0.23	0.22	0.68	0.66
Methane	0.83	1.52	3.03	4.22	11.76
Ethane	0.78	1.71	2.53	2.82	4.68
Ethene	2.19	5.33	6.84	10.81	26.86
Propane	0.76	0.84	0.83	0.83	1.25
Propene	1.82	4.79	5.64	9.10	18.59
Butane	0.50	0.55	0.21	0.55	<0.01
Butene	2.91	6.39	4.95	11.07	7.63

Accordingly Kaminsky et al. reported ethene as the dominant gas in the fluidized bed pyrolysis of LLDPE, followed by propene. At higher temperatures larger paraffines and olefins produced from decomposition are cracked into H_2, CH_4 and lighter hydrocarbons. Similar to butadiene, ethene and propene had maximum yields at 700°C. The yield of butenes reached the highest value at 600°C (Kaminsky et al., 1994).

Williams et al. analyzed the molecular weight distribution for the derived pyrolysis oils and waxes at 600, 650 and 700°C and their results are illustrated in figure 1.5. This parameter also gives an indication of the boiling point range and it is useful to determine the compatibility of the recycled plastic products with the conventional petrochemical feedstock derived from crude petroleum oil. For both oils and waxes, as the temperature had increased, molecular weights were shifted to lower values; however, this shift was less marked for waxes, which have weights much higher than the oils and ranged up to almost 4000 Da.

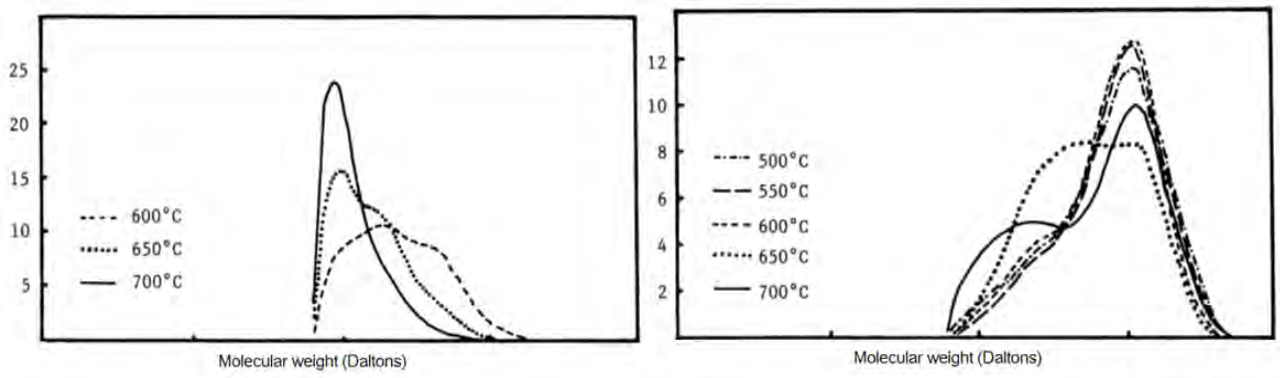

Figure 1.5 Molecular weight distribution of oils (left) and waxes (right) with refractive index detector (Williams et al., 1998).

Furthermore, gas chromatograms showed that the range and concentration of the carbon number species in the wax remained fairly constant, where even at the 700°C pyrolysis temperature, alkadienes, alkenes and alkanes were present up to C_{57}. So waxes composition does not depend upon temperature (Williams et al., 1998).

On the contrary, in the oils, concentrations of aliphatic species above C_{30} were greatly reduced at higher temperatures; instead these of single ring aromatic compounds and polycyclic aromatic hydrocarbons (PAH) were increased. In fact oils at 500 and 550°C contained no aromatic hydrocarbons, but these at 700°C had PAH equal to 25% of the total oil fraction. Benzene and toluene dominated the aromatic composition; among all only phenanthrene showed any biological activity, the other PAH have no reported carcinogenic or mutagenic activity (Williams et al., 1998).

Consistently with the above, Kaminsky et al. demonstrated that the degree of unsaturation increases with temperature so the C/H ratio becomes higher and, as a consequence the gas become richer in H_2, as showed in table 1.11.

Table 1.10 C/H ratios of the product fractions from fluidized bed pyrolysis of polyolefins (Kaminsky, et al., 1994).

Experiment	PE 1	PE 2	PE 3
Temperature (°C)	600	700	800
Fluidizing gas	H_2O	H_2O	H_2O
Starting material	HDPE	HDPE	HDPE
C/H ratio			
Gas	0.50	0.49	0.41
Oil	0.56	1.04	1.15
Distillation residue	0.53	1.27	1.60

Eventually it is clear that oils composition change with final temperature, if it is lower than 700°C, they will be mostly aliphatic, whether higher mostly aromatic. Higher temperatures favors secondary (i.e. post-pyrolysis cracking of the alkenes) and condensation reactions and more thermodynamically stable products (i.e. aromatics).

Char composition is mainly constituted by carbon, and the hydrogen and ashes content decrease with temperature. It was estimated by Cozzani that the weight of the ash fraction present in the char is roughly equal to that of ashes in the virgin PE (Cozzani et al., 1997).

%	500 °C	700 °C	800 °C
C	50.86	75.76	88.37
H	2.09	0.12	0.20
N	traces	traces	traces
ashes	47.05	24.12	11.43

Figure 1.6 Analysis of the Char from PE different Temperatures (Cozzani et al., 1997).

1.4.2. Residence time

It is believed that an extended residence time in the hot zone will result in higher amount of char, gas and thermally more stable products due to the secondary cracking reactions of waxes and oils (Williams et al., 1998). Commonly, to change this parameter, inert flow rate is varied, but Cozzani put polyethylene sample holder in different positions (l_1, l_2, l_3) along a fixed bed horizontal reactor, (figure 1.8). In this way sample heating was not affected by changing gas diffusion phenomena.

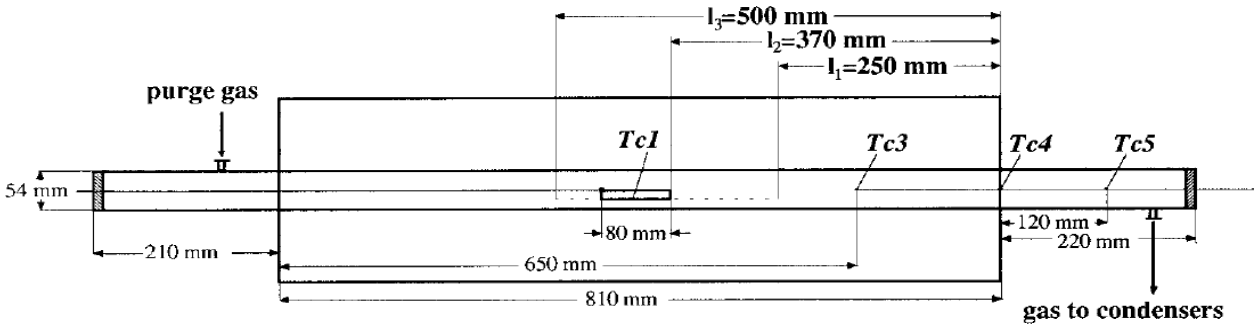

Figure 1.7 Fixed bed horizontal reactor (Cozzani et al., 1997).

Residence time had a significant influence on the products yields only above 500 °C. In figure 1.8 it is clear that the longer residence time resulted in lower tar yields and in greater char and gas yields.

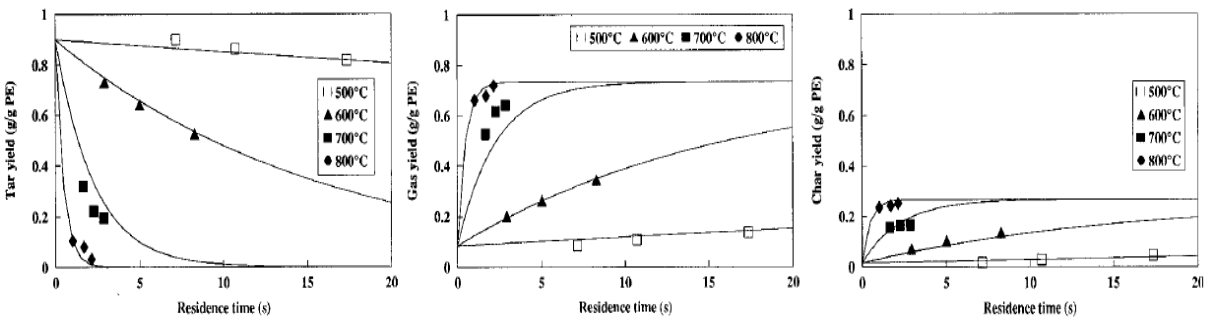

Figure 1.8 Yields of tar, gas, and char from LDPE pyrolysis as function of time and temperature (Cozzani et al., 1997).

Accordingly, McCaffrey et al. obtained high yields of liquid products with long residence time from the degradation of LLDPE at the temperature of 445°C; they also investigated oil composition in relation with time. In figure 1.9 are showed total condensable yield and straight alkane and alkenes yields on the total tar weight.

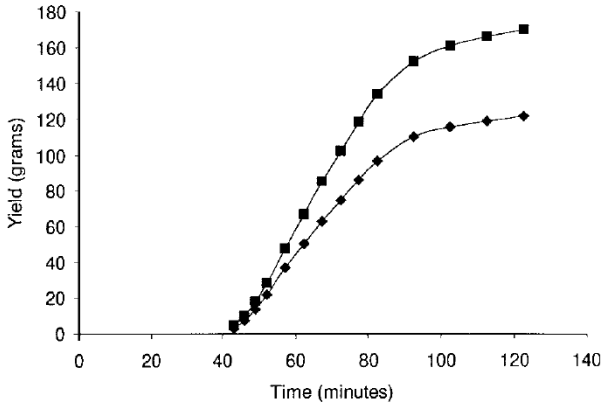

Figure 1.9 Cumulative yields of the total liquid products ■ and alkanes and alkenes ● (McCaffrey, 1997).

As the reaction progresses, the distribution of both the alkenes and alkanes was skewed towards smaller chain lengths; the molecular weights tended to become more normally distributed around the mean molecular weight. In figure 1.10 the distribution of the chain lengths is illustrated after 43 and 122 minutes.

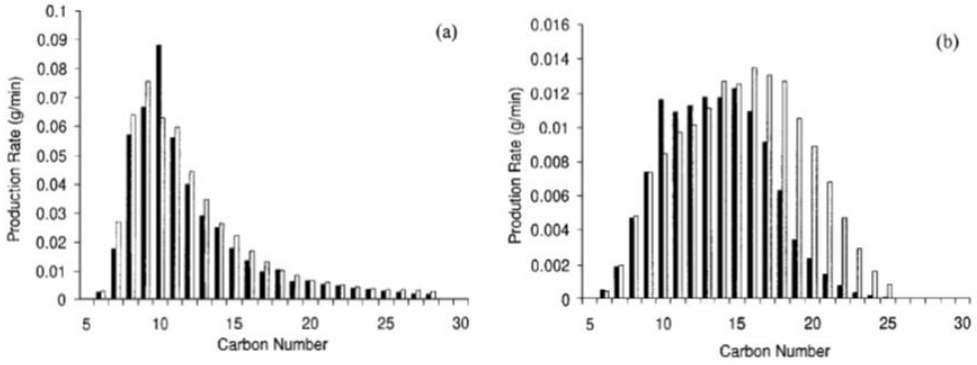

Figure 1.10 Distribution of n-alkenes■ and n-alkanes□ in tars after (a) 43 and (b) 122 min (McCaffrey et al., 1997).

1.4.3. Heating rate

Kinetic tests on pyrolysis of polystyrene and polypropylene were carried out by Kim, at the heating rate of 0.5, 1, and 2 °C/min in a stirred batch reactor.

Figure 1.11 shows the conversion curves versus temperature for different heating rates, decomposition of both PS and PP began at lower temperatures for slower heating rate. In fact pyrolysis of PS started at 360, 370, and 384°C for the heating rates of 0.5, 1, and 2°C/min, respectively. Likewise behaved PP, which, even at temperatures slightly higher, decomposed at 387, 405, and 411°C for the same heating rates.

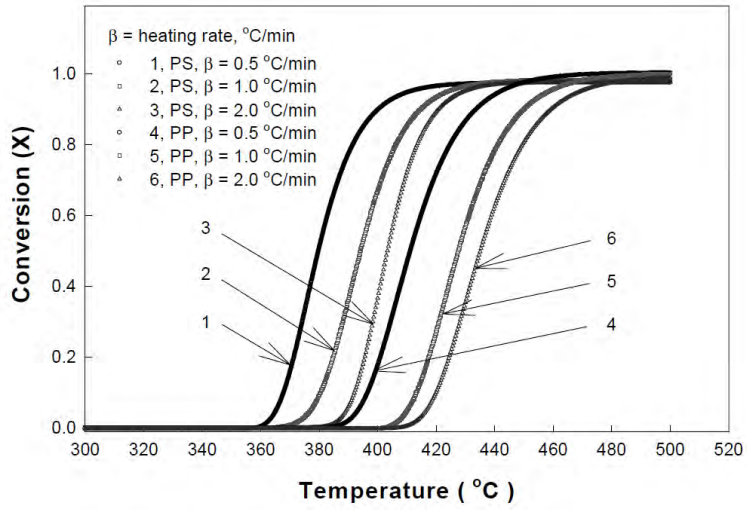

Figure 1.11 Effect of pyrolysis rate of PS and PP on heating rate (Kim et al., 2003).

Slower heating rates caused also a slight increase in lighter hydrocarbons, due to the deeper cracking, as it clearly deduced from figure 1.12, where bars represents weight fractions of each carbon atom number on the total oils' yield.

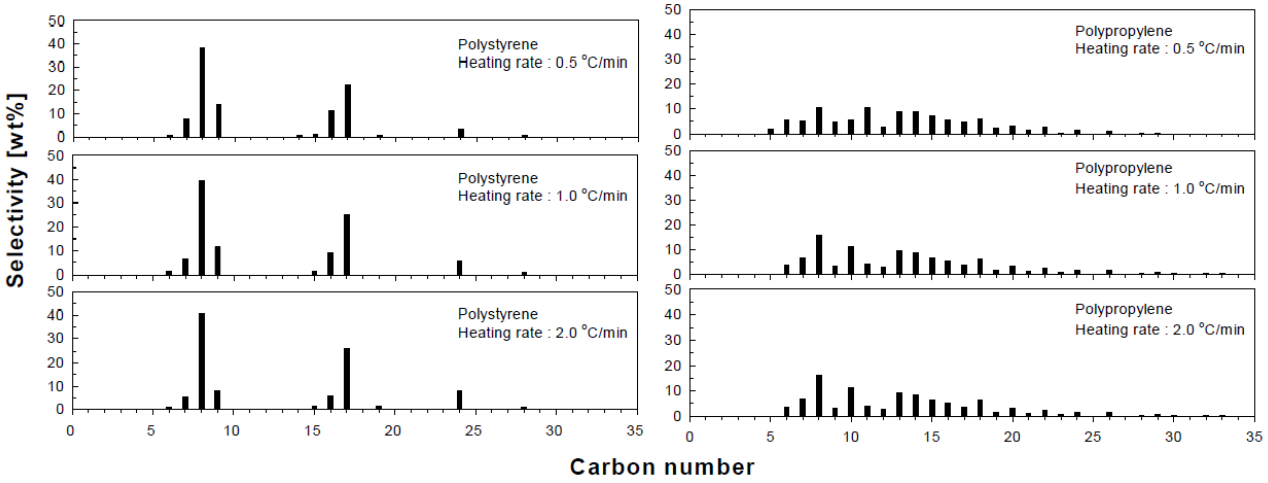

Figure 1.12 Effect of heating rate on carbon number distribution for PS and PP oils (Kim et al., 2003).

Finally, it is clear that in order to enhance plastic degradation slow heating rates shall be provided; these will favor a better heat transfer throughout the material, due to its low heat diffusivity capacity.

1.5. Economic viability

Pyrolysis sustainability depends upon products quality and oil price, which is continuously rising; so there are the premises that it could become viable. According to an economic feasibility study on plastic waste treatment drawn by Buekens et al. in 1998, the investment cost for a 25000 t/y size plant in Belgium amount on 20 million dollars. The resulting treatment cost is 250 dollars per ton, but naphtha price is only 180 dollars per ton, leaving a 'gate fee' which shall be covered by a subsidy to allow economic viability. During 2011 Islam developed in Bangladesh a pilot plant configuration for waste tyres treatment, as summarized in figure 1.13.

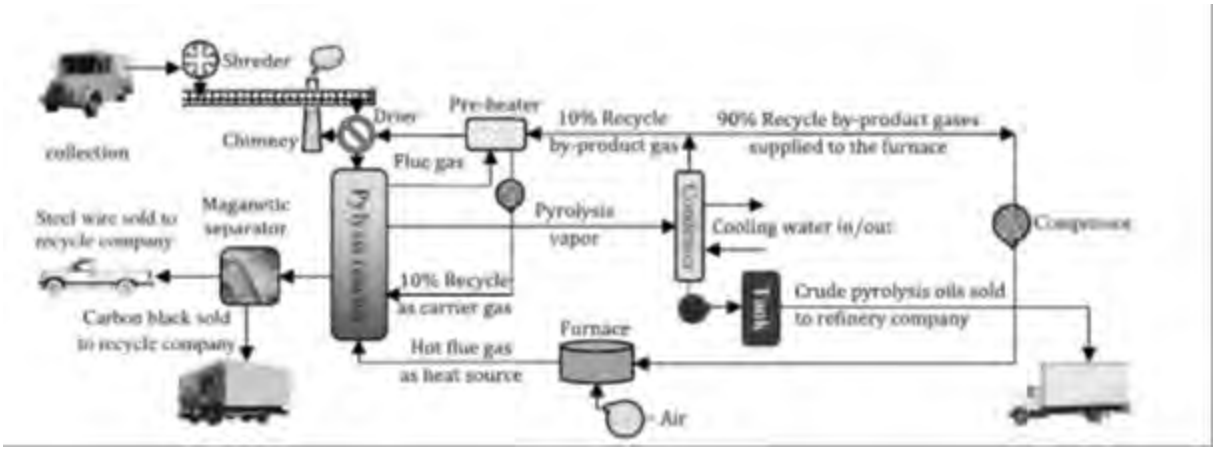

Figure 1.13 Conceptual design for pilot pyrolysis plants (Islam et al., 2011).

The economic analysis was run in three different scales, with treatment capacities of 144, 36 and 3 ton per day. The medium scale plant is the most probable, but it is clear that a larger plant reduces treatment costs per ton and abates investment efforts in less time. For the greater capacity, the Unit Production Cost (UPC) 136 dollars per ton, which is lower than oil price in this country; it can be further reduced by selling by-products such as carbon black and steel.

Table 1.11 Production cost for three different scale plants (US$) (Islam et al., 2011).

Plant capacity	144 tons/ day	36 tons/ day	3.6 tons/ day
Base equipment cost	2.5×10^6	1×10^6	0.20×10^6
Fixed capital investment (FCI)	5.69×10^6	2.27×10^6	0.45×10^6
Total capital required	6.54×10^6	2.62×10^6	0.52×10^6
Annualized capital cost/Capital charges	768123	307249	61455
Fixed operating cost:			
Salary for employee	190304	110176	17528
Maintenance + overheads + taxes and insurance + other fixed operating costs	398125	159250	31850
Variable operating cost:			
Feedstock	901440	225360	22536
Electricity	450720	135216	22536
General overheads	114182	66105	10516
Total operating cost	2054771	696107	104966
Total production cost of pyrolysis oil	2822894	1003356	166421
Unit production cost of pyrolysis oil (US$/ton)	136	193	321

Feedstock cost was a little underestimated (20 $/t) even considering that no pre-treatment had taken place; also energy price (0.10 $/KWh), insurance, taxes and salaries are related to the location, which is a developing country. However oil selling price was considered to be 400$/t, which is a significant demonstration that oil price had risen during last years.

1.6. Feedstock recycling

Pyrolysis of plastic waste allows increasing the sustainability of plastic use because it closes the cycle of hydrocarbons, as it is shown in figure 1.14, which represents the flow sheet of polyoleifins' life cycle, where solid-line connectors create a closed loop.

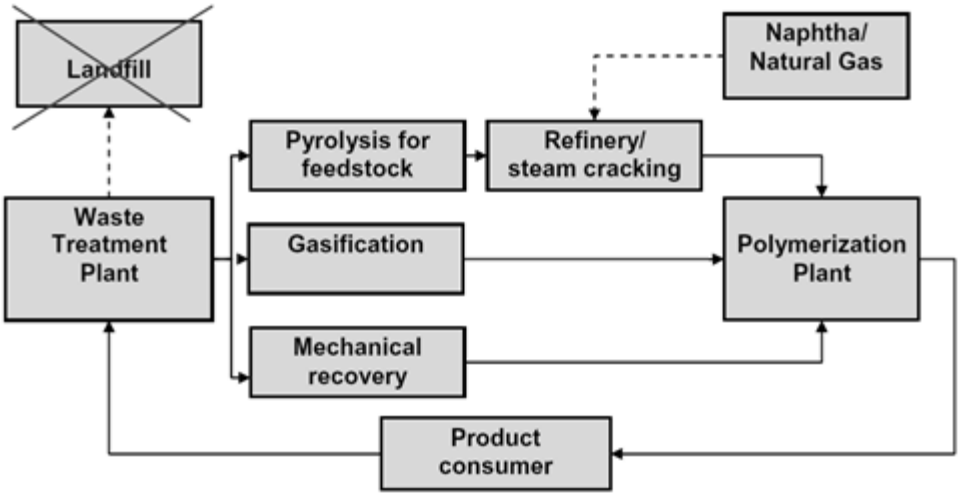

Figure 1.14 Polyolefins' life cycle (Donaj et al., 2011).

Feedstock recycling of oils highly depends on its quality but also on the needed applications, i.e. for heating and combustion a highly aromatic composition (BTX) is more desirable (Kaminsky et al., 2004). In the case of steam crackers, the aromatic are thought to lead to increasing coking rates in the process, so an aliphatic composition is preferred. A conventional steam cracker can be fed with a mixture of naphtha and plastic waxes up to 20% weight, without significantly enhancing coke formation and affecting yields of ethene and other alkenes, which are then used to make new plastic polymers (Williams et al., 1998). Alternatively, oils and waxes can be further refined in a conventional fluidized catalytic cracker to produce gasoline and thereby replace petroleum gas oils.

Treating polyolefins' as a single fraction is highly convenient, due to similarities in the chemical and physical properties between the components and of the high content of this fraction found in total plastic waste. Among others, polyethylene is by far the major plastic occurring in waste throughout the world, for example, the plastic fraction of European municipal solid waste is estimated to contain over 40% of polyethylene (Williams et al., 1998). For this reason this master thesis will deal with a low temperature pyrolysis of PE to gain waxes and aliphatic oils. This will allow an easy manageability and marketability of liquid products

Chapter 2
Differential scanning calorimetry

The Differential Scanning Calorimetry is an analytical technique that allows studying different properties of a generic sample with respect to temperature. It measures the difference between heat fluxes absorbed by a sample and a reference cooled or heated at the same rate; it can also provide the temperature of thermal events and its nature (exothermic or endothermic) and calculate the enthalpy of reactions. The sample pan and the reference one (usually void) are placed in the same furnace above two thermocouples (figure 2.1).

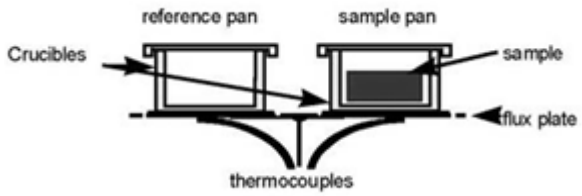

Figure 2.1 DSC main principles.

The instrument utilized in this thesis is a DSC Q10 of TA INSTRUMENTS (figure 2.2), its cell is a Q Series Pressure Cell and can be pressurized until 7MPa; it allows to run defined heating programs and the atmosphere in the sample chamber may be purged with an inert gas or air.

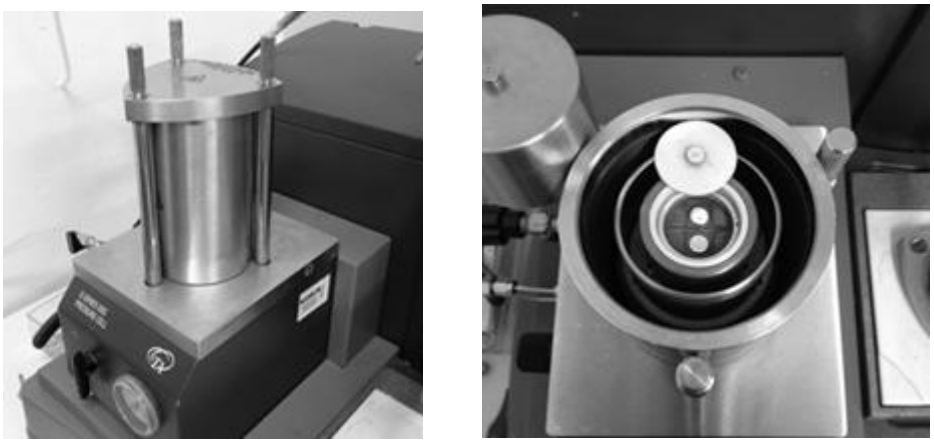

Figure 2.2 DSC instrument.

A DSC analysis allows deducing the behavior of a generic material; in particular the following phenomena can be observed:

- Fusion (Endothermic)
- Crystallization (Exothermic)
- Evaporation (Endothermic)
- Condensation (Exothermic)

- Sublimation (Endothermic)
- Glass Transition
- Chemical Reactions

In figure 2.3 is illustrated the generic behavior of a polymer: it can be identified the glass transition temperature (Tg) and the melting temperature (Tm). The intermediate peak is given by the crystallization process (Tc) and it quantifies the crystalline index of polymer, which tends to form ordered crystals, increasing the temperature. Crystallization is exothermic, while fusion is endothermic, so peaks are opposite.

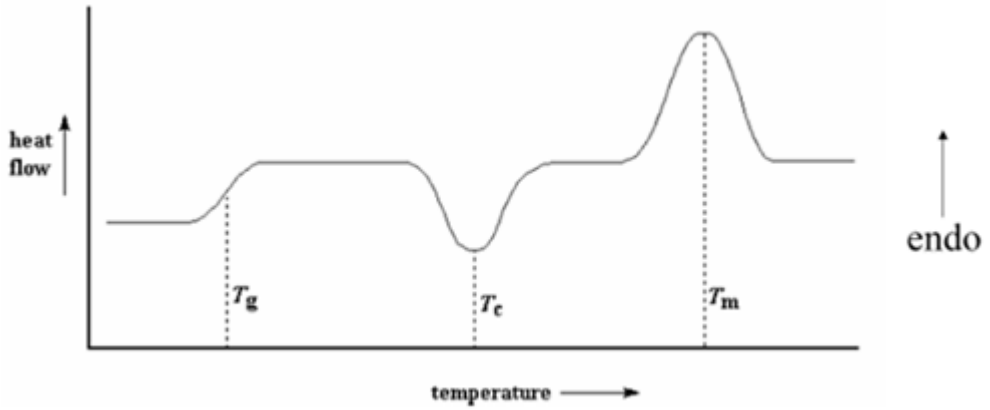

Figure 2.3 DSC chart of a generic polymer.

In order to obtain a reliable curve is necessary to calibrate the cell to minimize experimental errors; in fact the DSC method it is based on a series of assumptions:

- Perfect evenness between the two pans;
- Perfect symmetry of the cell and of its properties (thermal resistance and heating capacity);
- No influence given by the carrier in the analysis;
- No thermal resistance between sample holder and oven (this effect is scanning rate dependent).

Three parameters need to be calibrated before the tests:

- *Baseline* serves to straight the line and to shift it nearer to the zero, it has slope equal to 0.0014 and offset to *-1.9852*;
- *Cell constant* accounts for signals conversion (from micro V and W/g) and it is based on the enthalpy of fusion of a known material (Indio). The cell constant K is given by the ratio between the experimentally measured enthalpy and the known one. This parameter is also an indication of the instrument state; if it is good, it shall be comprises between 0.7 and 1.3 and results to be 1.522.
- *Temperature* is useful to calibrate the thermocouples, it compares the real melting temperature of Indio (156.60°C), which is a calibration standard to the experimental one (158.13°C).

2.1. Measurements

A series of tests was run on different samples available in the laboratory, in order to decide the conditions to be used in the pyrolysis reactor. All samples were identified as polyethylene polymers and they shall show two main properties, which are an evident melting peak and oxidation at a quite low temperature. In Appendix A are reported all the technical sheets regarding them.

Tests were run without flux, sample were placed in a closed crucible and heated to 250°C with a ramp of 10°C/min. They were not prosecuted far above this temperature to avoid fouling of the cells that will happen with evaporation reactions. All the curves in figure 2.4 are compared on the bases of the same sample weight (3 mg); the fact that they are not perfectly overlapping clearly shows baseline dependence from the sample kind. The curve of PE 9 starts after the others because the cell temperature was a little higher than in the other tests, but this is irrelevant for the analysis.

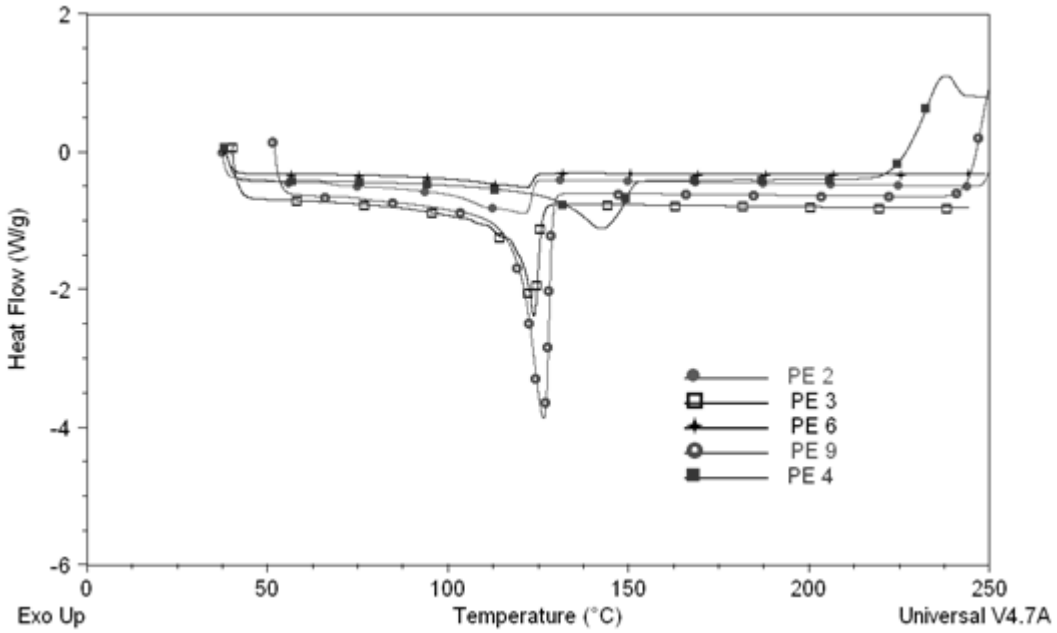

Figure 2.4 DSC of different PE samples heated at 10°C/min to 250°C without flux.

Two samples PE 2 and 6 don't show a marked fusion peak with respect to the others, while PE 9 shows the deepest fusion one, hence it was chosen for further considerations about the solid-liquid transition. In sample 2 and 3, the initial part of the fusion peak present some irregularity due to the presence of some additives that melts together with the plastic and cause some little peaks.

As regard as degradation PE 4 oxidized at the lowest temperature, so seems to be the easiest to be degraded; PE 3 and 6 don't oxidize in the temperature range studied. For completeness the Melt Flow index of each sample is reported in table 2.1, although no correlation was found with fusion temperature or enthalpy.

Table 2.1 Melt Index, fusion temperature and oxidation temperature of different polyethylene samples.

Sample	MFI (g/min)	Fusion T (°C)	Oxydation T (°C)
PE 2	2.3	121.45	252.69
PE 3	1-3	123.83	n.a.
PE 4	2	143.3	237.25
PE 6	1.1-2.3	112.08	n.a.
PE 9	0.4	126.55	252.24

2.1.1. Fusion transition

Fusion enthalpy can be calculated from the integration of the fusion peak and the function most adapt for the integration is the Sig-horizontal, which compensates the baseline variation with an s-shaped curve, changing its slope before or after a peak. Enthalpy together with fusion temperature shall not depend upon the heating rate; so other tests have been run at different heating rates in order to verify this assumption. In figure 2.5 are presented the curves of sample PE 9 heated to 300°C at 5-10 and 20°C/min, without any flux of gas.

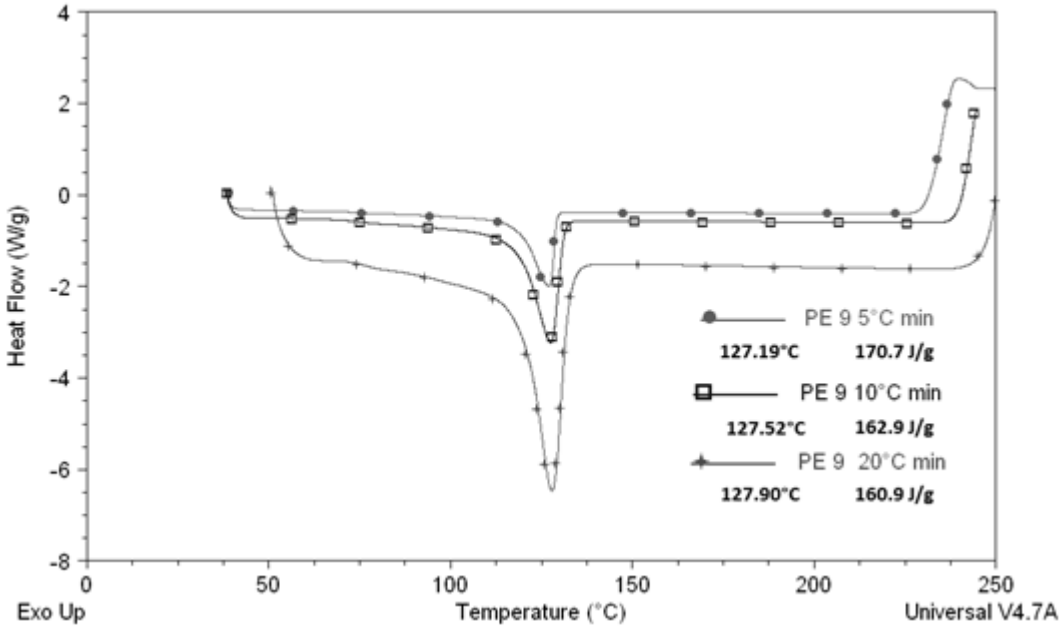

Figure 2.5 PE 9 heated at different heating rates (5-10-20°C/min) to 300°C without flux.

Values of fusion temperature and enthalpy related to each heating rate are shown in figure 2.5; it is evident that peaks are broader and less intense at higher heating rate, but this does not affect the integration, because melting temperature and enthalpy don't have appreciable variation with heating rate.

Curves appear to be ordered with increasing HR; the initial slope of the curve is steeper when sample is absorbing more heat in the same given time and this determines the baseline position in the chart. The initial part of the curve in the Indio chart (figure 2.6) is very short and collocates the baseline almost on the zero; hence the baseline position depends from both the heating rate and the material.

Furthermore it is known from literature that the descendent part of the fusion peak depends on the material, while the right part on the instrument; in fact in the Indio chart (figure 2.6) is much steeper than the one of PE (figure 2.5).

As for polyethylene, also for Indio melting temperature and fusion enthalpy don't have any considerable change with heating rate (figure 2.7); however the fusion chosen for integration is linear, not s-shaped, because the peak is narrow and straight.

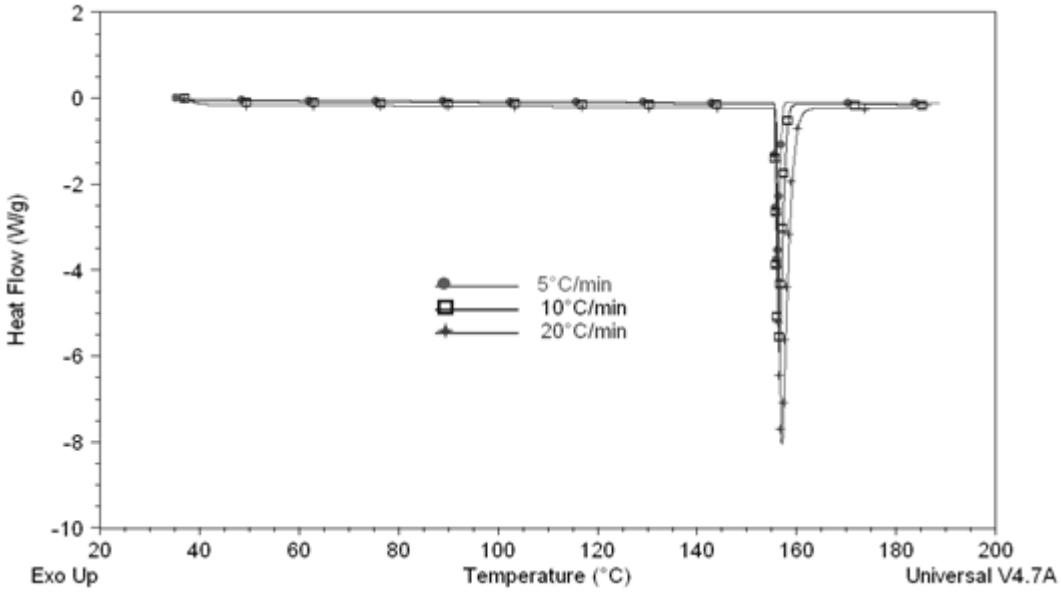

Figure 2.6 Indio heated at different heating rates (5-10-20°C/min) to 200°C without flux

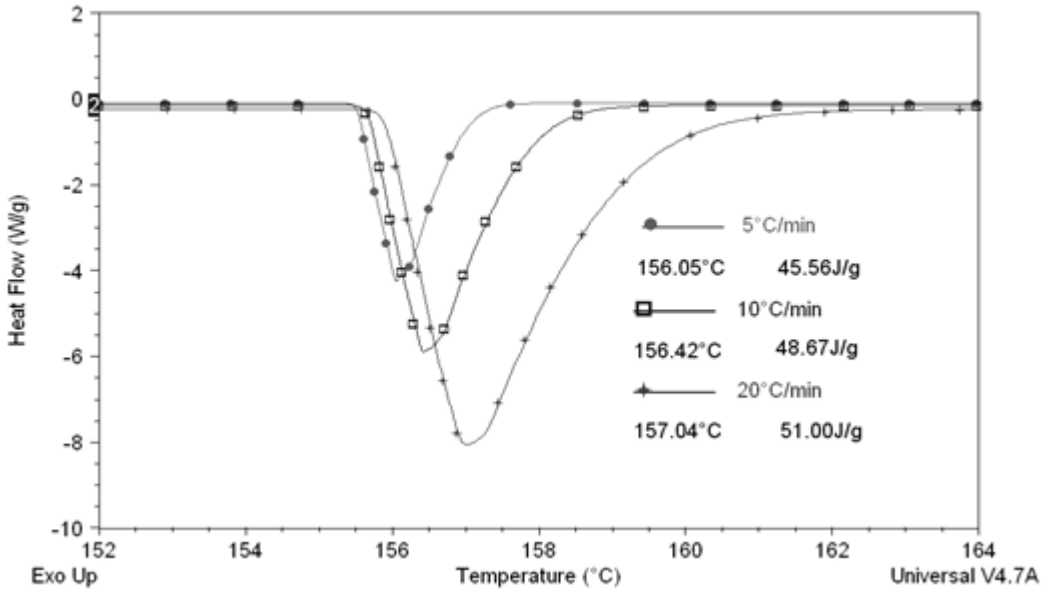

Figure 2.7 Zoom on the fusion peak of Indio heated at different heating rates (5-10-20°C/min) to 200°C without flux.

The heating rate dependence of the melting temperature distribution is in apparent contrast with the solely thermodynamic nature of this process. However the observed differences between melting

curves obtained at different heating rates can be explained considering the thermal inertia of the sample: speeding up the increase of temperature, broader thermal gradients, responsible for heat transfer in DSC samples, will take place. The existence of temperature gradients, during melting of the polymer, has its relevance, even in a 0.1 mm thick sample (Greco et al, 2007).

2.1.1.1. Specific heat

The DSC is capable to estimate the specific heat at constant pressure (Cp), starting from two curves, related to the same sample mass, at different heating rates. The Cp is the amount of heat per unit mass required to raise the temperature of one degree Celsius. It is known from literature that a generic polyethylene has a specific heat equal to 0.55 cal/°C/g at 23°C.

The Cp at a given temperature (T), is calculated from the formula 2.1, where HF stays for heat flux (cal), HR for heating rate (°C/min), m is the sample mass (g) and K the cell constant.

$$C_p\,(T) = K * \frac{HF1-HF2}{(HR2-HR1)*m} \tag{2.1}$$

In this case the cell constant is equal to 1.522, heating rates 5 and 20°C/min are compared over a sample mass of 3.25 mg and the Cp at 70°C results to be 0.47 cal/°C/g.

2.1.2. Glass and crystalline transition

In order to observe the glass and crystalline transition, PE curves in figure 2.4 were compared to a PET's one (figure 2.8) where they're very evident. Glass transition is represented by the step between 65 and 67°C and is a second order transition, since it involves only the Cp (specific heat at constant pressure) and not also the latent heat. The crystalline transition happens at 130°C and that favors the alignment of its molecular chains in an exothermic reaction.

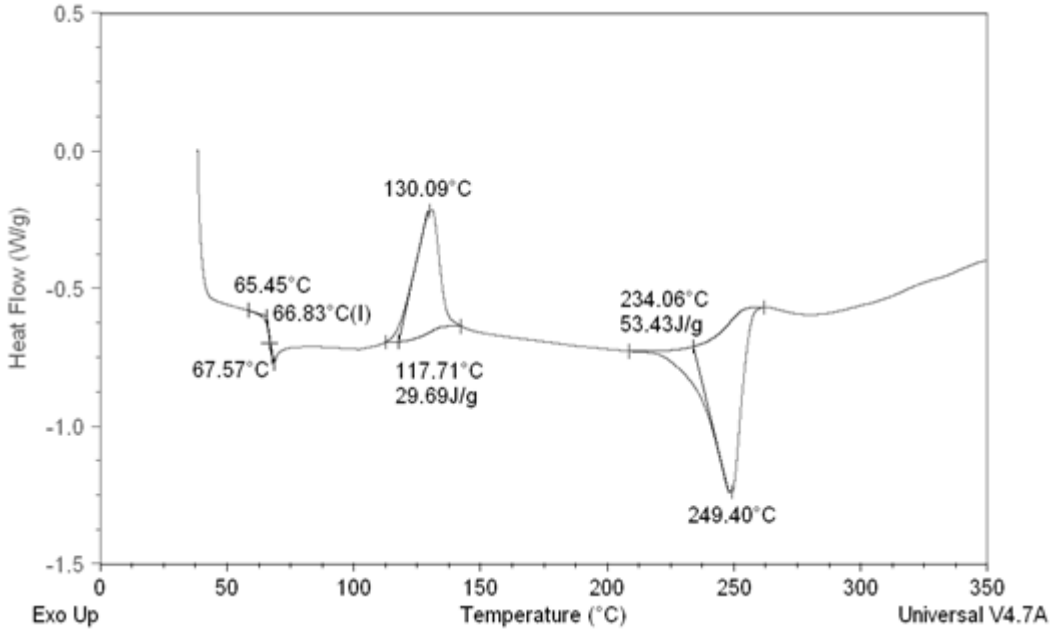

Figure 2.8 DSC diagram of PET.

It is clear that in PEs a glass transition does not occur and they're also amorphous since no crystalline transition has been seen.

2.1.3. Oxydation reaction

The positive peak, at higher temperature, well above melting, is likely related to oxidation reactions, which are highly exothermic. Among others, the sample oxidizing at the lowest temperature is PE 4 (figure 2.4). In figure 2.9 are shown oxidizing peaks of PE 4 in different atmospheres. If the reaction taking place is an oxidation one, it shall not happen in inert atmosphere; hence the PE 4 was tested without flux, in air, and in Helium. In this last one atmosphere, it was tested in both open and closed a sample holder.

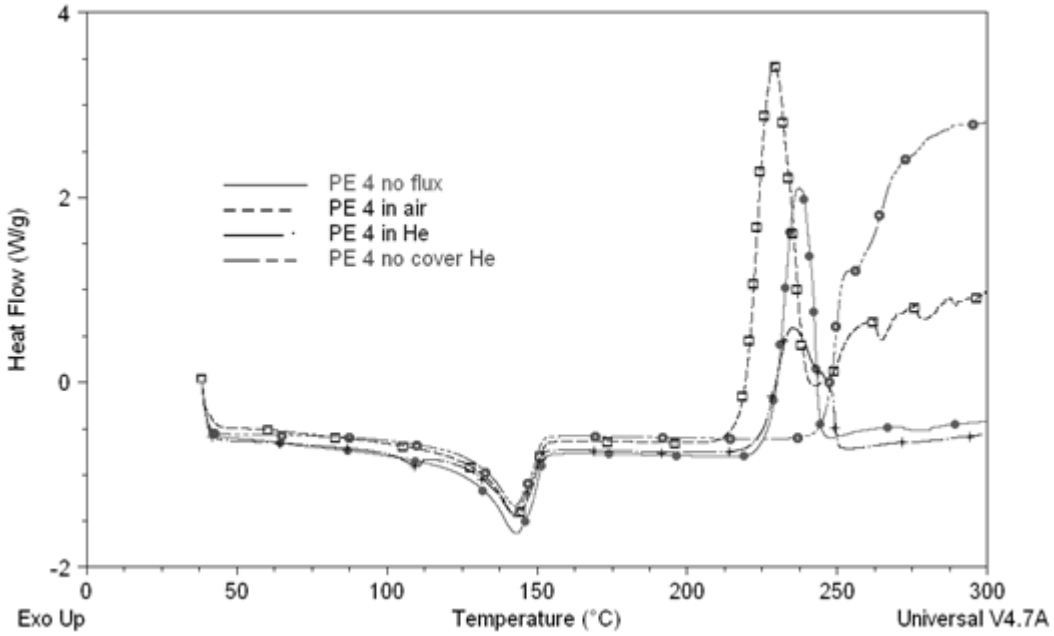

Figure 2.9 PE 4 in different atmospheres and without sample holder cover.

It is evident that oxidation peaks in figure 2.9 are reduced according to the quantity of air present in the sample holder and cell during tests. The more pronounced is in air atmosphere, followed by the one without flux and by the one in helium with cover. The fact that oxidation takes place also in the test performed with Helium means that in the cell was surely present a little amount of oxygen, probably in the sample holder itself. In fact in the test without the sample holder cover, in a completely inertized atmosphere, oxidation did not happen. However in this case the lack of the cover had favored PE volatilization before 300°C, as it is demonstrated by the tale's curve rapid ascent.

In table 2.2 are reported oxidation peak and initial volatilization temperatures; it can be seen that the polyethylene oxidizes first and reaches the peak temperature in air, while the temperature of oxidation in helium and without flux are about the same. Volatilization starts first in air, then without flux and in Helium and at last in Helium without cover, so it is happens at lower temperatures if it is preceded by a strong oxidation.

Table 2.2 Oxidation peak and initial volatilization temperature of PE 4 in different atmospheres.

Sample	Oxidation T (°C)	Volatilization T (°C)
PE 4 no flux	237.13	249.75
PE 4 in air	228.74	247.82
PE 4 in He	239.98	255.42
PE 4 no cover He	n.a.	246.39

2.1.4. Volatilization

As said before if the curve assumes an upward swinging trend, volatilization has taken place. In the test with air, sample loss was very little and not detectable, because the difference in sample weight from after and before was beyond balance's sensitivity. This is consistent with the curve in figure 2.9, in fact the oxidation peak had almost returned to baseline, thus only a very little sample volatilization had happened. On the contrary, in the test in helium without cover sample loss amounts to the 30 % of the initial mass.

In figure 2.10, a test is added to the previous in figure 2.9; it is without flow and without cover. In this case, the all air in the cell supports oxidation of the sample and the absence of the cover facilitates its dispersion, as happened for the test in Helium without cover. At the end of the test, the entire amount of sample (3.9 mg) has volatilized.

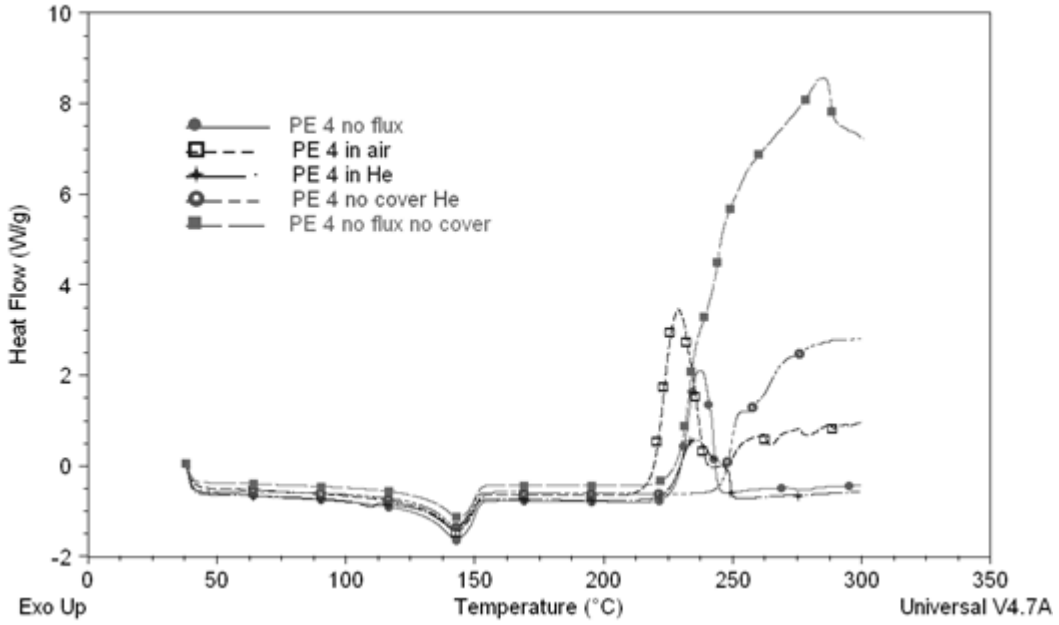

Figure 2.10 Heat flow in mW measured on PE 4 in air, without flux and in Helium with cover and in air and Helium without cover.

Sample volatilization is strongly enhanced without any cover, but is also related to oxidation; the deepest is the sample oxidized, the easiest it volatilizes. Moreover, the elimination of the cover, promotes volatilization, even apart from the oxidation, as shown in the test in Helium without cover; however, mass loss occurs at a slightly higher temperature if it is not preceded by an oxidation.

The DSC instrument, differently to TGA, is not able to detect the loss of sample mass and delivers the same heat flux of less plastic, so the analysis becomes distorted because sample emits more heat than the reference.

2.1.5. Sample weight

The sample weight influence is clearly observable, because it shifts the curve up and down when the sample mass is greater or lower. In figure 2.11 curves related to different amounts of sample (same PE 4) from 1 to 5 mg are compared. Reducing the sample weight, the heat flow difference between sample and reference lowers, so the curves shift downward or vice versa.

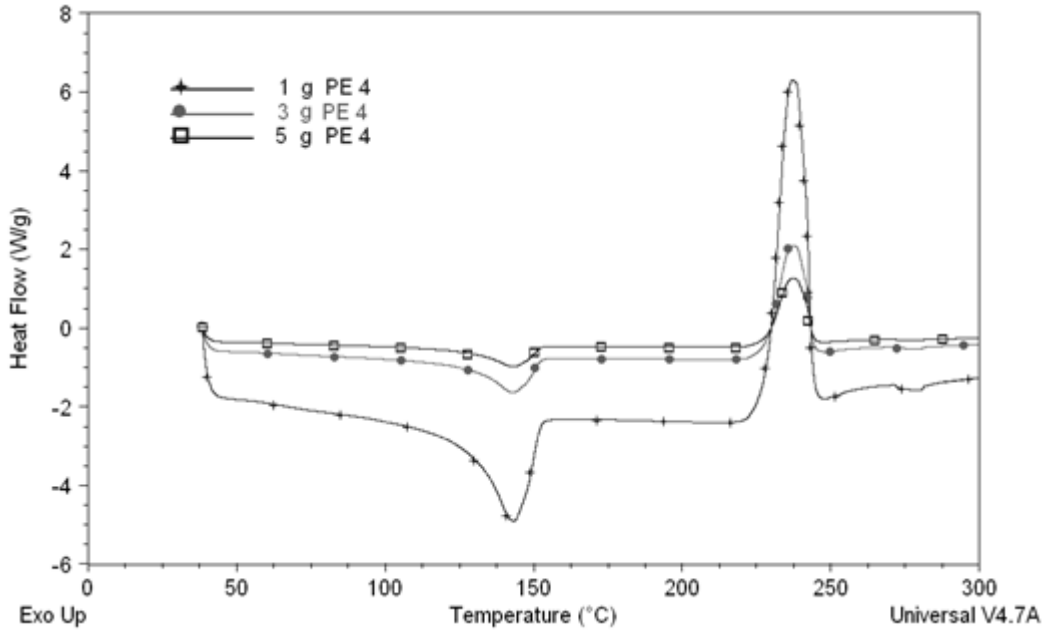

Figure 2.11 Different amounts of sample PE 4 heated to 300°C at 10°C/min without flux.

2.1.6. Reproducibility

Due to the fact that the Cp calculation depends on the baseline position that is determined by the initial slope of the curve, it shall remain the same repeating some the tests In conditions of clean and well calibrated cell, Indio shows a very good reproducibility (figure2.12) and also the replica of PE 4 (figure 2.13) has given good results, in fact enthalpy and fusion temperature has not shown any sensible change.

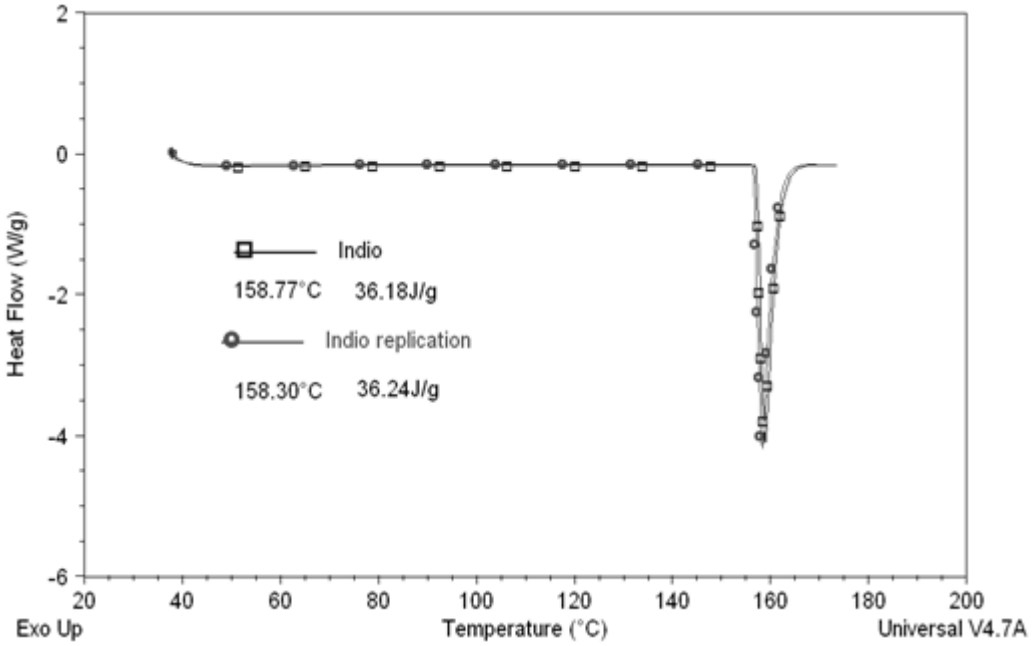

Figure 2.12 Indio's reproducibility.

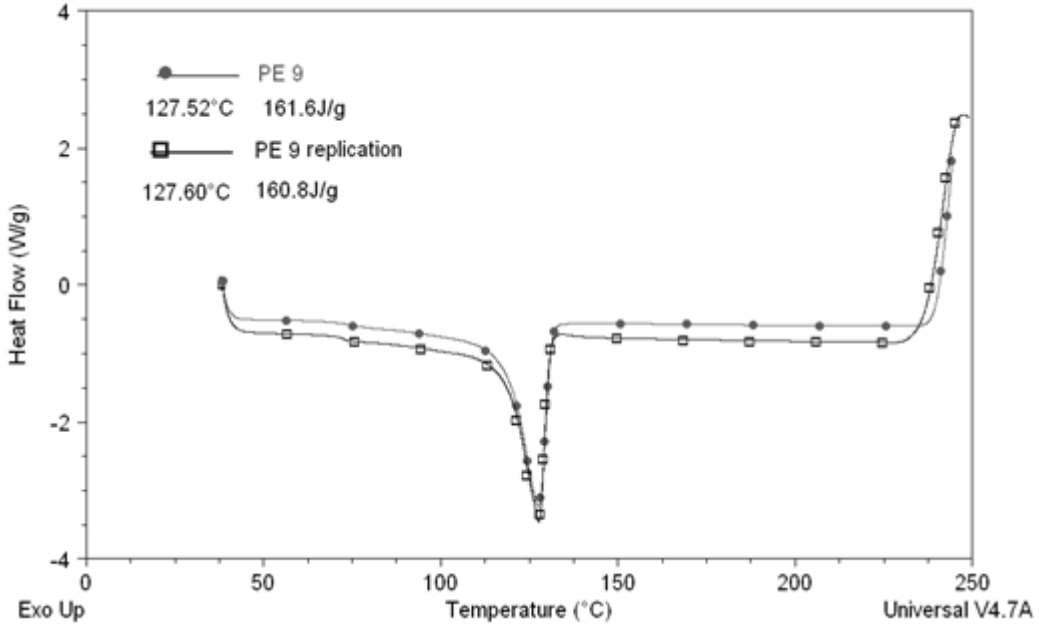

Figure 2.13 Reproduction of the test with PE4

However experimental inaccuracies cannot be completely eliminated cleaning or calibrating the cell, because the thermal diffusivities of calibration standards (i.e. Indium and Zinc), are much higher compared with that of polymers. Calibration is necessary in order to account for convective thermal resistance and to ensure that, during DSC, external surfaces of the aluminum pan are at the programmed temperature of the oven. Nevertheless, due to the very low thermal conductivity of polymer samples, the programmed temperature of the oven can be only partially representative of the actual temperature of the sample. So, results will always depend upon temperature gradients within the sample, scanning rate, sample mass and thickness (Greco et al., 2007).

On the contrary, initial test temperature shall have no influence on the analysis. With the DSC it is possible to choose an isothermal equilibration time before starting the test. The curves in figure 2.14 are obtained starting from the same amount of indium (7.2 mg), with a preliminary isothermal time equal to 2 or 40 minutes. The initial isotherm seems to have no influence on the curve itself, in fact, the two diagrams are identical.

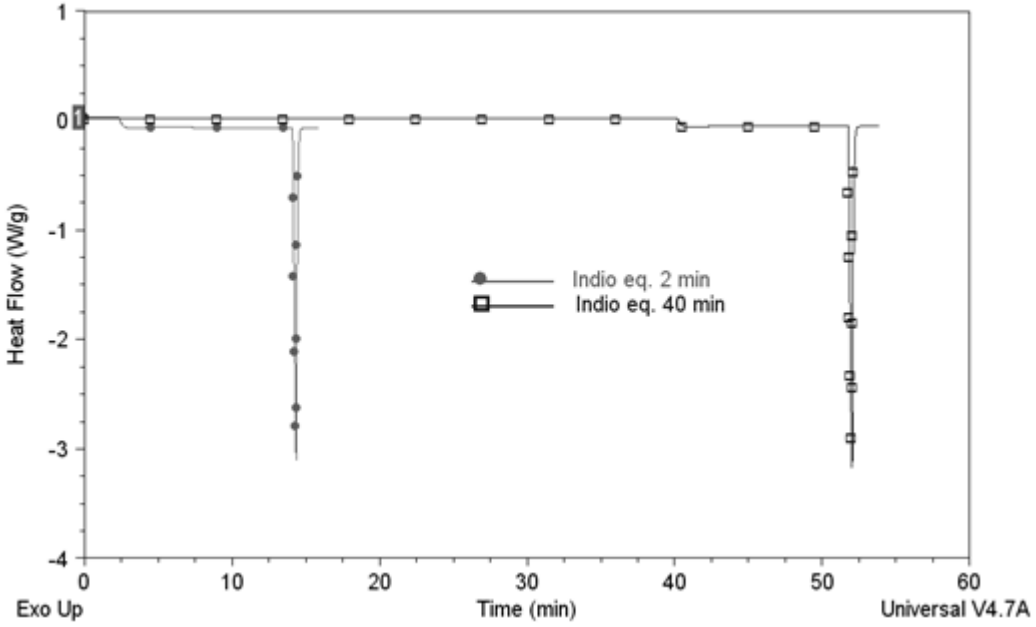

Figure 2.14 Indium fusion peak with an initial isothermal of 2 and 40 minutes versus time (left) and versus temperature (right).

Chapter 3
Preliminary degradation tests

Before proceeding with pyrolysis in a tubular reactor, some tests were made in a simple laboratory oven (figure 3.1), in order to evaluate plastic melting behaviour. The oven cannot guarantee a controlled atmosphere because it has a top opening of about 5 cm^2 that was closed with a little steel sheet but not perfectly sealed; so test were run in ambient air and stopped before any sort of degradation proceeds significantly.

Figure 3.1 Laboratory oven equipped with PID regulation.

Heating is provided by a PID temperature controller Eliwell EWPC907T that relies on an internal thermocouple placed in air as close as possible to the sample. The PID function allows minimizing the error between the measured temperature and the desired one by properly setting a group of parameters: *It* (Integral time), *dt* (Derivative time) and *Pb* (Proportional band). Tuning was performed by using a reading thermocouple placed nearby the regulation one that furnishes temperature continuous measurement. In figure 3.2 is reported the performance of the regulator before and after parameter settings. Temperature seems far more stable and close to the chosen set-point (150°C) even if it was not possible to eliminate the initial overshoot. Due to the quite considerable volume of the oven (about 400 litres) and its uncontrolled atmosphere, it is clear that the temperature inside it is not uniform, but regulation and control thermocouples are placed nearby the sample, so that its temperature is certain.

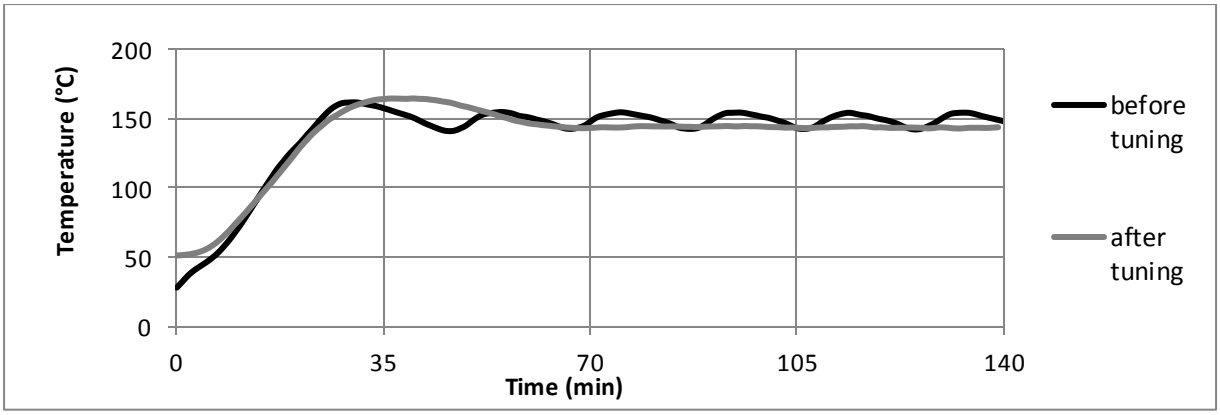

Figure 3.2 Regulation performance before and after tuning.

3.1. Thermal conductivity

It is well known that plastic has a very low thermal conductivity and this causes high energy requirements and the possibility of uneven temperature distribution. For these reasons, a good thermal conductor was added to plastic and the behaviour of the mixture was compared to the polymer alone.

The chosen conductor is the silicon carbide (SiC) that has an high sublimation temperature (approximately 2700°C), does not melt at any known pressure, has excellent corrosion and oxidation resistance, high mechanical strength at elevated temperature, low thermal expansion and high thermal shock resistance. So it can be considered chemically inert, moreover its thermal conductivity is 64.6 W/m K at 25°C, about 160 times the one of polyethylene, which is 0.4 W/m K at the same temperature.

Three couples of glass crucibles containing only PE (0.5 g) and a mixture of PE (0.5 g) and SiC (0.15g) were heated at about 5°C/min until 100, 150 and 200°C and then maintained in the oven for 30 minutes at each temperature. Samples' aspect after each temperature is presented in figure 3.3. Accordingly to the previous analysis in DSC, the melting temperature of this PE (classified as PE 9 in paragraph § 2.1) is about 123°C; so it is reasonable, that at 100°C no fusion has taken place. At higher temperatures (150-200°C) samples are clearly melted, but these with silicon carbide do shows any qualitative difference with the others, thus it seems that SiC does not have any effect in speeding the melting process.

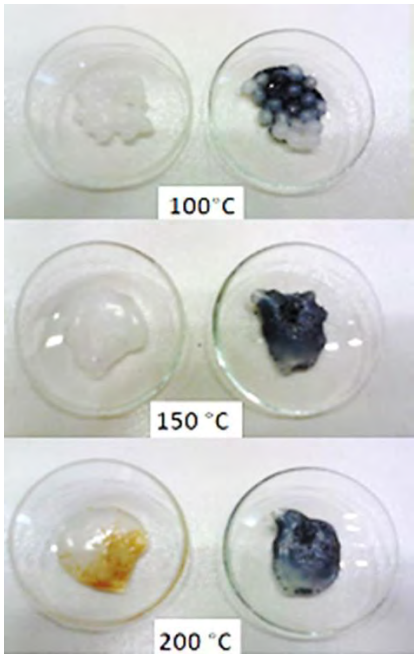

Figure 3.3 PE 9 (left) and PE 9 with SiC mixture (right) after 30 min at the indicated temperatures.

On the contrary, gas conversion seems to be clearly enhanced by the Silicon Carbide; in fact, sample weight losses are grater for these with SiC and increase at higher temperatures. In table 3.1 are reported sample mass losses for each temperature, evaluated on the initial grams of charged polyethylene.

Table 3.1 Sample mass losses at 100, 150, 200°C.

T (°C)	PE	PE and SiC
100	0%	8.68%
150	0%	8.84%
200	0.16%	10.00%

3.2. Fluidity

Fluidity is usually quantified through the Melt Flow Index and increases as melting proceeds. It seems useful to make some test to evaluate as much the sample can became fluid in order to better handle plastic in the reactor and possibly avoid clogging and leaks. Due to the fact that fluidity is the inverse of viscosity, they will certainly share a dependence with temperature and they will be influenced also by chemical transformations possibly taking place during heating (Lam et al., 2011).

Fluidity was studied by means of different shapes crucibles, rectangular or circular inclined on a support as shown in figure 3.4. The chosen polyethylene was classified in paragraph § 2.1 as PE 4 and it is the one that manifest the oxidation peak first, so it is the most easily degraded; it was also mixed with SiC in one of the two rectangular crucibles.

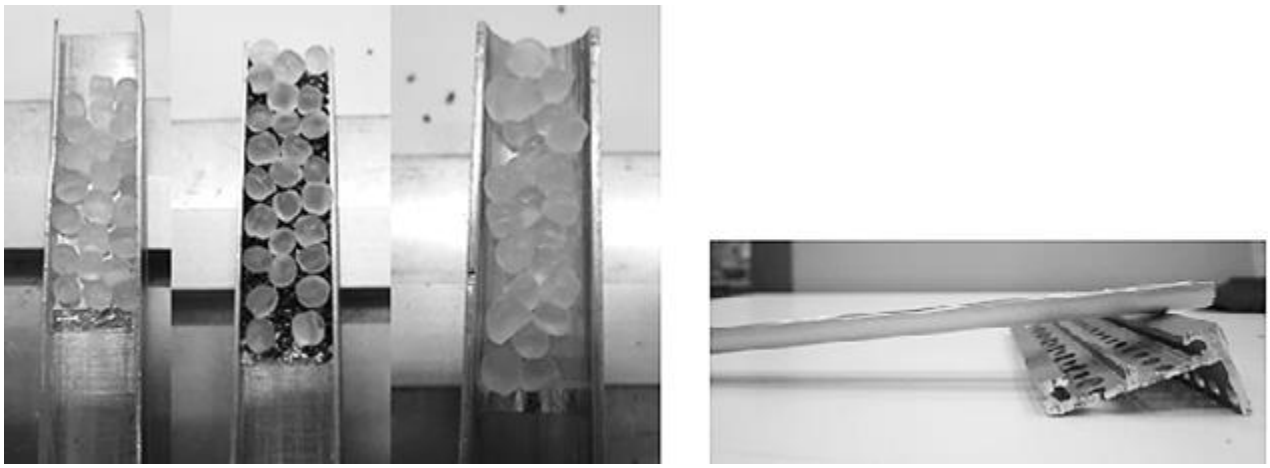

Figure 3.4 Rectangular and circular crucibles lying on a support.

Samples were inserted together in the preheated oven at 240°C and as plastic melts, it shall slide along the crucible accordingly to its fluidity. The inert reveals to be useless also in this case, because it hinders plastic sliding. The circular crucible proved to be the best solution, and in figure 3.5 a distinct plastic descent along the round crucible can be observed.

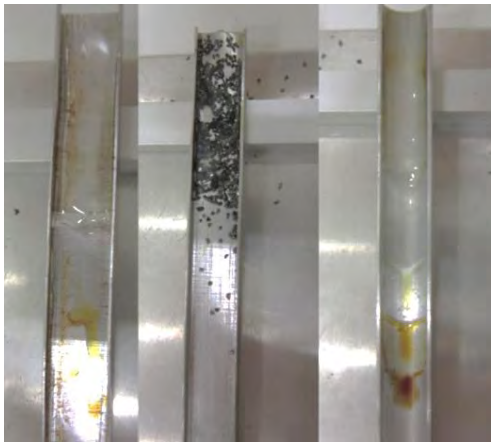

Figure 3.5 Melting behaviour in different crucibles at 240°C.

Using this last crucible, other tests have been carried out and plastic was kept at temperatures gradually higher for a fixed time interval (30 minutes) starting from 220°C that is the lowest temperature at which any sliding was manifested.

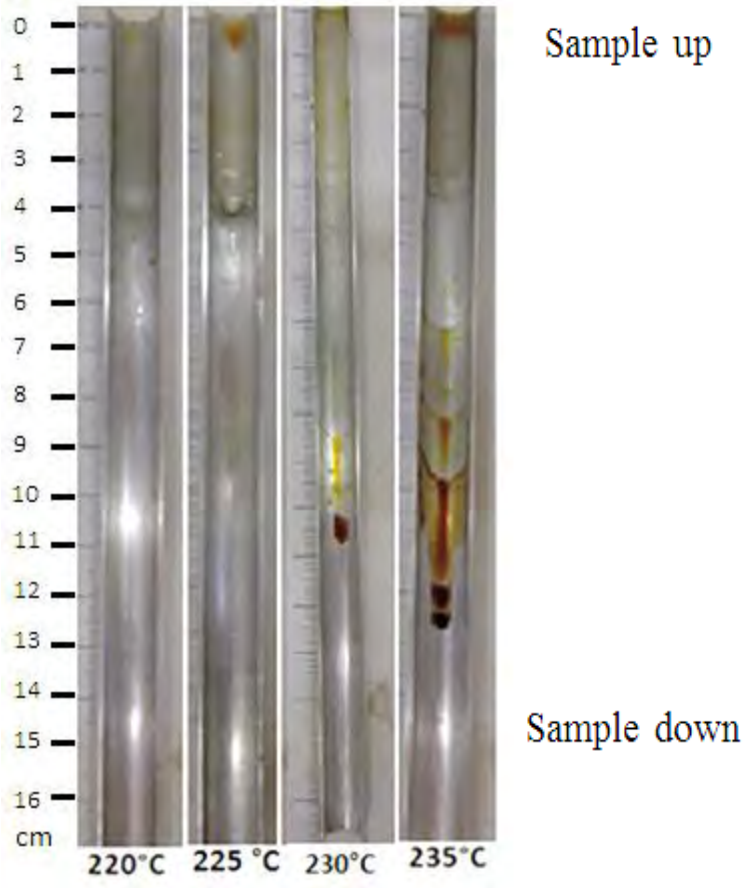

Figure 3.6 Sample's sliding along the crucible at different temperatures for a fixed time (30 min.).

From figure 3.6 it appears that at higher temperatures (235°C), sample slides for more centimetres along the crucible in the same time (30 min); so it flows faster, i.e. it has lower viscosity. It is also clear that the sample will reach the end of the crucible at any temperature but the time it needs is longer as the temperature is lower. Thus resistance to sliding (i.e. viscosity) is lower at higher

temperature, but no proportional trend could be found, since a concurrent oxidation influence has happened. It can be deduced from figure 3.6 that this reaction starts at 230°C, because the sample assumes a yellow-brown colour; oxidation can lead the polymer to reticulate and to become more refractory to slide.

Visually the products obtained in these tests are comparable to a pyrolysis wax, because they're viscous, sticky and yellow-brown coloured. To verify this assumption, two samples, taken from the upper (sample up) and the lower (sample down) part of the crucibles were analysed with the DSC instrument and results are reported in figure 3.7. Test were run in Helium (70 ml/min) or air (40ml/min) atmosphere without sample holder cover starting from ambient temperature till 300°C, with an heating rate of 10°C/min.

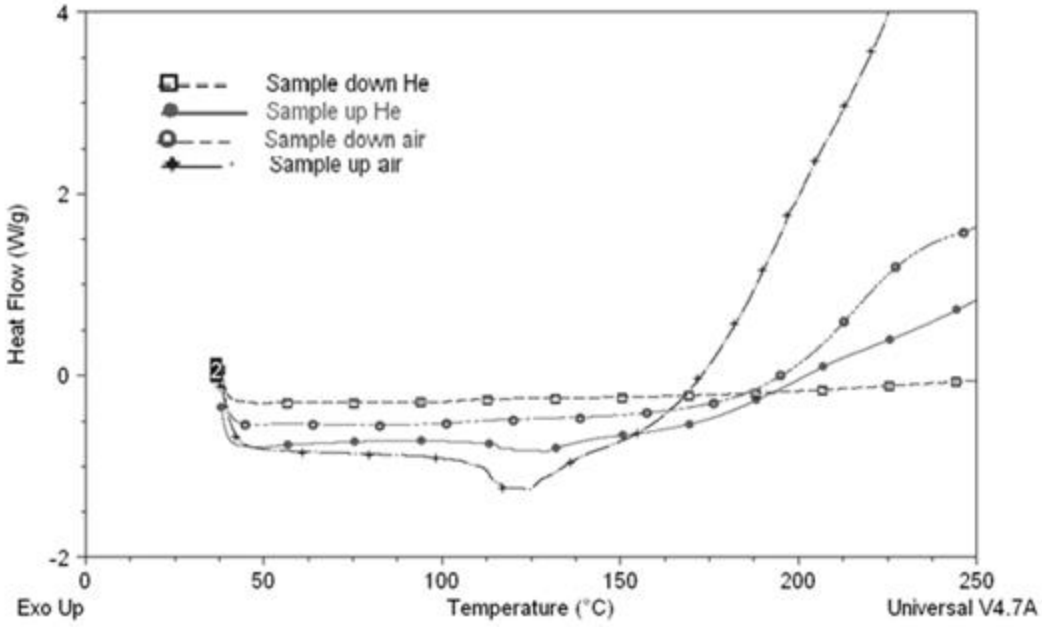

Figure 3.7 DSC curves of samples from upper and lower part of the crucibles in inert (He) or oxidizing (air) atmosphere.

A wax-like compound shall manifest a broad and undefined fusion peak, due to its very variegated composition. This is evident in the curves referred to the 'sample up' in both atmospheres, even in it is clearer in the air's one. On the contrary, 'sample down' does not show any fusion peak, because the curves remain fairly straight; only in air atmosphere it shows a moderate oxidation above 200°C.

Sample 'up' is certainly more volatile, because it is subjected to a marked evaporation above 160°C promoted by the presence of air and to a subsequent degradation; in Helium this phenomenon is a little inhibited, but not eliminated. As a consequence, weight losses are much more significant for 'sample up', as it is clear from table 3.2, where weight losses during the DSC test are reported. 'Sample down' has a higher resistance to volatilize and this is probably due to the fact that it has already undergone in the oven to a more extended degradation.

Table 3.2 Weight losses of the oven samples in the DSC in different atmospheres.

SAMPLE	ATMOSPHERE	% MASS LOST
up	He	30%
down	He	29%
up	air	54%
down	air	37%

3.3. Morphological characterization

Plastic behaviour during initial heating was investigated also from a morphological point of view, i.e. the same polyethylene used in paragraph § 3.2 (PE 4) was put in a Pyrex test tube and heated in the oven. So melting and bubble formation could be observed with respect to temperature and atmosphere.

Experiment set up is illustrated in figure 3.8: the test tube holds about 0.7 g of polyethylene and in its upper part are inserted two thermocouples (a reading and a controlling one) and a metallic pipe. The reading thermocouple is immersed in the sample and the heating rate is set to 5°C/min. With respect to the experiments described in paragraph § 3.1, the thermal control is clearly improved, because it was possible to place the control thermocouple inside the sample and not in air above the crucible. The pipe can eventually provide a flow of inert gas (nitrogen) to keep the atmosphere controlled, so the same test was run in nitrogen atmosphere (30ml/min) and in ambient air.

Figure 3.8 Test tube placed in the oven holding polyethylene in oxidizing atmosphere (left) and inert (right).

Melting occurs at about 170°C, as it is visualized in the figure 3.9 for both inert and air atmosphere; until this point no qualitative differences between the two samples are detectable. Melting temperature is higher than the one detected by DSC in paragraph § 2.1 (146°C), because heat transfer and insulation are not optimized as inside the DSC cell.

Figure 3.9 Melting of polyethylene samples at 170°C in oxidizing atmosphere (left) and inert (right).

At 220°C, the sample exhibits a moderate yellowing (figure 3.10), which is less evident under nitrogen flux; thus it is proven that yellowing is a symptom of oxidation, because it is inhibited in the inert atmosphere, even if the test tube is not completely hermetic. Throughout the sample mass some bubbles can be seen, these are formed by the gas trapped between sample particles during melting.

Figure 3.10 Melting of polyethylene samples at 220°C in oxidizing atmosphere (left) and inert (right).

After other 20 minutes of permanence at 220°C, oxidation had proceeded in air atmosphere, as it is clear from the increased yellowing in figure 3.11. It can also be noticed an increase in the gas bubble volume inside the sample viscous mass which is caused by degradation taking place. Due to the fact that the sample is maintained at the same temperature, the enlargement of these bubbles cannot be attributed to expansion of the gas already present in interstices between plastic granules.

Figure 3.11 Polyethylene samples after 20 minutes at 220°C in oxidizing atmosphere (left) and inert (right).

In order to favour a more homogenous melting and to avoid the trapping of gas bubbles, the same technique of the tilted crucible is adopted for the Pyrex tube: a larger one is placed inside the oven, inclined so that the liquefied plastic can flow toward the bottom (figure 3.12). Sample quantity is a little higher (1.8 g) and a metallic pipe is used to guarantee a 30 ml/min of flux inert gas (Argon) in one of the two tests. The flow is deliberately low to favour the gas recirculation inside the sample holder.

Figure 3.12Polyethylene sample in inclined test tube.

Plastic, after being subjected to a temperature of 180°C for 60 minutes looks like in figure 3.13; as for the last test, the yellowing in the left photo, where no inert was used, is due to oxidation.

Figure 3.13 Polyethylene samples after 40 minutes at 180°C in oxidizing atmosphere (left) and inert (right).

In controlled atmosphere, even raising the temperature and enhancing the residence time in the oven, oxidation does not appear, as proved by figure 3.14, which represents polyethylene after 160 minutes of permanence at 240°C in 70 ml/min of Argon flow.

Figure 3.14 Polyethylene after 160 minutes at 240°C in 70 ml/min of Argon flux.

Among all the tests performed with the test tube, only in this very long one sample weight losses have been detected and amount on 3.5% of the initial sample mass.

Other attempts to characterize pyrolysis stages through image analysis were carried out by Wang et al., 2012. They heated 10 grams of PE under nitrogen atmosphere from 20°C to 600°C in 40 minutes taking an image every 40 seconds. Experiments showed that pyrolysis involved four stages: melting, two stages of decomposition and ash deposition (figure 3.15). Decomposition and melting stages are the key step of pyrolysis since they take up half or more of the total time.

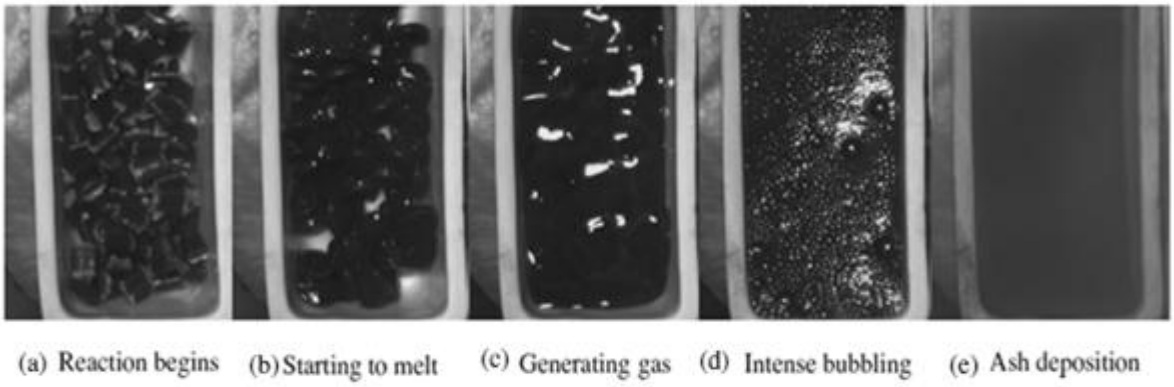

Figure 3.15 Morphological changes during pyrolysis of PE granules (Wang et al., 2012).

Two morphological signals were investigated: polyethylene area (PA) on the total pixels of the picture and bubble ratio (BR) that is the area of the bubbles on the total pixels of the figure. The bubble formation is due to the trapping of gas in the liquefying mass during melting and to volatile evaporation during degradation. The trends of the two parameters and their changes during pyrolysis stages are illustrated in figure 3.16 with respect to image sequence. Melting began at about 170°C, meanwhile interstices between granules were disappearing so PA was increasing and BR was decreasing. This reaction was completed at 300°C (corresponding to image sequence 30) when PA and BR reached it maximum and minimum value, respectively. Thereafter started the first stage of decomposition, which was characterized by volatile evaporating and BR sharp increase; the second stage began after BR drop and brought it to a second peak value, lower than the first. As ash deposition happened, the BR dropped to zero or very low values.

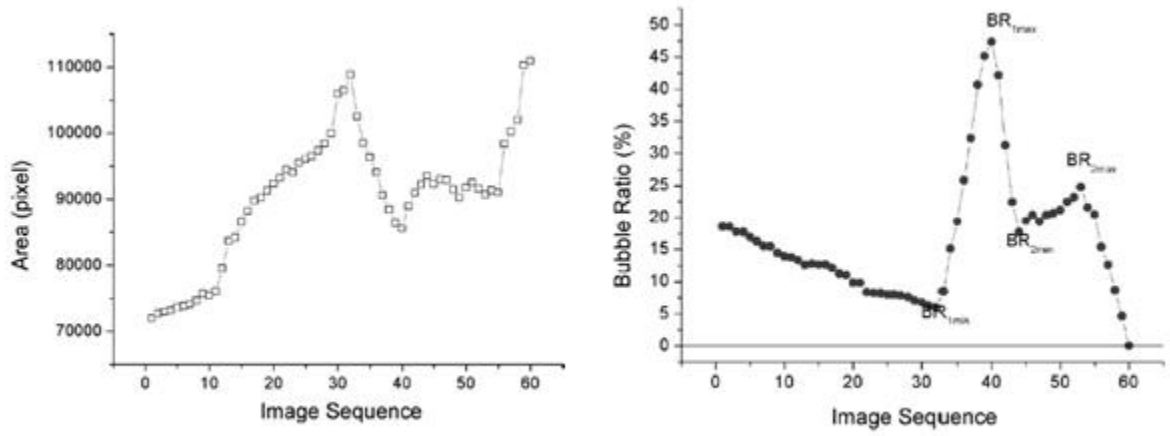

Figure 3.16 Morphological signals Plastic Area (left) and Bubble ratio (right) of PE pyrolysis versus image sequence (Wang et al., 2012).

BR is strongly correlated with temperature and time: it provided a precise signal for process characterization. On the other hand, PA only gives the extremes of melting, because no distinct change in its trend happened with first and second decomposition stages. Only ash deposition causes an upper switch to the curve.

3.4. Summary

It can be concluded that the SiC is not so useful in the initial melting stage, that is the most critical to guarantee a complete sample degradation. The fact that it can enhance gas conversion is of little interest, because the main aim of this thesis work is to produce oils, so its use was abandoned.

The observation of bubble formation in the melted mass is of great importance not only to characterize pyrolysis steps, but also to acquire a good control of the process in order to ensure a homogeneous melting. Besides this reaction, also oxidation or degradation and volatilization shall be understood to choose the heating policy, which better fits to the sample

Chapter 4
Tars

The term tar is referred to each hydrocarbon with a molecular weight greater than benzene (Abatzglou et al., 1999). This definition was agreed during the redaction works of the Wurzburg protocol (Brussels, 1998), which was an attempt to standardize tar sampling and analysis methods. Its focus was specifically directed on tars originated from biomasses, but it is still interesting considering that no analogue protocol was developed for tars originated from plastic pyrolysis.

4.1. Properties

In the pyrolysis process tars' quality is crucial for its future use as a fuel, as discussed in first chapter. On the contrary in biomass gasification tars are considered as organic contaminants in the flue gas, because they can condense and damage engines when temperature lowers. Once the gas becomes over saturated, they can lead to fouling, aerosol formation and depositions inside the installation. These fouling phenomena don't take place as long as all tars stay in the gas phase, therefore the concern disregards the tars' quantity, but focuses on their properties and composition. So a great effort is made in both sectors in order to get a satisfactory characterization and/or quantification. The main parameters considered in this work are heating value, dew point, boiling point and viscosity.

4.1.1. Dew point

In both pyrolysis and gasification, the tar dew point is a very important parameter to evaluate the performance of the condensation trap or the gas cleaning system. Due to the fact that tar is a complex mixture of condensable hydrocarbons, which includes single ring to five rings aromatic compounds along with complex polycyclic aromatic hydrocarbon (PAH), their properties are easier analysed by classes. Moreover tars originated from biomasses will have oxygen-containing hydrocarbons, phenols and alcohols. In table 4.1 are listed compounds which are expected in five different tars classes.

Table 4.1 Biomass tar compounds in five different tar classes (Li et al., 2008).

Tar class	Class name	Property	Representative compounds
1	GC-undetectable	Very heavy tars, cannot be detected by GC	Determined by subtracting the GC-detectable tar fraction from the total gravimetric tar
2	Heterocyclic aromatics	Tars containing hetero atoms; highly water soluble compounds	Pyridine, phenol, cresols, quinoline, isoquinoline, dibenzophenol
3	Light aromatic (1 ring)	Usually light hydrocarbons with single ring; do not pose a problem regarding condensability and solubility	Toluene, ethylbenzene, xylenes, styrene
4	Light PAH compounds (2–3 rings)	2 and 3 rings compounds; condense at low temperature even at very low concentration	Indene, naphthalene, methylnaphthalene, biphenyl, acenaphthalene, fluorene, phenanthrene, anthracene
5	Heavy PAH compounds (4–7 rings)	Larger than 3-ring, these components condense at high-temperatures at low concentrations	Fluoranthene, pyrene, chrysene, perylene, coronene

As the temperature of the gas drops below the dew point, the tars will either directly condense or form aerosols. However, even at temperatures well below the boiling point a certain amount of each component will remain in the vaporous phase, as long as temperature does not decrease further. When the vapour pressure exceeds the saturation pressure, the gas becomes over saturated according Raoult's Law and this leads to condensation of the saturated vapour. So the tar dew point is the temperature at which the partial pressure equals the saturation pressure and it is determined by the vapour pressure of each component. Condensation curves were deduced with a calculation tool (Li et al., 2008) and are reported for the five tar classes in figure 4.1; each tar component contributes to the total concentration on mass basis.

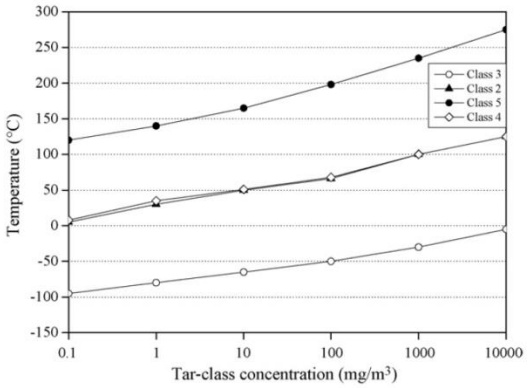

Figure 4.1 Dew point of the different tar classes in relation to concentration (Li et al., 2008).

The dew point calculation excludes tar class 1, as the components are not known, but it is believed that these start to condense already at 300-350°C, quickly followed by class 5, which, even for very low concentrations (e.g. <1 mg/m^3), has a dew point above 100°C. In an energy production plant, classes 2 and 4 will create the heaviest problem, because will condense at room temperature, so they need to be partially removed. On the contrary class 3 won't condense at concentration as high as 10,000 mg/m^3, and play an unimportant role in this matter. With respect to single aromatic specie, in figure 4.2, the saturation concentration of some hydrocarbons is plotted over temperature for an ideal mixture with nitrogen.

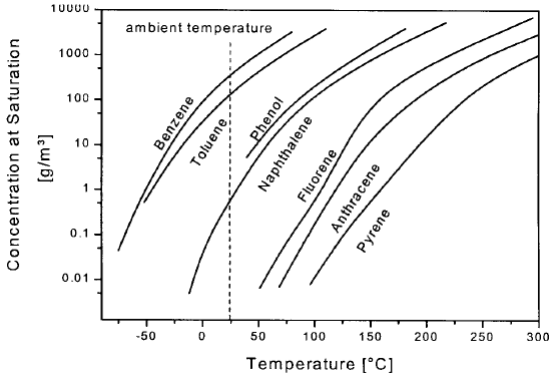

Figure 4.2 Saturation concentration of aromatics in system with nitrogen (Moersch et al., 1999).

It is clear that even at room temperature, benzene and toluene will not cause any problems due to condensation in a gasifier, since they show saturation concentrations of about 100 g/m^3 and their concentration in the gas is at least one order of magnitude lower. For higher aromatics (e.g. fluorene) saturation concentration is of a few mg/m^3, hence, almost complete condensation of these compounds has to be expected. Naphthalene and phenol are in between with a saturation concentration of about 0.5 mg/m^3 at 25°C.

4.1.2. Boiling point

The boiling point of a substance is the temperature at which the vapour pressure of the liquid equals the pressure surrounding the liquid and it changes into a vapour. Boiling points of traditional fuels were investigated (Lam et al., 2011) in order to compare a microwave pyrolysis oil with the original waste automotive engine oil. From figure 4.3, where are plotted simulated distillation curves, it can be seen that pyrolysis was useful for the waste oil, shifting its boiling point closer to these of traditional fuels and that pyrolysis oil contains components that have a lower boiling point range than diesel, but higher than gasoline.

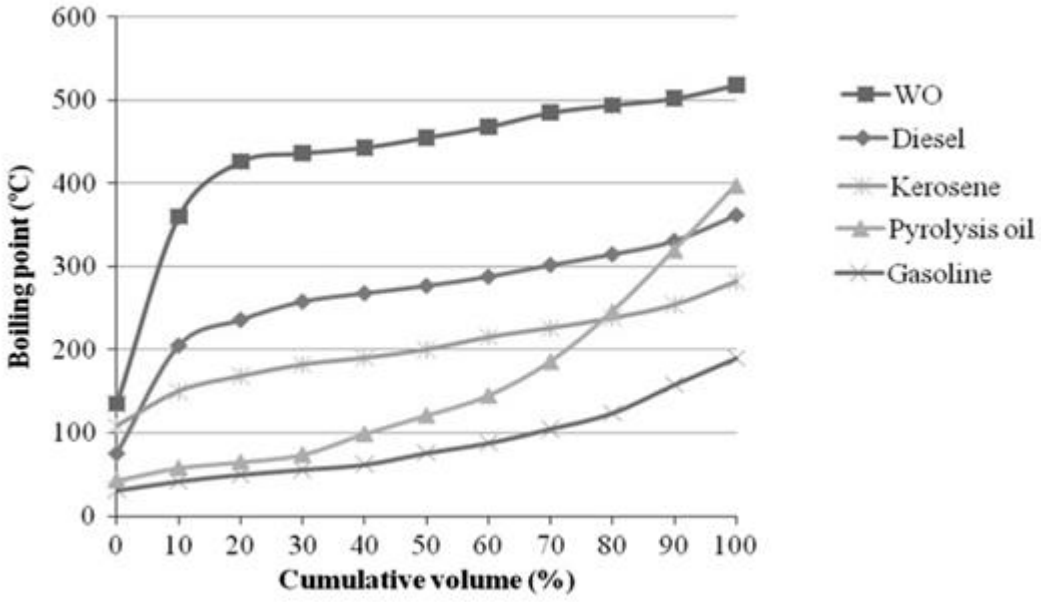

Figure 4.3 Simulated distillation for pyrolysis oil, waste oil and commercial fuels (Lam et al, 2011).

4.1.3. Calorific value

The calorific value indicates the gross energy output of combustion in the engine chamber and it can be quantified using a bomb calorimeter. High energy oils can be obtained by pyrolysis (Lam et al, 2011): the calorific value of a pyrolized oil (46‑47 MJ/kg), is higher than the one of the original waste oil and close to that of traditional liquid fuels derived from fossil fuel (43‑48 MJ/kg). So it was proven that the oxygen content and H/C ratio are inversely proportional to the heating value, in fact the waste oil matrix presented long-chain carbon compounds.

4.1.4. Viscosity

Viscosity is an effective parameter for oils characterization, especially lubricants, and it is determined by means of viscometers (e.g. capillary Brookfield or Hopper). Fluidity is the inverse of viscosity; it is quantified through the Melt Flow Index, which is used to select the most adapt machining process for a material. It is also an oil quality parameter, because if it is constant throughout time, is symptomatic of oil stability. Lam et al. checked the pyrolysis oil viscosity over a time period of 9 months and it showed negligible change, thus it exhibit good stability features.

Table 4.2 Viscosity of pyrolysis oil over time in mm^2/s (Lam et al., 2011).

3 months	6 months	9 months
6.4	6.5	6.5

Lam's pyrolysis oil possess higher kinematic viscosities than diesel (2–4 mm^2/s) and gasoline (0.7 mm^2/s); so further treatment were needed since a lower viscosity is desirable and represents a favourable feature when it comes to handling and transportation.

It is well known that viscosity is influenced by temperature, but it is also demonstrated that depends on oxidation and it increases with it. Oil oxidation normally results in the sequential addition of oxygen to base oil molecules, causing the formation of oxygenated by-products with hydroxyl (O-H) and carbonyl groups (C=O), e.g. aldehydes and carboxylic acids. Carboxylic acids, in particular, are undesirable as they are the common cause of acidic corrosion and sludge formation (as a result of polymerisation in which carboxylic acids combine to form larger molecular species), which can lead to increased oil viscosity and cause problems such as filter plugging and system fouling.

Very little oil oxidation can occur in the pyrolysis process, eventually the use of a carbon bed can be beneficial acting as a reducing environment.

The densities of the pyrolysis oils (757–773 kg/m^3), are quite close to that for gasoline, and it is also within the prescribed range of 720-775 kg/m^3 given in British Standard of Unleaded Petrol (Lam et al., 2011).

Another feature that shall be considered is particle content, which can lead to coke formation in the steam cracker, but it can be easily removed by filtration. This is also a measurement technique, because a 0.1 μm polycarbonate membrane filter can hold particles, which can then be weighted.

4.2. Analysis

Generally tar sampling is performed by methods based on cold trapping on cold surfaces, filters or impinger trains with a solvent, by absorption in a cold organic solvent or by adsorption on a suitable sorbents. The subsequent analysis is most often performed by gas chromatography (GC) or gravimetrically (by weighing the collected tars, after careful evaporation of the solvent and condensed water).

4.2.1. The European Protocol

Recently, on-line methods have been developed, such as the European tar protocol, which was developed in Brussels. This guideline provides a series of steps for the measurement of organic contaminants and particles in producer gases from biomass gasifiers. The procedure includes gas preconditioning, particle filter, tar collection in isopropanol, volume metering, and finally GC analysis, as it is shown in figure 4.4.

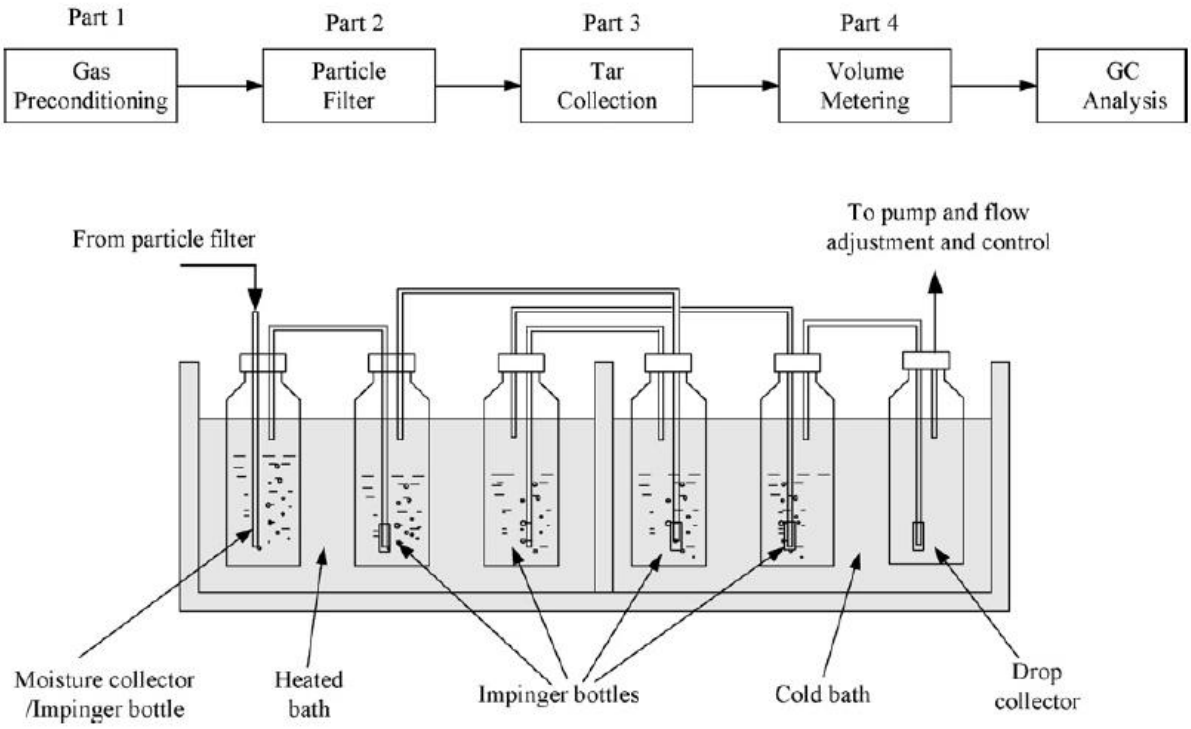

Figure 4.4 Tar collection procedure (Li et al., 2008).

Collection of tar is performed in a series of 6 impinger bottle, where the first acts as moisture collector, in which water is absorbed in isopropanol, then the gas is passed through a series of other 4 impingers with solvent and an empty one. Solvent is necessary, because the direct condensation of the liquid effluent without diluting media, can result in further reaction of the trapped compounds. The heat released by gas cooling and condensation is removed either in an external water bath or through a liquid quench system of isopropanol. Cooling fluid and cooling temperature can be selected arbitrarily.

As the protocol says, the gas chromatograph is the core of the analysis apparatus and shall be fitted with a capillary column, a flame ionization detector and a data processing system. The stationary phase of the capillary column should be bonded poly(5%diphenyl/ 95%dimethyl)siloxane, the internal diameter of 0.25–0.32 mm and the length of 30–60 m.

The typical gas chromatograph parameters are:

- injector: split, 1:75;
- injector temperature: 275°C;
- detector temperature: 300°C;
- injection volume: 1–2 ml;
- carrier gas: hydrogen or helium;
- column pressure adjusted so that the linear velocity of H_2 He are 30–55 cm/s and 20–40 cm/s, respectively;
- column temperature program: 50°C for 5 min, up to 325°C at 8°C/min and stop for 5 min.

4.2.2. Other methods

Notwithstanding the common protocol, other methods had been developed to analyse tars. The one set by Moersch et al. is based on the difference between the total content of hydrocarbons in the gas and the remaining concentration after condensation; so two subsequent measures are taken with the gas chromatograph, as it is illustrated in figure 4.5.

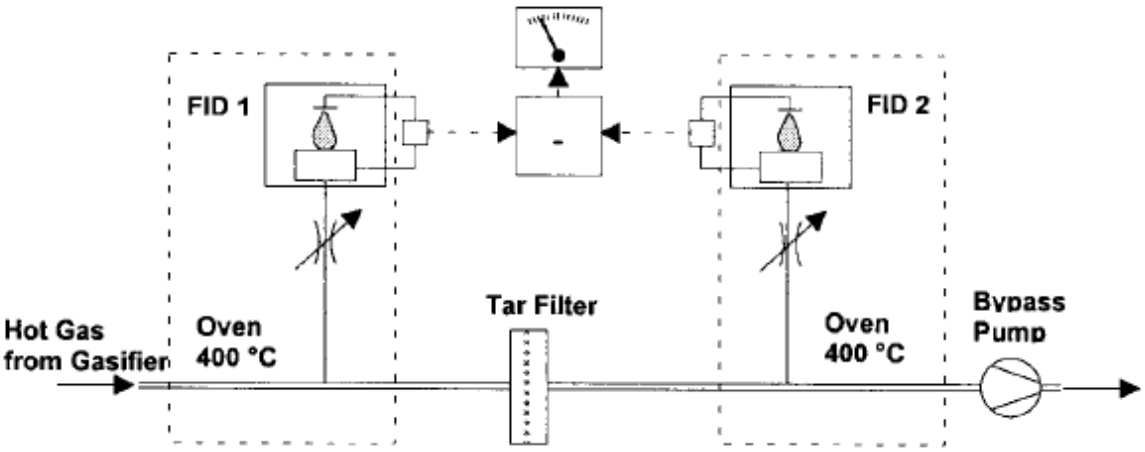

Figure 4.5 Basic principle of the tar measurement system (Moersch et al., 1999).

For the determination of the hydrocarbon content a flame ionization detector (FID) is well suited, since it has a high sensitivity and linearity. Further, the signal is for most of the typical

tar components with sufficient accuracy directly proportional to the mass of organic carbon in the sample and each tar component can be classified and characterized.

The second measurement is performed to determine the amount of non-condensable hydrocarbons, so the system registers as tars only those components that are retained by the filter. To be on the safe side, the filter temperature should, therefore, be chosen below the lowest temperature in the process.

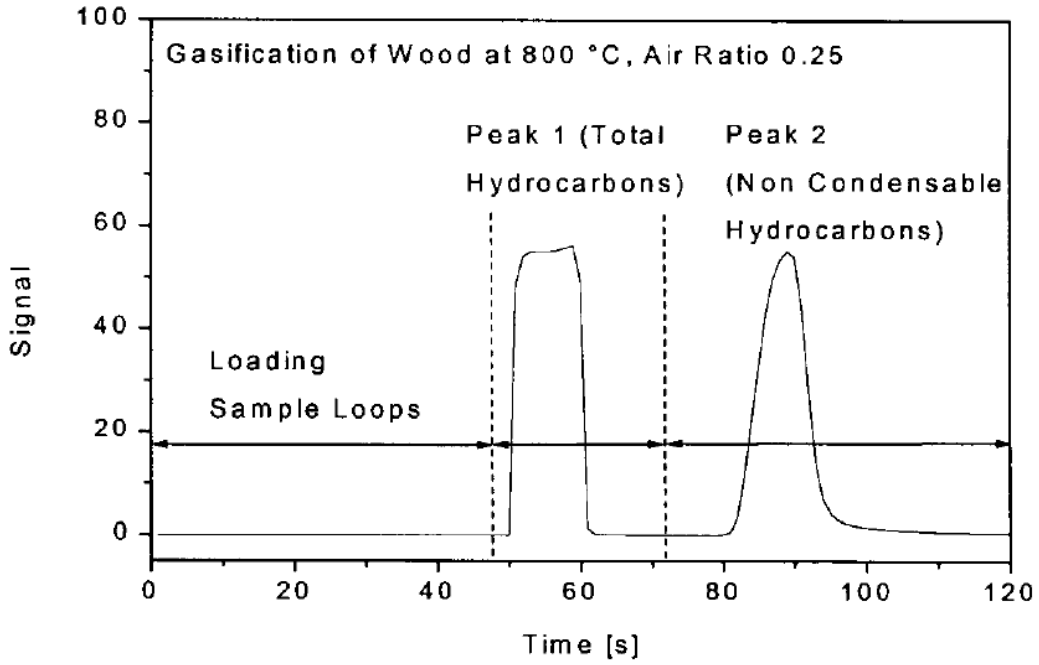

Figure 4.6 FID-signal during analysis cycle (Moersch et al., 1999).

The major difficulties that hinder the application of this principle are that for low tar contents, the difference of the two measurements is very small compared to their absolute value and possible fluctuations of the gas composition require analysing exactly contemporaneously.

Chapter 5
Instruments

5.1. Gas chromatography

Gas chromatography allows analysing gaseous or liquid samples and it is based on the peculiar distribution of a substance between a stationary and a mobile phase, as a function of its affinity to each one.

The mobile phase is a carrier gas, which shall be chemically inert, low viscous and highly pure (99.9%), such as nitrogen, helium or argon. The stationary phase is generally made from a non-volatile liquid, supported on a powder, which uniformly fills a column (packed column), or distributed as a thin film on the inner wall of a column (capillary column). Stationary phases differ in the first place for polarity, so substances which have a polarity similar to the stationary phase will be longer retained in the column.

In figure 5.1 it is schematically illustrated the operating principle of a gas chromatograph. Liquid samples can be injected with a syringe and vaporized above the injector and gaseous samples are typically introduced on the top of the column by a sampling valve pneumatically operating; after that they have been eluted from column, they are collected by two detectors, which are distinguished as front detector (FID) and back detector (TCD). The TCD is made by a filament, which varies its conductivity if alternately exposed to the carrier or to a transported mixture. On the contrary, the FID is based on the ionization changes of a chemical species exposed to a hydrogen flame.

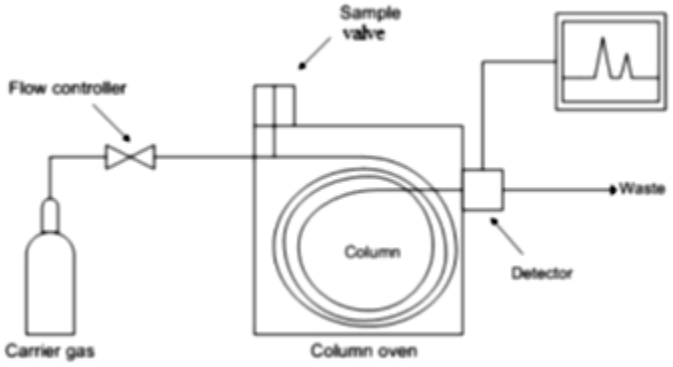

Figure 5.1 Gas Chromatograph main principle.

Detectors produce a continuous signal, which varies when a substance, different from the carrier is passing through them and peaks will be as many as compounds in the mixture.

The chromatogram displays signals of both detectors as a function of time and can furnish information on both the identity of the substance on the basis of its elution time and on its mass concentration integrating the area under the peak.

Optimizing chromatographic analysis means improving separation of substances in order to obtain distinct and well-resolved peaks. It is possible to vary a set of variables such as oven temperature, heating rate, pressure, duration of the analysis and carrier flow and type. Temperature is a very important variable to improve separation which can be kept constant or varied according to a temperature program.

The instrument used in this work is a Gas Chromatograph – Hewlett Packard 6890 (figure 5.2), controlled through the software Agilent Chemstation, equipped with a Porapack Q 80/100 packed column and crossed by a constant flow of Helium.

Figure 5.2 Gas chromatograph Hewlett Packard 6890.

Packed colums are well suited to separate hydrocarbons and specifications of this specific one are reported in table 5.1.

Table 5.1 Packed column's characteristics.

Porapack Q 80/100		
Lenght	30	m
Particle dimension	80-100	mesh
Superficial area	550	m^2/g
Density	0,34	g/ml
Maximum temperature	250	°C

The method utilized in order to analyse the produced gas was evolved starting from a series of preliminary trails in order to clearly separate peaks and to ensure that all the gases have been eluted from the column.

5.2. Mass spectrometry

This analytical technique is applied to identification of compounds or to the analysis of trace substances and it is commonly coupled to gas chromatography. The gas chromatograph allows separating the various substances, as explained in paragraph § 5.1, and the mass spectrometer furnishes a spectrum, which is unique for each compound.

The mass spectrometer distinguishes ions on the bases of their mass/charge ratio: the mixture is passed through a beam of electrons with known energy so that the ionized molecules will fragment into smaller ions, according to their chemical structure. Separated ions will reach a detector where the energy received is converted in suitably amplified electrical signal to produce a mass spectrum.

The most common ionization technique is the electronic impact, where a tungsten filament emits a beam of accelerated electrons, which transmits their energy to the molecules causing their deep fragmentation. The detector is capable to separate ions on the basis of their mass/charge (m/z) ratio and it often uses a quadrupole, which is a squared space crossed by magnetic static and dynamic fields. It forces ions along sinusoidal trajectories so that these will fragment instead to go straight the detector and this allows scanning the entire range of the corresponding masses (figure 5.3).

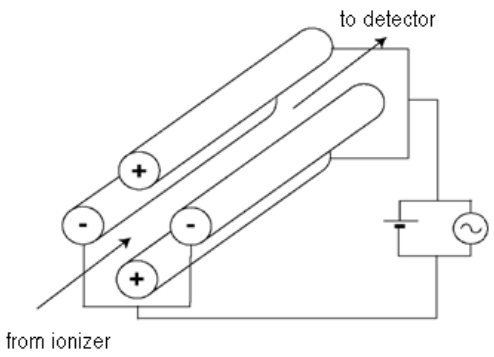

Figure 5.3 Quadrupole main principle.

Detectors are able to amplify the weak current produced by ions and signals are transmitted to a computer, which plots the abundance of each ion versus its mass, as a function of the greatest one (base peak) and finally identify a compound according to its spectrum. The parent peak, instead, is usually the lowest and corresponds to the ionized molecule, so it is useful to determine its molecular weight.

Generally, the more stable a molecular ion is, the higher is its probability of reaching intact to the detector; the compound, after having lost an electron, becomes a radical-ion which decomposes into other radicals and ions.

$$M \longrightarrow M^{+\bullet} + e^{-}$$

The first, being neutral, are not detectable, but their mass can be deduced from the difference between the molecular weight of the parent peak and its fragments.

The mass spectrometer used in this thesis work is a Carlo Erba Instruments (figure 5.4) and it is controlled through the software Mass-Lab, which allow choosing the mass range to analyse and to set the time of the test. It is also possible to calibrate the instrument with a reference gas hold in an ampoule and released when necessary. Detector sensibility is focused on four reference masses (69,

131, 264, 502), which comprehend the whole range to analyse and the clarity of the referring signal shall be optimized through a series of parameters.

Figure 5.4 GC-MS by Carlo Erba Instruments.

The gas chromatograph is equipped with a capillary column of the series Restek-Rtx, which is specific to solvents, pesticides, heavy hydrocarbons or PCBs and the analysis conditions such as carrier gas pressure, oven temperature and sample split are set by an analogue control.

Table 5.2 Capillary column's characteristics.

Restek Rtx- 5MS		
Lenght	30	m
ID	0,25	mm
DF	0,25	µm
Stationary phase	5% 95%	Diphenilpolysiloxane Dimethylpolisiloxane
Max temperature	380	°C

A pump guarantees the vacuum conditions necessary to eliminate any molecules of atmospheric gas, which may interfere with the ions bringing the signal/noise ratio to values lower than 100.

Few microliters of sample are introduced into the injector through a liner and are vaporized at 250°C; after being eluted from column, they will enter the mass spectrometer. The out coming chromatogram and the relative spectra are elaborated with the software Mass-Link.

Chapter 6
Experimental apparatus

The main constituents of the experimental installation are a heated tubular reactor and a water-cooling condenser; the auxiliary heating apparatus was composed of two nozzle heaters and a tubular resistance.

6.1. Reactor

6.1.1. Kettle-type reactor

The first configuration tested in order to carry on pyrolysis experiments, was a kettle-type one, which is characterized by input and output of the gases at the same level, on the upper cover of the reactor (figure 6.1). It was constituted by a steel cylinder with a threaded hole in the bottom and a screw cap with two possible gas ways and a slot for the control thermocouple. The threaded hole in the bottom was of no use in this case, so it was close with a screw. The screw cap shall be sealed by a graphite gasket, which is able to bear the quite high temperatures needed for the pyrolysis tests without run into melting or deterioration. This cap was then substituted by a flat one, to improve sealing (figure 6.1). The cylinder is 100 mm high and its internal and external diameters are 45 and 60 mm, respectively.

Figure 6.1 Kettle-type reactor with screw (left) cap, flat cap and inner configuration (right).

Sample will be placed inside a crucible and above some fillings (figure 6.1), which will raise it to the cover level. Heating is provided by a Watlow cylindrical steel resistance with a 50 mm diameter and 50 mm wide. It furnishes 450W and it is regulated by a thermal controller Eliwell eWPC 90T.

Preliminary leaking tests performed on this reactor gave positive results; flow rate entering or exiting it were measured with a bubble flow meter and they were the same at both room temperature (25°C) and at pyrolysis temperature (400°C), so no gas seemed to be diverged from its main path. However, after a deeper test, this cover arrangement revealed to be ineffective, because gas seeped through splits between the cover and the gasket. This test is called expansion test, because evaluates the degree of gas expansion during a temperature ramp and it is illustrated in figure 6.2.

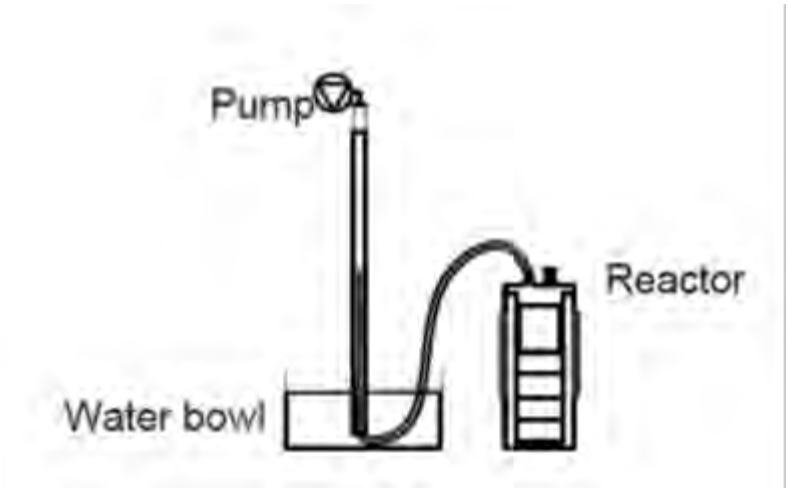

Figure 6.2 Expansion test set-up.

The reactor was sealed with gasket and cover at ambient temperature; the gas entrance was closed with a cap and the exit was connected through a polyamide tine pipe to a vertical plastic tube set above a bowl of water. The tube was sealed in its top with a valve; with this one opened, water had been sucked from the bowl into the tube with a pump until it became almost filled of water, then the valve was closed. This ensured that the water column remained stable inside the tube. Then a temperature ramp was set starting from room to working temperature with a heating rate equal to 5°C/min; so that the gas held inside the reactor will enlarge its volume with increasing temperature and expand through the pipe into the tube lowering water level. Since no descent of the water level had happened, gas is leaked instead of being conveyed into the water tube; so the reactor sealing system was substituted with one better performing, characterized by ISO-KF aluminum seal of 55 mm diameter and chain clamp.

Figure 6.3 ISO-KF Chain clamp and Helicoflex Seal.

The ISO-KF Helicoflex seal resists to temperatures up to 280 °C, impedes gas permeation, is mantled with aluminum, has a centering ring made by Inconel (which is a Nickel and Chromo alloy) and contains an Inconel spring and stainless steel spacing material. The spring deforms under the stress applied by the aluminum clamp and ensures the seal.

On the top of the reactor cylinder was welded a circular steel annulus, perfectly polish, on which shall adhere the seal and the reactor screw cap was substituted with a new flat steel one, which shall compress the seal.

Also this configuration was subjected to an expansion test: the reactor was connected to the tube filled of water and heated till 400°C at 5°C/min. The expected increase of gas volume together with temperature was calculated by means of the ideal gas law, starting from room temperature (25°C) and reactor volume (78.83 cm^3). Unfortunately the amount of water descent along the column happens to be less than expected, revealing that some leaks were still occurring. In the figure 6.4 is represented the ideal volume calculated in comparison with the measured one.

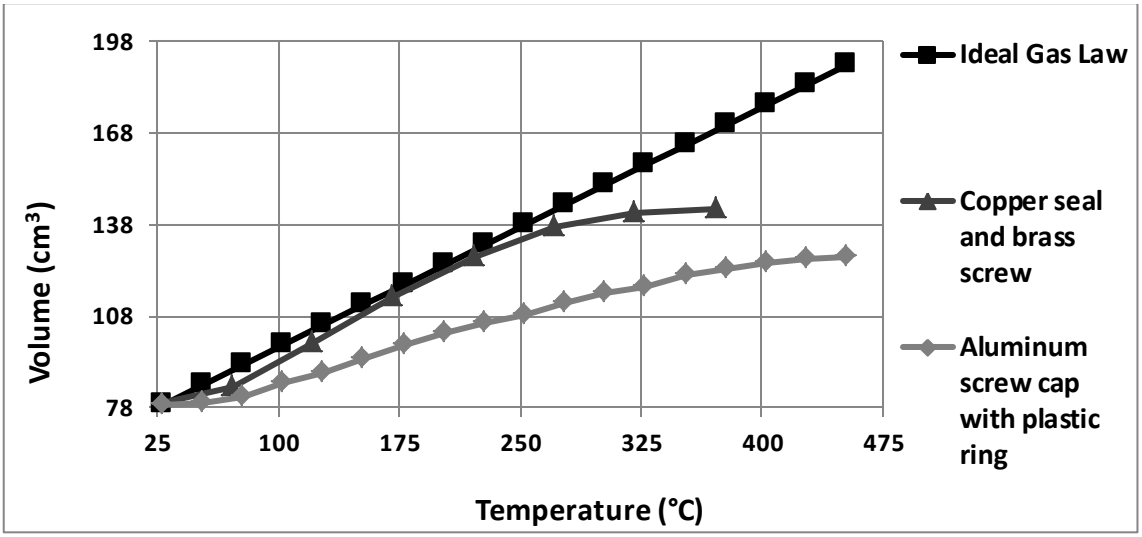

Figure 6.4 Expansion curves with different bottom caps.

The aluminum screw cap used to close the bottom hole had a very low performance, because its curve lies far below the ideal one. This is probably due to the fact that temperature at the bottom remained quite above plastic melting point and so that the plastic ring couldn't have any sealing function.

Therefore it was substituted by a copper seal coupled with a brass screw; which worked well until 275°C, but then its curve drifted apart from the ideal one, possibly because copper and brass expanded differently with temperature and didn't anymore perfectly adhere to each other. This phenomenon cannot be attributed to non-stationary effects, i.e. not all the gas had reached the final temperature, because even if temperature is increased very slowly or the reactor is maintained at 275°C for one hour, still the copper seal-curve doesn't get closer to the ideal one.

The tests performed so far were run at constant pressure, thus raising temperature, volume would result increased. A last test was carried on keeping the volume constant; so the reactor was connected to a manometer with both the gas inlet and outlet closed and then heated to 400°C. The relative pressure increase shall be around to 1.2 bars, but it didn't happen.

Limitations of this reactor had become evident, so the experimental configuration was switched to a more performing one.

6.1.2. Tubular reactor

The second set-up, which proved to be the well-functioning, is compost of a cylindrical steel reactor (figure 6.5), vertically displaced, two steel caps with connectors for gas inlet and outlet and a slot for the control thermocouple. The main cylinder has and inner diameter of 38 mm, a thickness of 2 mm and a height of 120 mm. The control thermocouple is inserted from the bottom cover, allowing a simple charge and discharge of the reactor.

Figure 6.5 Tubular reactor with covers, control thermocouple and tubular resistance.

Heating is provided by two cylindrical steel nozzle heaters, 30 mm high and 40 mm wide, which are placed on the steel cylinder and perfectly adhere on it (figure 6.6). The cylinder diameter was chosen starting from the nozzle dimension in order to uniformly warm the reactor's walls and to avoid any spacing or heat losses. Heaters provide a power equal to 275 W and work till 400°C and are regulated by a thermal controller Eliwell eWPC 90T with analogic control. Also the exit tube is heated by a tubular resistance modulated by a power reducer, which maintains a temperature of about 350°C inside it. Sealing is ensured by two ISO-KF aluminum seal, which were described in the previous paragraph, but in this case are compresses by two ISO-KF Bolt Clamps composed by three parts, fixed by screws with hexagon sockets (figure 6.6). These are perfectly suitable for metal seals, because are made of steel, can bear a maximum pressure of 1.5 bars and work at temperature as high as 200°C. The clamp inner diameter was chosen to be 40 mm as the one of the seals in order to fit on the reactor.

Figure 6.6 Tubular reactor (left) and particular of nozzle heaters, clamp and seal(right).

Finally reactor is insulated with rock wool to minimize the heat losses to the outside.

The performance of this set-up was evaluated with an expansion test; from figure 6.7 it can been seen that the curve of volume increments of the reactor is close to the ideal one up to 340°C; this was considered good to enough to adopt this configuration.

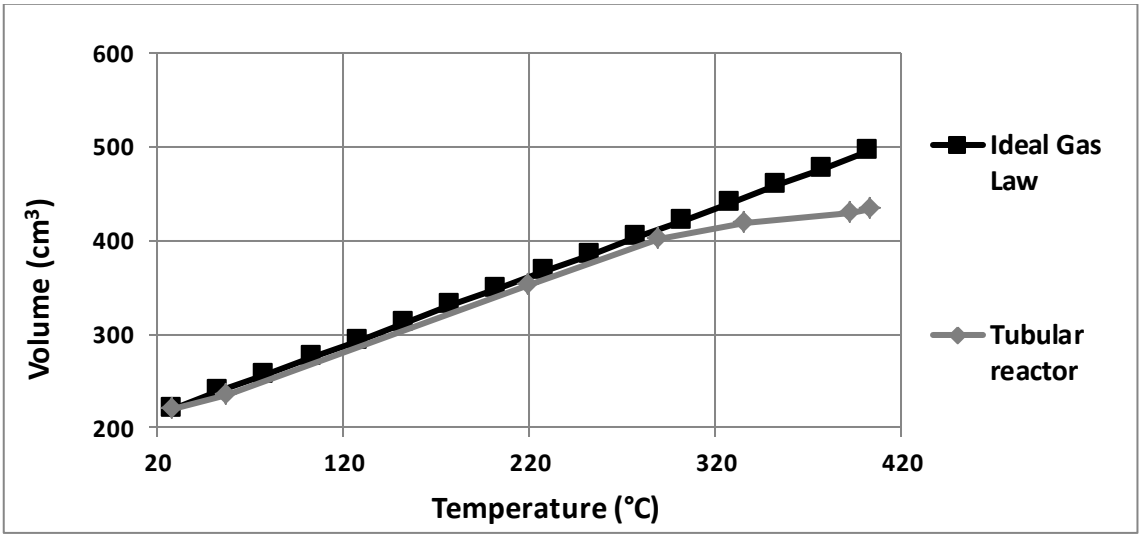

Figure 6.7 Expansion curve of the tubular reactor.

The inside of the reactor is filled with a system of grids and cylinders in order to support the sample and the fillings (figure 6.8), which are placed above and under the sample and have the function to preheat the gas or to protract its permanence in the hot zone enhancing sample decomposition.

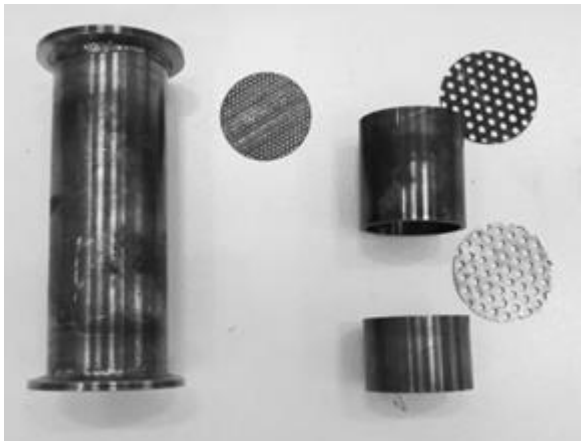

Figure 6.8 Reactor's cylinders and grids system.

On the bottom of the reactor is placed a hollow cylinder, that sustains a grid with large mesh (4-5 mm), and second hollow cylinder, which in turn holds an identical grid. These serve to retain the fillings spheres and allow the passage of the thermocouple. Inside the upper cylinder and exactly in the middle of the reactor there is a slot for a smaller grid, with a tighter mesh (1-2 mm). It serves as a sample holder and its littler holes shall retain it until it is degraded; the control thermocouple is inserted until it reaches contact with this grid in order to precisely determine sample temperature.

Filling material is constituted by 12 mm diameter spheres of alumina (Al_2O_3), which is acid-resistant, has a high thermal conductivity, melts at a temperature of about 2000°C and has refractory properties, so it should not interfere with the pyrolysis process.

The gas is fluxed in the reactor from the top, it is preheated passing through the upper filling, then it encounters the sample, it is degraded filtering through the lower filling and finally it is conveyed into the condenser.

6.2. Condenser

Condenser is probably the key part of this plant, because it cools the hot vapours turning them to oils. The various condensers present throughout the laboratory glassware were investigated, but none seemed to fit to pyrolysis oils, due to the serious risk of clogging and the impossibility to open them or remove parts for cleaning, as it is clear from figure 6.9, which represent the Liebig condenser.

Figure 6.9 Liebig condenser.

This glass condenser has an inner-tube straight, so it is cheap to manufacture and it is much more efficient than an air condenser, because it uses water as cooling fluid, that can absorb much more heat than the same volume of air, and its constant circulation through the water jacket keeps the condenser's temperature constant.

Hence water was chosen to be the cooling fluid for its high performance, not to mention its easy availability. Also glass as material, allow to visually analysing condensates, the presence of more phases and their colour; thus a condenser was designed starting from a large glass test tube, were gas shall condense.

The test tube is low cost, replaceable if necessary and easily cleanable. It will be sealed by an aluminum cap with a rubber O-ring and inserted in a capacitor with a hollow space, where water shall flow. The capacitor is equipped with a second O-ring to guarantee sealing.

In figure 6.10-11 is presented the original project of the condenser and its appearance after the realization.

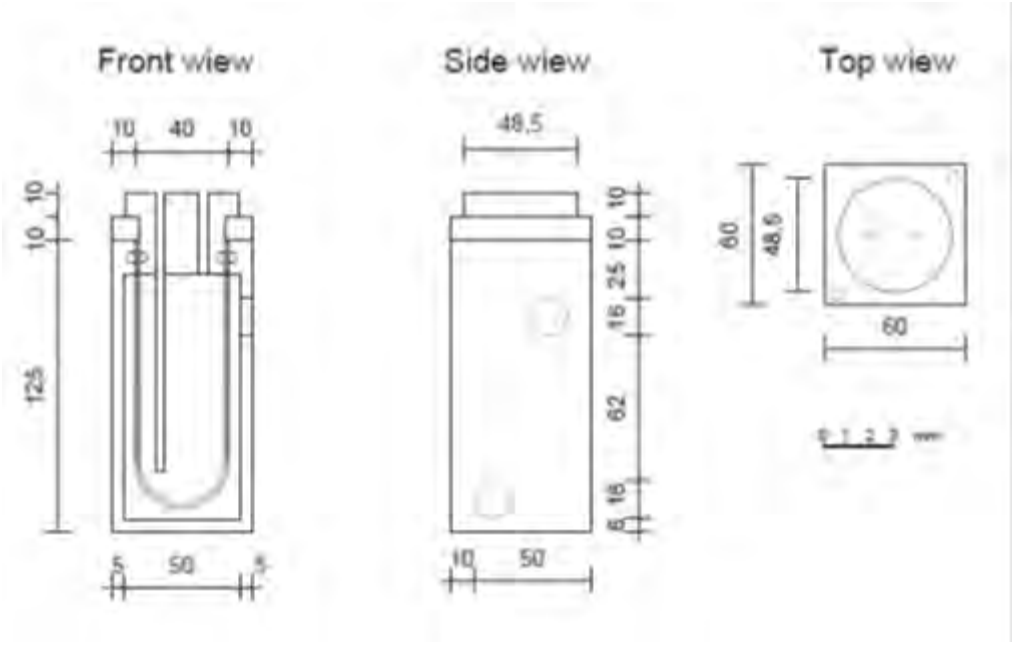

Figure 6.10 Condenser design.

Figure 6.11 Water-cooling condenser.

The outer shape capacitor was initially designed to be cylindrical, but a parallelepiped turned out to be most easily feasible by the mechanics, because the connections for water pipes were more readily welded on a straight surface.

It is also equipped with a squared block, which serves to keep the test tube from jumping out from the container for the over-pressure generated by the cooling fluid circulation.

6.3. Thermal profiles

After that the reactor was tested for sealing, so that no gas losses had happened; its thermal performance was evaluated. Different aspects of the thermal performance were investigated, starting from the amount of insulation material, to resistance and holding pliers position, to type and size of filling and ending with control thermocouple position.

6.3.1. Initial pliers and resistance configuration

The first configuration tested is showed in figure 6.12, where heating bands are placed between the two holding pliers.

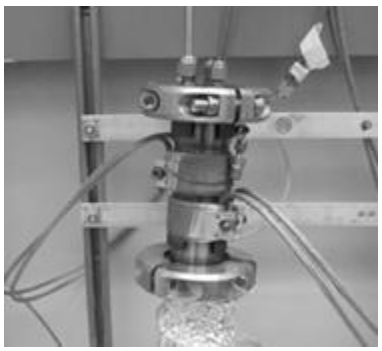

Figure 6.12 First resistances and pliers' configuration along the reactor.

Insulation is provided by one or more layers of rock wool, which is essential to minimize the heat dispersion from the reactor. Its importance was demonstrated by two preliminary tests, run with different degree of covering with rock-wool, as it is shown in figure 6.13.

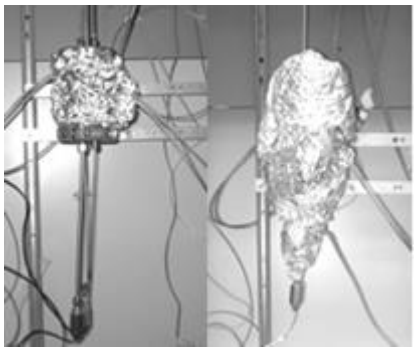

Figure 6.13 Initial (left) and improved insulation (right).

Thermal tests were carried on in a flux of 100 ml/min air; the void reactor was heated to three different set-points 300, 350 and 400°C with a constant heating rate of 5°C/min. Set point temperature was maintained for half an hour and was regulated by a control thermocouple placed outside the reactor, adjacent to its outer wall.

In all the three cases it was evident that the initial insulation was insufficient to keep warm the exit of the reactor, so a further layer of rock wool was added in its lower part and this allow a gain of 50 degrees more in the exit, as it is shown in figure 6.14.

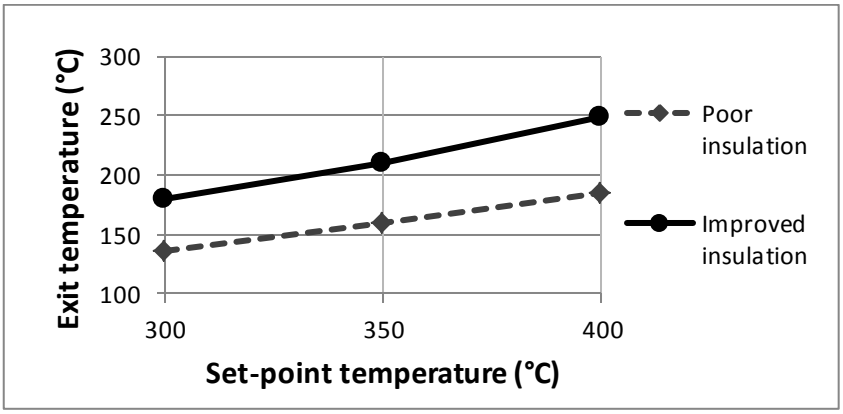

Figure 6.14 Exit temperatures at different set-points with two levels of insulation.

Then more accurate tests were drawn in order to establish the performance of the resistances' position along the reactor and the consequent placement of the holding pliers.

As reactor fillings some alumina spheres were chosen; alumina (Al_2O_3) is particularly adapt for this function because it possess a high thermal conductivity, melts at a temperature of about 2000°C and has refractory properties, so it should not interfere with pyrolysis products. In laboratory alumina spheres of different sizes were available; those with greater diameter (about 12 mm) are easier to remove than those of a smaller size (6 mm).

Four different sampling points are necessary along the reactor: above and below each filling to evaluate its efficacy and at the exit of the gases, their precise location is illustrated in figure 6.15.

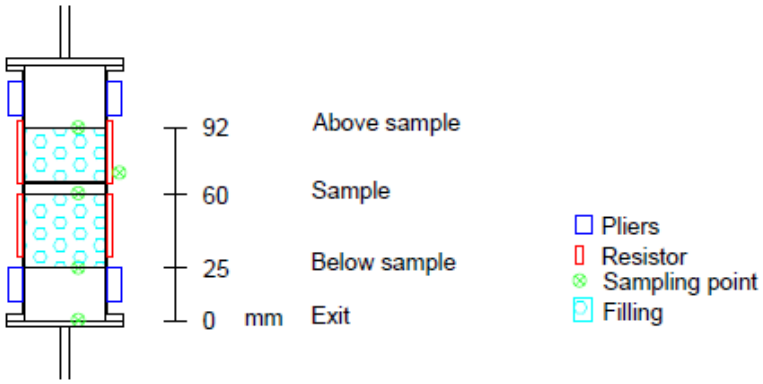

Figure 6.15 First resistances and pliers' configuration along the reactor, longitudinal section.

The test procedure is the same used to evaluate insulation performance: the reactor was fluxed with 100 ml/min of air and heated to three set-points with a heating rate of 5°C/min., but differently from before, the reactor was also filled with alumina spheres.

In figure 6.16 are illustrated thermal profiles after an isothermal time of 30 minutes at 300-350 and 400°C. The curves are referred to three different test conditions: void rector; upper and lower filling of 13 mm diameter; upper filling of 13 mm and lower of 6 mm diameter.

The differentiation between the upper and the lower filling was forced by practical reason: in order to charge and discharge the reactor easily, it was not possible to use 6 mm diameter spheres also for the upper part. Furthermore, the smaller spheres diameter lead to smaller interstitial space between them and this could be cause of clogging.

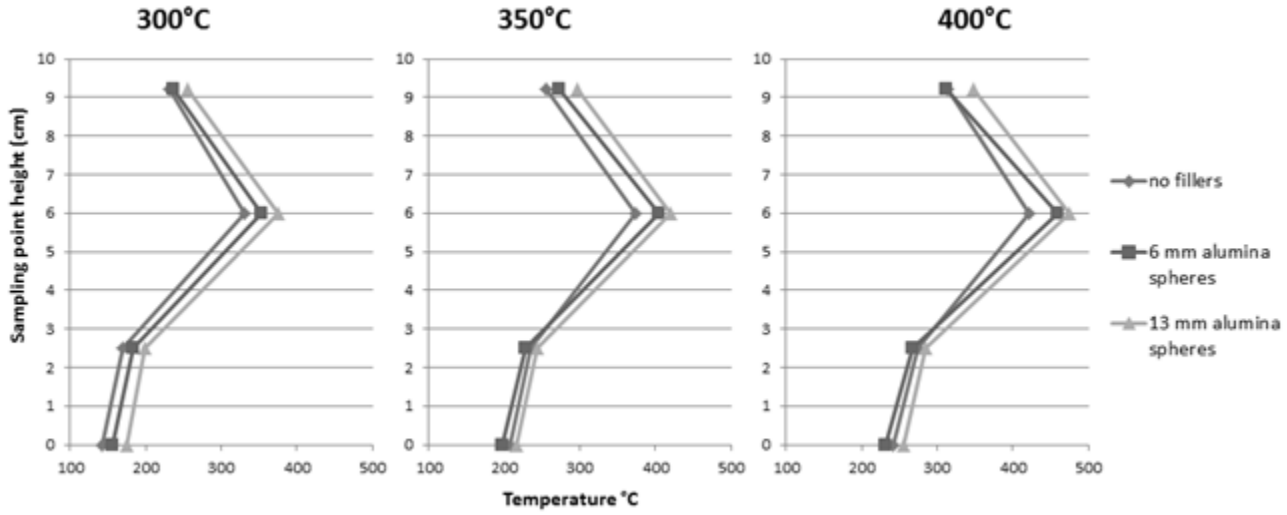

Figure 6.16 Thermal profiles at three set-points with different filling condition.

From the graphs it can be seen that the upper filling allows gas preheating, while the lowest is not so useful from a thermic point of view. The bottom filling of smaller diameter seems to slow down the gas, which exits in all cases at a temperature even lower than the curve without fills. On the contrary the one of greater spheres seems to maintain the gas at a higher temperature in the exit.

Finally the best filling from both, thermal and practical point of view is made by 13 mm spheres as for the upper part and for the lower one. The following three graphs (figure 6.17-19) report the thermal control during the three tests. In total were used six thermocouples, five for monitoring temperature and a last one to control the regulator. The reading thermocouple on the wall is placed nearby the controlling one, to be on the safe side; so the set points can be easily identified in the graphs. The other thermocouples (above, below sample and exit) were used to evaluated the effect of the fillings. From these graphs it can be deduced that temperatures registered by the thermocouples reach stationary after a quite short time.

In spite of the use of fillings, the exit temperature remains quite low, so another configuration for the heating bands along the reactor was thought and it is developed in paragraph § 6.3.2.

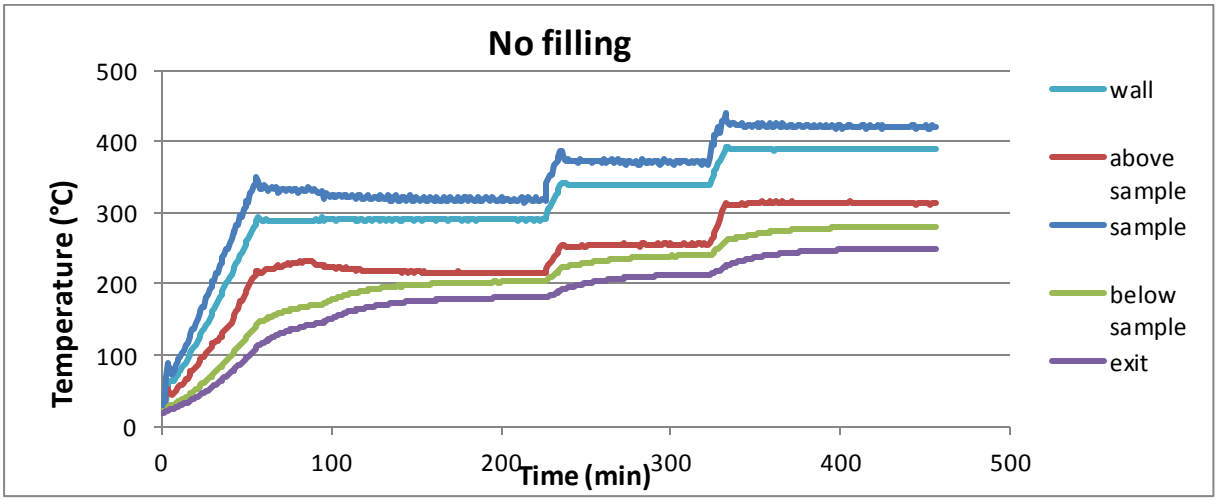

Figure 6.17 Thermal control without fillings at 300-350 and 400°C.

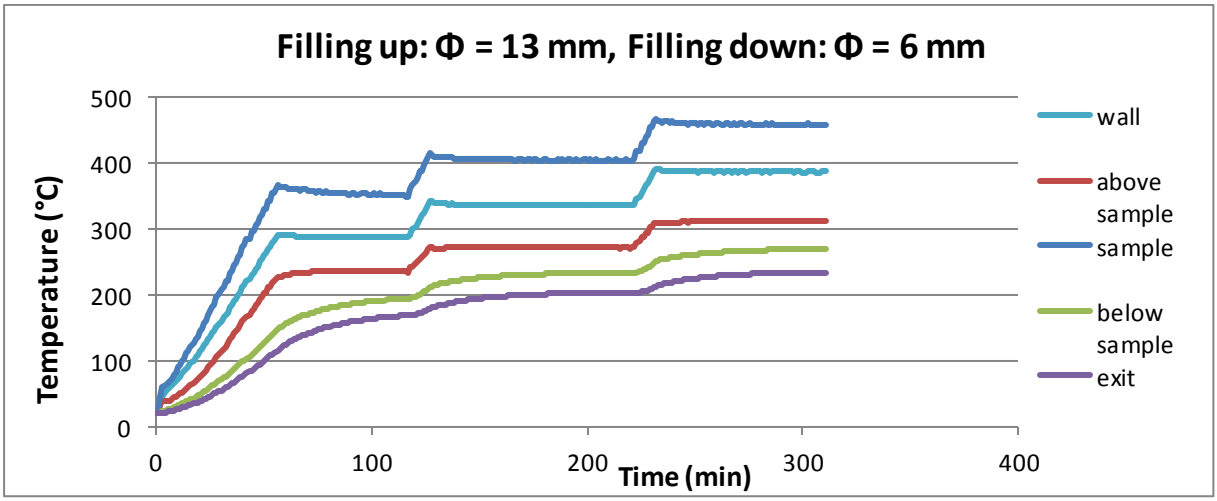

Figure 6.18 Thermal control with 13 mm diameter spheres as upper filling and 6 mm spheres as lower filling at 300-350 and 400°C.

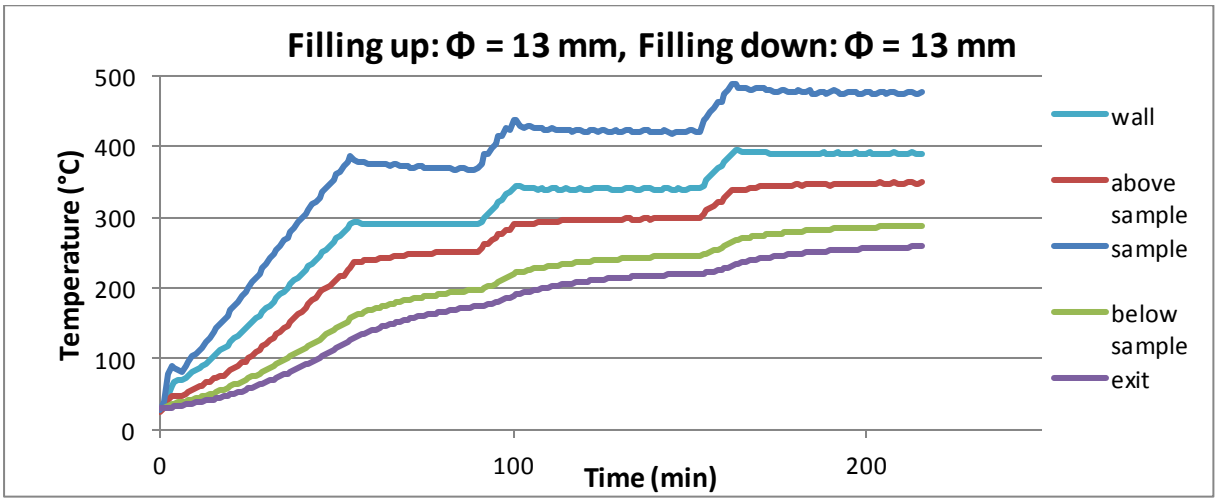

Figure 6.19 Thermal control with 13 mm diameter spheres as upper and lower filling at 300-350 and 400°C.

6.3.2. Second pliers and resistance configuration

The lower heating band was moved to the end of the reactor, consequently the lowest holding pliers stayed between the two resistances. The control thermocouple is always placed on reactor's outer wall, but a little lower respect than before, due to space constrains.

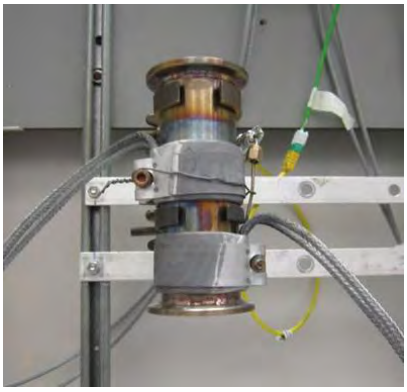

Figure 6.20 Second resistances and pliers' configuration along the reactor.

Considering the upper filling beneficial effect in preheating the gas; it was extended to the top of the reactor, adding some spheres, as it is shown in figure 6.21.

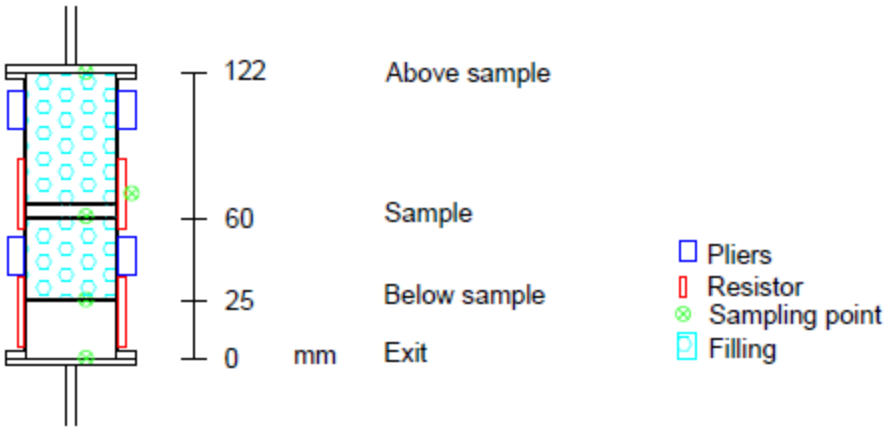

Figure 6.21 Second resistances and pliers' configuration along the reactor, longitudinal section.

The improved configuration of the heating bands allow to the curves related to different height to become closer and shifted downward demonstrating a better thermal control. In figure 6.25; the sample curve (blue) does not present clearly higher temperature than the others; unfortunately for this test only the set-points of 350 and 400°C are available. The solution to move the heating band lower along the reactor had demonstrated to be useful; in fact the thermal profile is far more homogeneous and the purple curve, related to the exit is almost overlying to the sample's one, and this shall inhibit any condensation to take place in the exit pipe. The most critical point of this configuration is below the sample (green curve), where the inferior filling terminates, but this does not seem particularly worrying because temperature is anyhow higher than before. In figure 6.22 is presented a comparison between the two configurations.

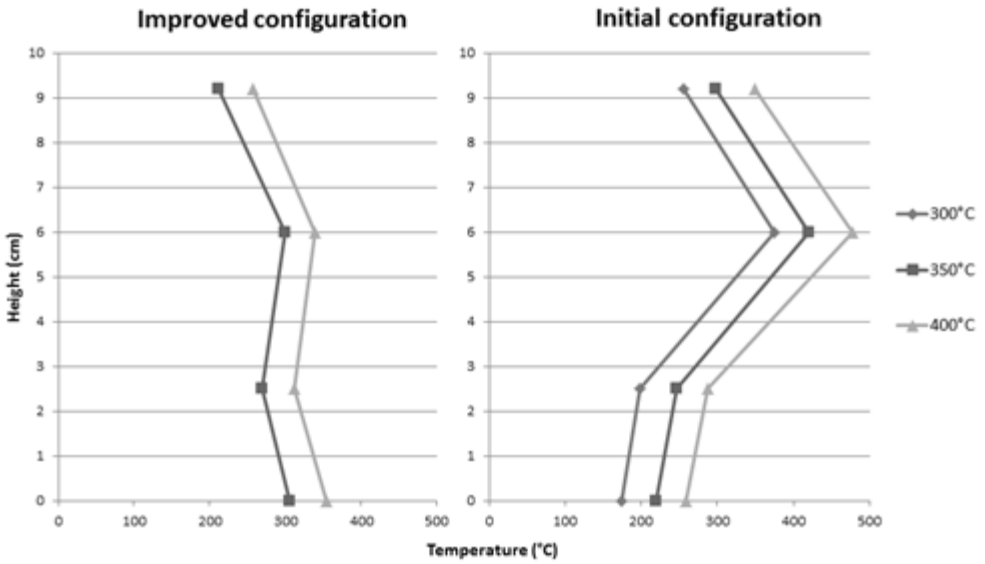

Figure 6.22 Thermal profiles at three set-points with different resistance and pliers position.

Finally the improved configuration ameliorates clearly the thermal profile, but the sample maintains itself at a temperature approximately 50°C lower than the set-point, as it can be seen from figure 6.22; so the choice to put the control thermocouple in the outer reactor's wall must be reconsidered; probably an inner control can reduce this discrepancy.

6.3.3. Inner control thermocouple

The thermocouple was placed on the inner wall above the sample. Unfortunately, from figure 6.26 it can be seen that the discrepancy between the thermocouple that registers sample temperature and the set-point is remained as before (about 50°C).

However the temperature below the sample (green curve) becomes nearer to the others and this in anyhow an improvement. For comparison in figure 6.23 are reported thermal profiles drawn at different set-points with the inner and outer thermocouple. Finally, for the future pyrolysis tests, it seems appropriate to put the control thermocouple on contact with the inner grid that holds the sample, in order to have a precise idea of the temperature to which it is subjected.

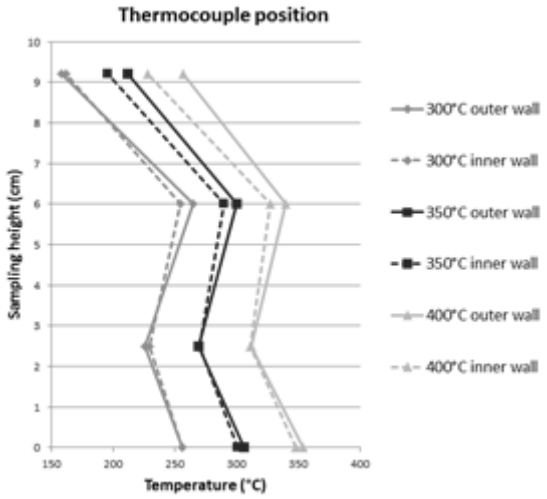

Figure 6.23 Thermal profiles at three set-points with inner or outer thermocouple.

6.3.4. Sic

An interesting test was developed in order to evaluate the use of silicon carbide as upper filling. Figure 6.24 shows the thermal profile detected with the SiC (red curve) and with alumina (green curve) at different set-point temperatures 300, 350 and 400° C.

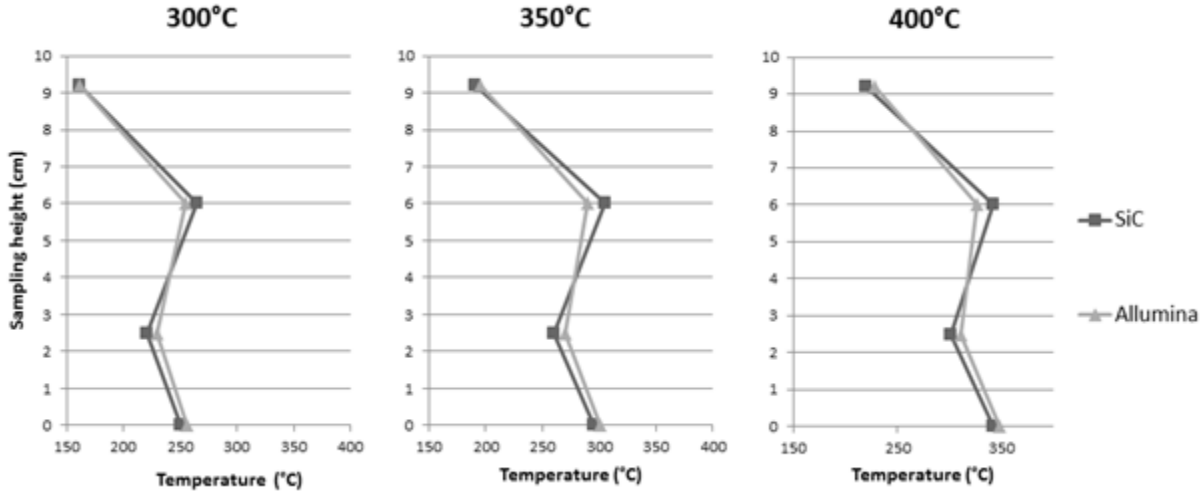

Figure 6.24 Thermal profiles at three set-points with Sic or alumina as upper filling.

Thermal profiles are very close, but it can be seen, where the upper filling ends (at cm 6) that the SiC favours a better heat diffusion than alumina so that the gas temperature above the sample became slightly higher, and it increases as the set-point raises. The temperature of the gas that has passed through the SiC is 10°C warmer than the other at 300°C; at 350°C is 15°C and reaches 20°C at 400°C. Finally the SiC had raised gas temperature of a quantity that is not sufficient to justify its adoption; in fact it makes difficult the charge and discharge of the reactor, because, it is of very fine particle size and it can infiltrate between grids and crucibles and prevent their sliding or, in the presence of partially melted polymer, it may also create agglomerations.

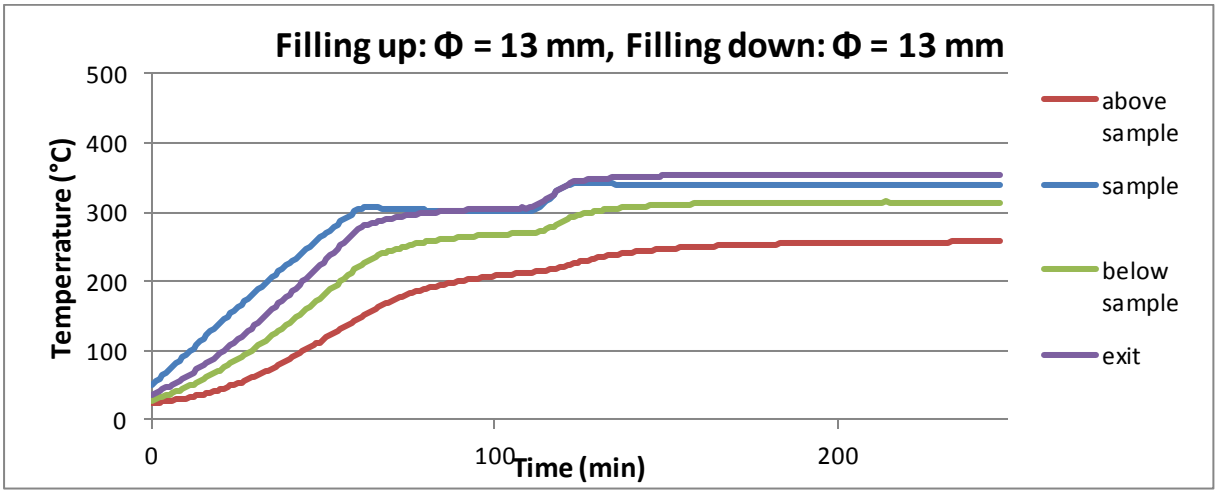

Figure 6.25 Thermal control with 13 mm diameter spheres as upper and lower filling with the heating bands in the lower part of the reactor at 350 and 400°C.

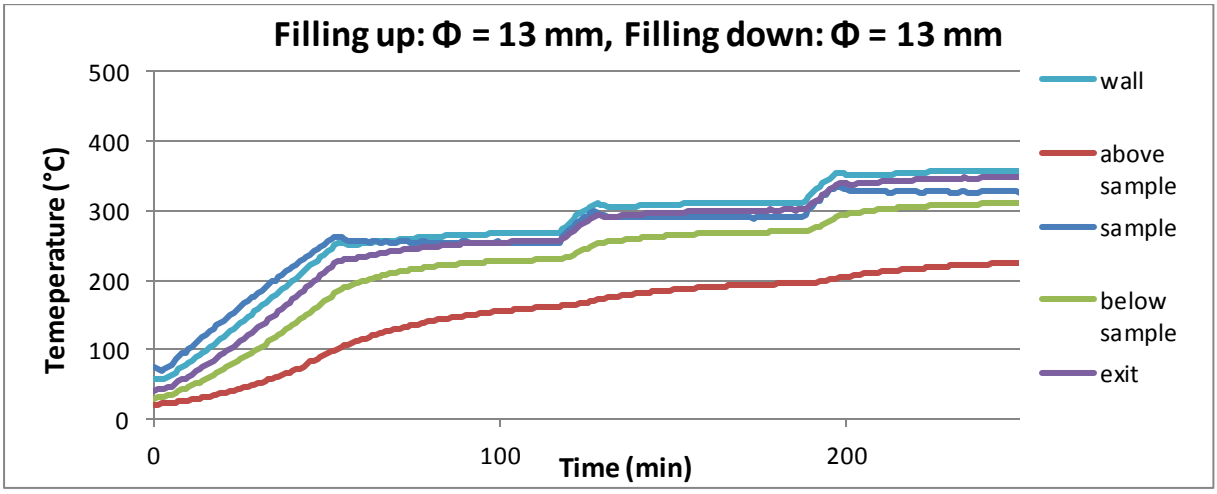

Figure 6.26 Thermal control with 13 mm diameter spheres as filling, for the improved resistance and pliers configuration at 300-350 and 400°C.

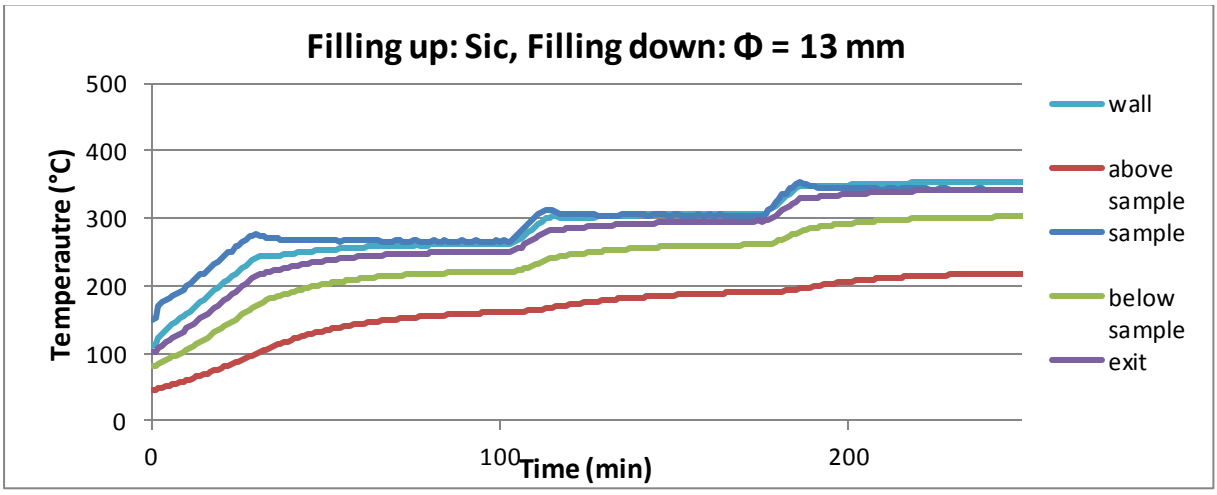

Figure 6.27 Thermal control with SiC as upper filling and 13 mm diameter alumina spheres as lower filling, for the improved resistance and pliers configuration.

6.4. Standard method development

The standard procedure provides to weight each piece of the reactor before starting a test, in order to evaluate eventually occurring deposits on grids, fillings or crucible. A filter, made of a plastic tube filled of cotton, is introduced on the gas exit in order to hold particles and not to damage instruments. It is also weighted before and after each test.

The pyrolysis temperature is chosen to be 400°C, because is the highest working temperature of the heating bands; it is preferable not to exceed it in order to preserve the resistance, considering also that the control thermocouple is not placed in contact with the reactor walls, but in the middle of it, in a flux of inert gas. The isothermal time was chosen to be at least 60 minutes, from a preliminary test. The Eliwell thermal regulator was calibrated to provide a heating rate of 5°C/min, which was the most common program temperature encountered in literature. As inert gas, Helium is preferred to Nitrogen, because it also used as carrier for the gas-chromatograph and won't interfere in the subsequent gas analysis. The standard sample quantity charged in the reactor was 1 gram of polyethylene.

First preliminary pyrolysis test served to optimize the procedure and eventually ameliorate some aspects regarding both the reactor and the condenser.

6.4.1. Reactor

The middle grid tight mesh revealed to be ineffective to retain the sample until it is degraded, in fact the melted polyethylene poured through the grid holes and then re-condensed on the bottom cover, because it is still too heavy to remain in the gas from at the exit lowest temperature. So a tiny aluminum crucible was used to contain the sample and was placed on the middle grid. In this way only the volatilized sample can leave the crucible and flow away from the hottest zone.

This crucible allows feeding the standard 1 g quantity of sample, but, in order to treat more polymer, a bigger one was built which can retain up to 4 grams of polyethylene and required a bigger hollow cylinder to be hold inside the reactor as shown in figure 6.28.

Figure 6.28 Different size crucibles and hollow cylinders to hold them.

6.4.2. Condenser

After the first tests it was clear that the polymer condensate as soon as it reaches the condenser; so the tube exiting the condenser cap, which serves to prolong gas path inside the test tube was not only useless, but cause of dangerous clogging and it was eliminated.

Oils precise measurement is very important, since they're the main purpose of this thesis so the little quantity that remains inside the cap is removed with a cotton swab and weighted. Furthermore, it seems difficult to deduce the oil weight inside the test tube, because it weighs about 50 grams, which is 100 times than the oils. So a tiny aluminum paper container (figure 6.29) is introduced inside the test tube and oils are weighted on an insignificant tare.

Figure 6.29 Condenser test tube without pipe and with aluminum paper inside.

Chapter 7
Pyrolysis tests results

After the optimization of the reactor configuration, pyrolysis tests are carried out and the first mass balances could be drawn.

7.1. Inert gas flow rate

Four different flow rates have been investigated to find the one that maximizes oil production. They were chosen in the range of the flow meters available in the laboratory; it was investigated a range span from no flow, followed by 20, 50 and 150 ml/min.

The standard heating procedure is a ramp of 5°C/min from ambient temperature to 400°C, which is maintained for one hour; the sample charged was about one gram for each test, using the smallest aluminum crucible. Figure 7.1 reports the results in terms of different fractions (gas is calculated by difference); it is clear that this pyrolysis plant can allow a good oil yield, up to 65% of the original material which is maximized by a 50 ml/min flow rate.

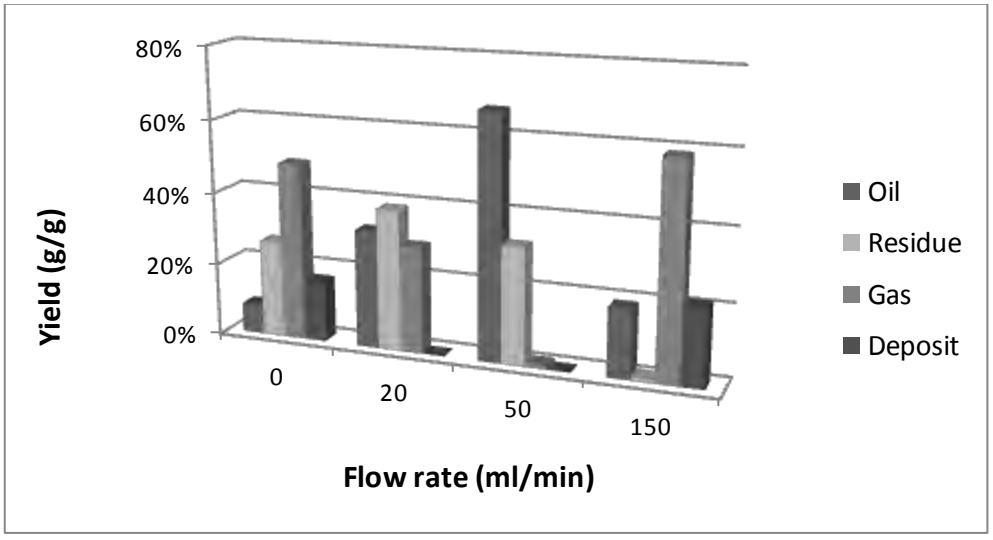

Figure 7.1 Products yields for different flow rates.

'Residue' is the remaining sample in the crucible, which is not degraded; deposits are fouling that accumulates on the reactor fillings or grids or on the filter. Yields are calculated as the ratio of the given product (or residue) by the initial mass of sample and gaseous products are deduced by difference.

The fact that the oil production presents and optimum at 50 ml/min is indicative of the presence of two opposite phenomena: the residence time of the volatile products in the hot zone and the residence time in the condenser. The longer the volatiles remains in the lowest heated zone of the reactor, the deeper the cracking achieved, so lighter molecular weight species are produced, which tends to escape the condenser and remain in a gaseous form, increasing the gas yield.

On the contrary, a 150 ml/min flow rate, provides a very little sample degradation and at the same time a very short residence time in the condenser, giving a high yield of gases but also a quite considerable amount of fouling, that although quite heavy, cannot completely condense and are dragged out the condenser and accumulate on the following filter, increasing the deposits. The 0 ml/min flow rate is useful, but not directly comparable with the others, because without flux kinetics is different.

7.2. Reproducibility

In order to found the previous considerations on more secure bases, some reproducibility tests are made and gave satisfying results. In figure 7.2-3 oil yields, gases, deposits and residue in two series of tests at different flow rates are presented; in the worst case they different by 10% (figure 7.3, residue at 150 ml/min) but frequently they overlap.

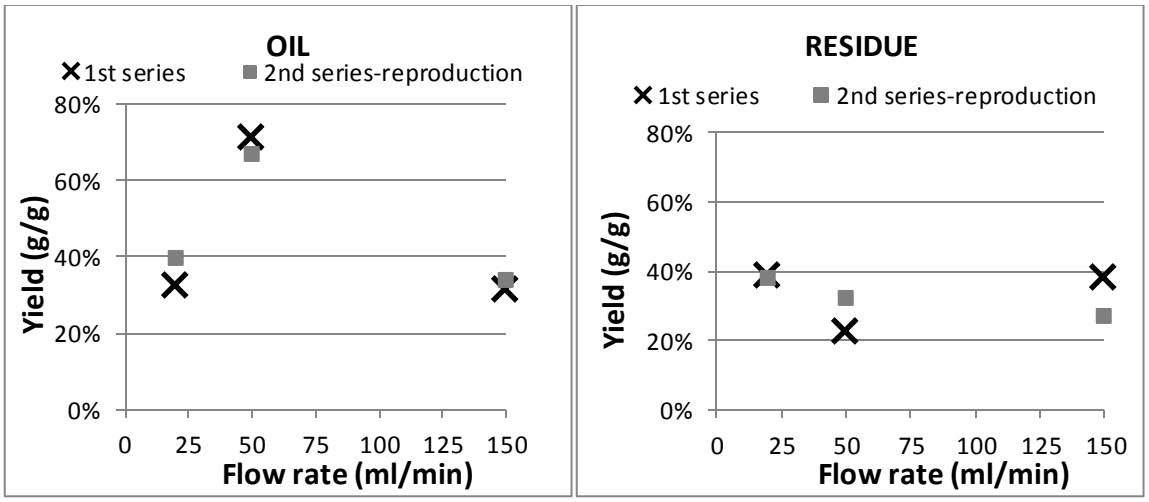

Figure 7.2 Oil (left) and residue (right) yields in two series of tests at different flow rates.

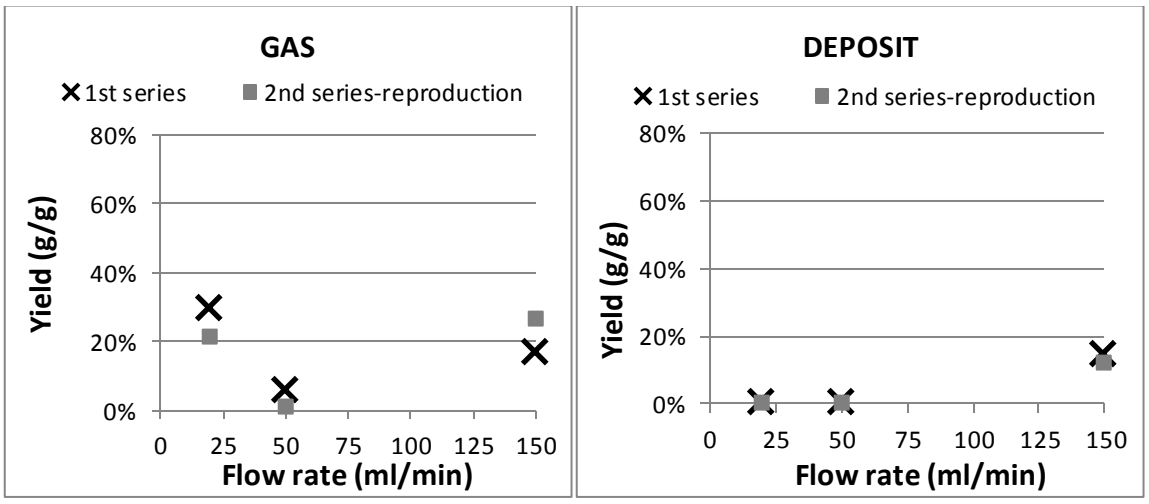

Figure 7.3 Gas (left) and deposit (right) yields in two series of tests at different flow rates.

7.3. Isothermal time

It was expected that increasing the time at the final temperature further degradation takes place and higher yields of gases and oils are obtained. Starting from the usual 60 minutes, the isothermal time was increased up to 150 minutes, following the standard heating procedure (5°C/min till 400°C) and using the optimal flow rate of 50 ml/min.

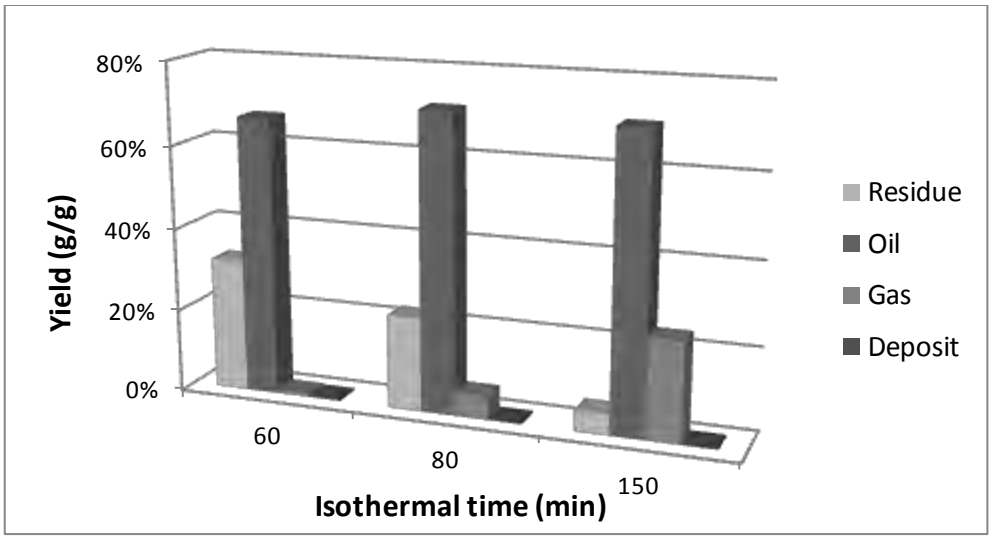

Figure 7.4 Yields after three different isothermal time (60, 80 and 150 min) at 400°C with an heating rate of 5°C/min and a flow rate of 50 ml/min.

It is clear from figure 7.4 that residue is progressively decreasing as long as the time is increased and it is converted into gases, while the oils yield increases slightly.

7.4. End temperature

The conversion efficiency was evaluated also with respect to the final temperature; as said before, it is preferable not to exceed the nozzle heaters working temperature (400°C), so the end temperature was lowered to 385°C and 375°C. It is quite obvious that a lower temperature means a lower conversion, not only in terms of gases, but also of oils. Results obtained from three different tests with the standard flow rate of 50 ml/min, heating rate of 5°C/min and isothermal time of 60 minutes are as expected and are showed in figure 7.5.

The residue on the crucible after pyrolysis at 375°C is definitely high and it is causes accumulation of degraded polymer on the bottom of the reactor, because the exit temperature remains too low to prevent condensation. Gas yield shows a moderate increase from 18 % at 375°C to 33% at 400°C; but oil's is far more marked: from 21% at 375°C to 58% at 400°C.

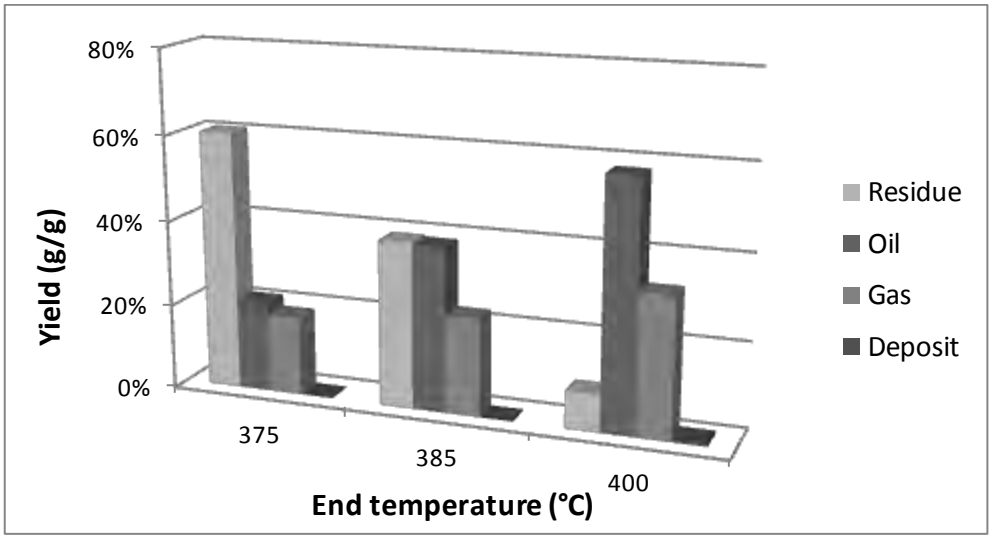

Figure 7.5 Yields at three end temperatures (375, 385 and 400°C) for 150 minutes with a heating rate of 5°C/min and a flow rate of 50 ml/min.

7.5. Heating rate

It is known from literature (Kim et al,2003) that a slower heating rate results in an increased yield of oils and this was experimentally verified by three test run at 3-5 and 10°C/min till the end temperature (400°C), which was maintained for 150 minutes. From figure 7.6 it can be seen that the slowest heating policy provides the highest oils yield.

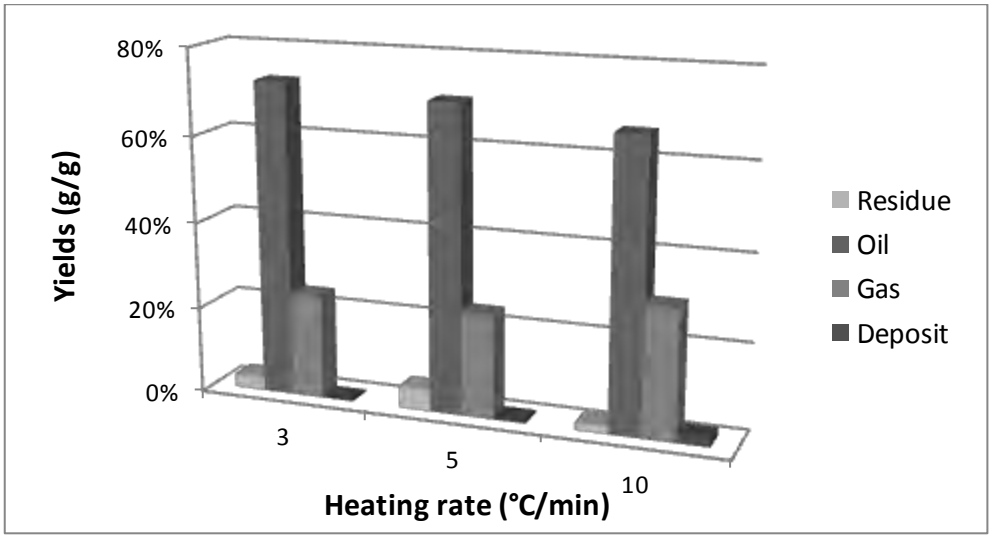

Figure 7.6 Yields with three different heating rates from room temperature to 400°C for 150 minutes.

It can also observed that keeping constant the isothermal time, a slower heating program means a longer residence time at high temperature in the reactor, causing a deeper cracking of the residue and higher product yields.

7.6. Sample amount

The larger crucible was tested with respect to the smaller one and it was charged with double the amount of sample (2 grams instead of 1 gram). The flow rate was the same for both tests (150ml/min), as well as the heating policy (5°C/min till 400°C for 1 hour).

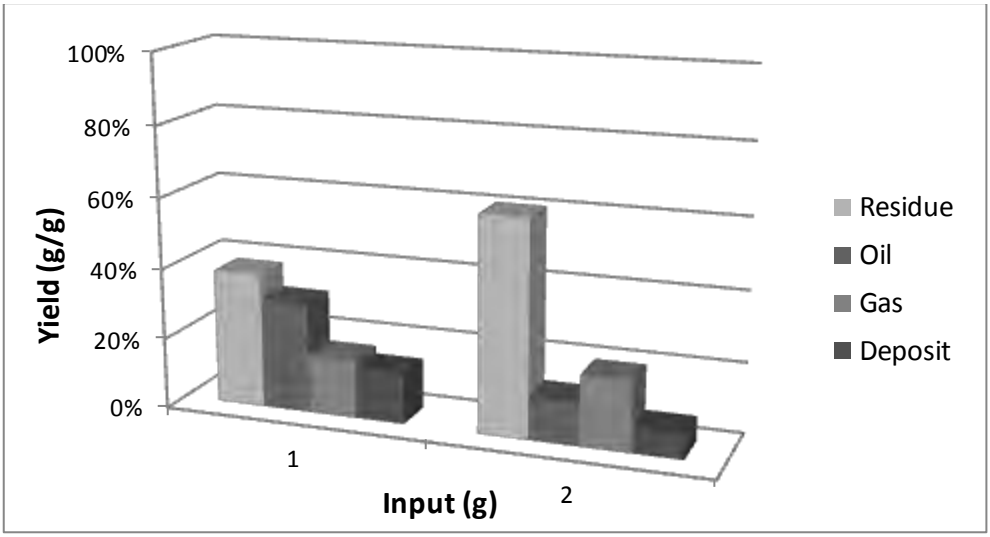

Figure 7.7 Smaller crucible yields (left) and bigger (right) after 60 min at 400°C with 150 ml/min flow rate on the initial mass of PE charged (1 or 2 grams, respectively).

The bigger crucible achieves less sample conversion, as shown in figure 7.7, where yields of the two crucibles are reported as fractions of the initial loaded mass. At the same flow rate the bigger crucible gives the higher residue yield, so that a stagnation phenomenon is taking place inside the bigger crucible: apparently the hot gas is not able to reach the bottom of the crucible.

7.7. Error estimation

Analyzing all the results, an estimation of the error on gases and oils yields can be attempted using the standard deviation (9.1), where x_i is the single measurement, $< x >$ is the arithmetic mean (9.2), and N is the total number of tests.

$$\sigma_x = \sqrt{\frac{\sum_{i=1}^{N} (x_i - < x >)^2}{N}} \tag{9.1}$$

$$< x > = \frac{1}{N} \sum_{i=1}^{N} x_i \tag{9.2}$$

The error (σ_x) was found to be between 8 and 13%; in figure 7.8 error bars ($\pm\sigma_x$) and mean values (dotted lines) are shown for two groups of tests run in different conditions. The group of five tests on the left is run with an isothermal time of 60 minutes, heating rate 5°C/min, end temperature 400°C and flow rate 50 ml/min. The other three tests on the right have a different isothermal time (150 minutes), but the same heating rate, end temperature 400°C and flow rate.

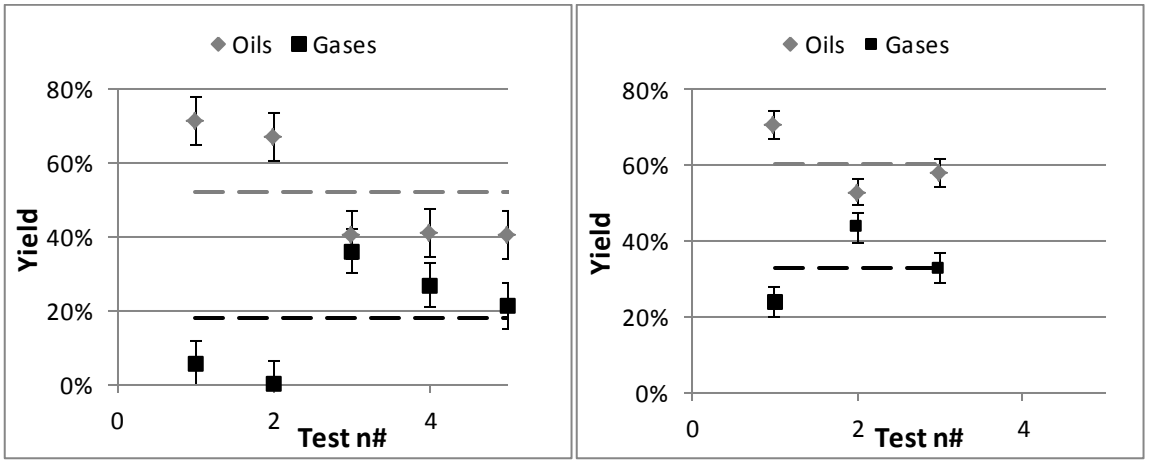

Figure 7.8 Gases and oils yields in two groups of tests with same flow rate (50ml/min) and heating rate (5°C/min), but with different isothermal time: 60 minutes (left) and 150 minutes (right).

Error value depends on the number of comparable tests used to calculate it; in fact error bars are longer for the group of five tests that has a greater variability. However, error does not depend on the product (i.e. oil or gas), because in the single group it affects in equal extent oils and gases. In the left graph error on oil is 14% and on gases is 13.2 %, in the right graph it amount on 7.5% for oils and 8% for gases. The fact that errors on gases remain similar to oils' confirms that the procedure of obtaining gas yields by difference is reliable.

Chapter 8
Products analysis

8.1. Residue analysis

The residue remained in the crucible obviously demonstrate to have undergone to some physical changes, as it is clear from figure 8.1, where the initial polyethylene sample is visually compared to a residue obtained after 60 minutes at 400°C with heating rate 5°C/min and flow rate 50 ml/min.

Figure 8.1 Initial sample of polyethylene and pyrolysis residue.

Residue was analyzed with the differential scanning calorimetry in Helium atmosphere (50 ml/min) with and heating rate of 10°C/min until 250°C and compared to the analysis of the initial sample. In figure 8.2 it shows an anticipated melting point respect to the original polyethylene; in fact it melts at 116.5°C instead of 143.8°C and it seems more refractory to be degraded, since it does not show a completed oxidation peak, but solely an upwarding trend of the curve, that can be identified as the beginning of it, so it may oxidize at higher temperatures.

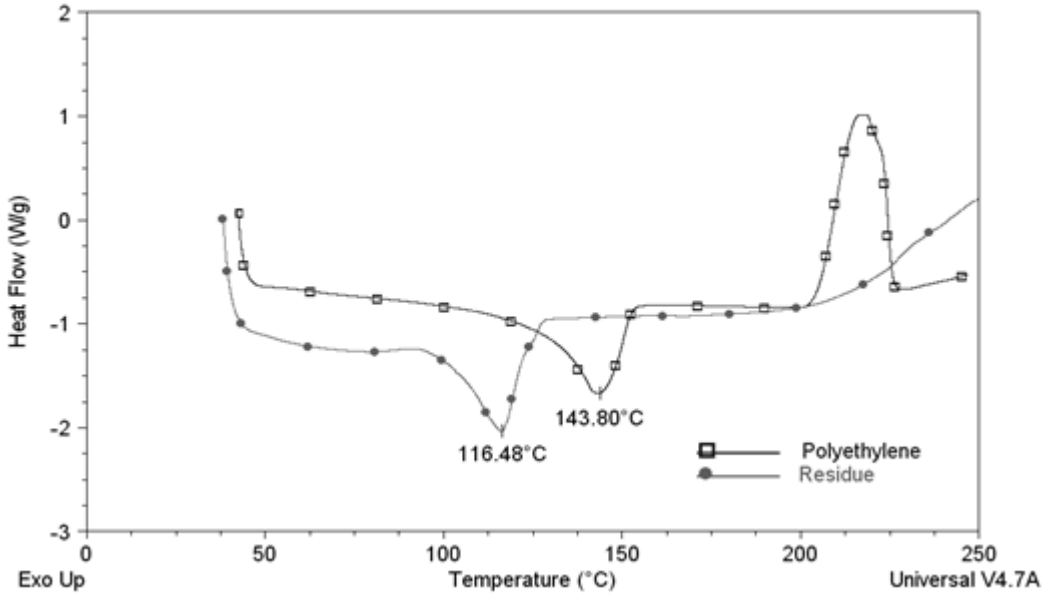

Figure 8.2 DSC of polyethylene and residue in 50 ml/min.

8.2. Gas analysis

8.2.1. Gas identification

The analysis of the gaseous products was performed with the Gas-chromatograph Agilent 6890, already described in paragraph § 5.2. The method developed for polyethylene gases has the following parameters that were partly deduced from the instrument's user guide and partly by experimental tests:

- Injector temperature: 120°C;
- Front and back detectors temperatures: 250°C and 200°C;
- He, H_2 and air flow rates: 60, 53, 270 ml/min, respectively.

The oven ramp aimed at eluting all the compounds in the shortest time, but separating them well is reported in table 8.1 and it lasts 25 minutes.

Table 8.1 Oven ramp in the GC 6890.

Temperature 1 (°C)	Time 1 (min)	Heating rate (°C/min)	Temperature 2 (°C)	Time 2 (min)
100°C	7	35°C/min	180°C	16

In figure 8.3 the gas composition from a polyethylene pyrolysis test run at 400°C for 60 minutes is reported. The gas first was stored in a suited bag then sucked out with a pump and analysed.

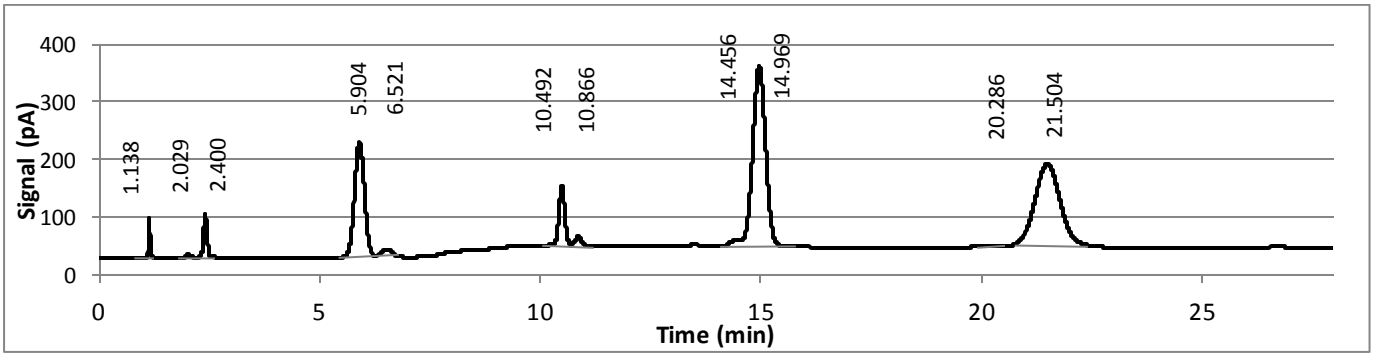

Figure 8.3 Chromatogram of polyethylene degradation at 400°C.

Gaseous compounds are found to be up to C_6 and almost all have been identified with certainty from comparison with available compounds. In table 8.2 are reported identified hydrocarbons residence times; they may undergo small variations among tests.

Table 8.2 Hydrocarbons elution time.

Hydrocarbon	Elution time (min)
Methane	1.138
Ethylene	2.029
Ethane	2.400
Propylene	5.904
Propane	6.521
Butene	10.492
Butane	10.866
Pentene	14.456
Pentane	14.969
Hexene	20.286
Hexane	21.504

It can be deduced that gases produced by polyethylene pyrolysis at low temperatures are mainly light paraffines and olefins, as verified by Donaj et al., 2001. In these operating conditions, the presence of aromatic hydrocarbons (Benzene, Toluene, etc.) was excluded from comparison with Toluene's residence time (6.114 minutes) that differs from all the other found in the chromatogram and from literature (Williams et al., 1998).

Gas compound identification was also attempted by spectra analysis with the Mass spectrometer described in paragraph § 5.1. Sampling of the gases was made through a gas sampling tube (figure 8.4) connected along the gas line. It has an upper hole sealed with a rubber gasket that allows inserting a syringe.

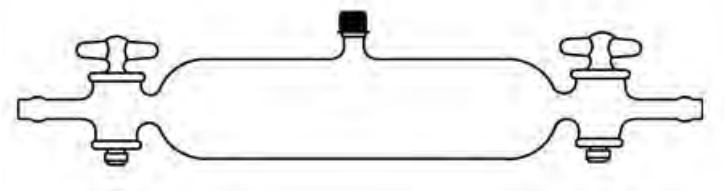

Figure 8.4 Gas sampling tube.

The GC-MS column configuration is suited to separate heavy hydrocarbons, not to analyse the lighter; so the oven heating program (table 8.3) starts from the lowest possible temperature to separate the peaks as much as possible and it is very long in order to detect any present compound. The mass scan is focused between 10 and 150 and the standard 30cc/min split was maintained, since the injected volume is quite considerable (0.7µl).

Table 8.3 Oven programmed temperature in the GC-MS.

Temperature 1 (°C)	Time 1 (min)	Heating rate (°C/min)	Temperature 2 (°C)	Time 2 (min)
36°C	6	6°C/min	180°C	10

Basically, all the compounds exits in the first 8 minutes and in figure 8.5 is reported the obtained chromatogram. They are not well separated and the lightest compound (from C_1 to C_3) are included in the first peak, together with air, that infiltrates during gas sampling. However the second and the third peak are better separated and are identified as Penthene (1.46 min) and Hexene (1.94 min).

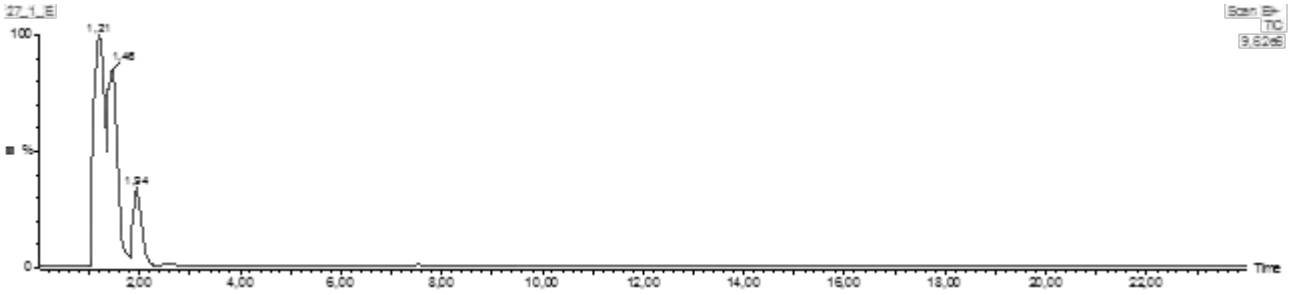

Figure 8.5 Polyethylene pyrolysis gas chromatogram obtained with GC-MS.

Unfortunately it is not possible to improve this analysis, but it allows identifying the presence of other trace gases, as shown in figure 8.6, which is a view of the previous image starting from 2.2 minutes (where Hexene peak ends), scaled on the largest peak. The present peaks are identified as Heptene or methyl-Hexene (2.61 min), methyl-Heptane (5.66 min) and Nonene or dimethyl-Heptene (7.53 min).

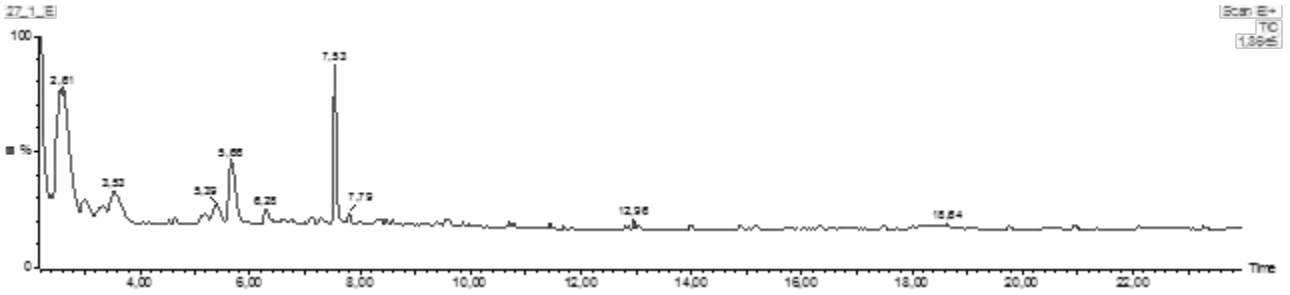

Figure 8.6 Polyethylene pyrolysis gas chromatogram obtained with GC-MS displayed from 2.2 minutes, with the largest peak view function.

Finally the GC-MS could be very useful in gas identification, since a satisfactory sampling method was developed, but it shall be equipped with a column able to separate light compounds, otherwise peaks will overlay as happened in this case.

Gases were also analysed in continuous and with three subsequent analyses it is possible to view the single gases production trend. Analyses start from the beginning of the gas production that happened to be at 75 minutes until the end of the test; each analysis has the duration of 29 minutes and uses the method described in table 8.1.

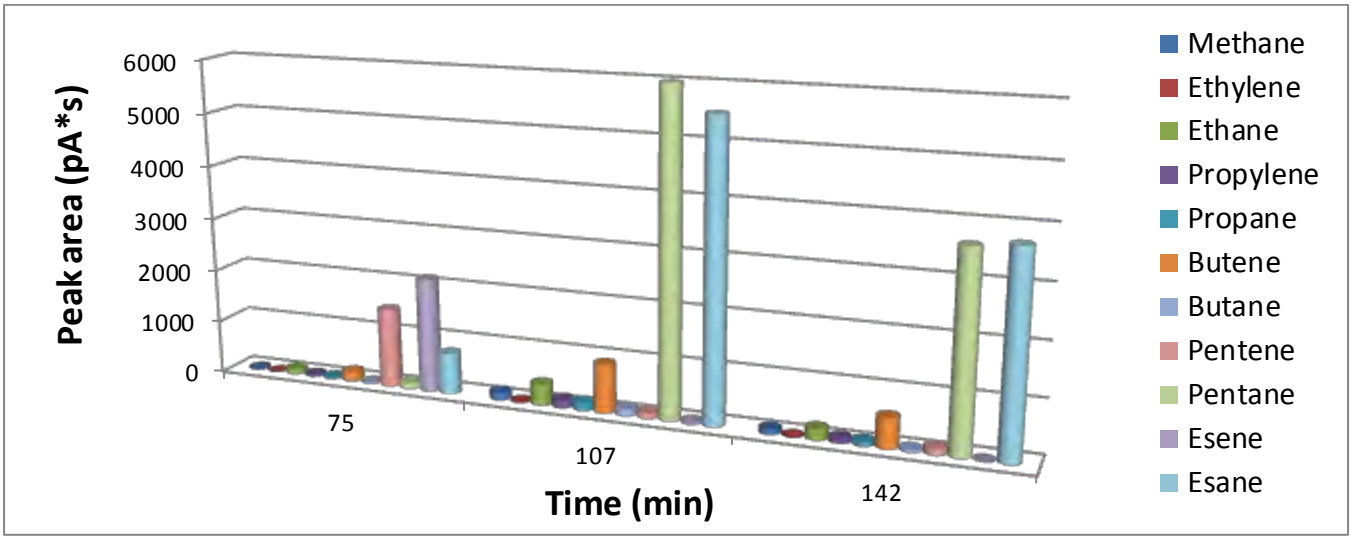

Figure 8.7 Gas production during a polyethylene pyrolysis test.

Even if the signal cannot be associated to a concentration, it is clear that heavier gases (Pentane and Esane) are far more abundant than the lighter (Ethylene, Propylene …). This is consistent with the total produced gas volume (47 ml) collected after a 400°C pyrolysis test lasted 1 hour. Since it is quite low, it shall be constituted prevalently by heavier gases that have a higher molecular weight. In fact higher temperatures (650-800°C) are needed to achieve mainly light gaseous olefins (ethene, propene, butadiene and other) (Kaminsky et al., 2003).

Another attempt for gas quantification was made using Argon as a tracer gas in the flow of inert (He). Its peak shall vary as the total flow rate increases because of gas production. This procedure requires first improving a method for good peaks separation and a sensitivity analysis to understand how and how much the tracer peak is influence by total flow rate and concentration.

The oven ramp used for the previous tests (table 10.1) reveals to be ineffective for the TCD detector, because it does not allow separating all the detected gases, such Argon (tracer), air (that can infiltrates) and Methane and Hydrogen (product gases). CH_4 stays separated from Ar if the oven temperature is not raised above 170°C, but H_2 can be distinguished from Ar only if the oven temperature is lowered to 50°C. It displays a negative peak but its signal is very scarce and thus negligible. Finally this detector cannot separate air from H_2 because the PPQ column is not suited for these gases.

Even doing some approximations (i.e. neglecting H_2 and air infiltrations), the tracer gas quantification method cannot be applied because the Ar peak is influenced by both variables: total flow rate and fraction, although it seems much more sensitive to this last one.

8.2.2. Gas production

To understand when gas is produced, some tests with a by-pass to the GC column were run. The by-pass drives the gases directly to the Front Detector (FID) that detects hydrocarbons and changes intensity of its signal when gas production is ongoing.

To avoid excessive fouling of the instrument, a filter and a bubbler are introduced along the line to clean the gas and a pump with adjusted flow rate serves to stabilize FID's signal.

The signal (S) is also normalized to its minimum value (equation 8.1); because from time to time the initial reading settles on different values and also it increment is greater if the minimum signal is higher.

$$|S| = \frac{S}{S_{min}} \tag{8.1}$$

For this reason FID's signal cannot be considered directly proportional to the quantity of produced gas, but it can serve for qualitative evaluations. In fact from figure 8.8 it is clear that gas production starts approximately at 72 minutes, a short time before the thermal program has reached the final isotherm.

Lower end temperatures (375-385°C) don't favour a consistent gas production, in fact their normalized signal stay far below the 400°C curve, proving that they are not sufficient to degrade the sample even if the isothermal time is quite long (150 minutes). On the contrary, the temperature of 400°C seems able to degrade almost all the sample, since the curve reaches a maximum and then drops.

Provided that 400°C is the suited temperature to degrade the sample, the heating rate was also varied from 3 to 10°C/min. It can be notice in figure 8.9 that with the faster ramp (10°C/min), gas production starts only after the isotherm has been reached.

On the contrary, if the heating rate is very low (3°C/min), degradation starts before, even during the temperature ramp. In this case signals (referred as S) are normalized using the norm function (8.2).

$$|S| = \frac{S - S_{min}}{S_{max} - S_{min}} \tag{8.2}$$

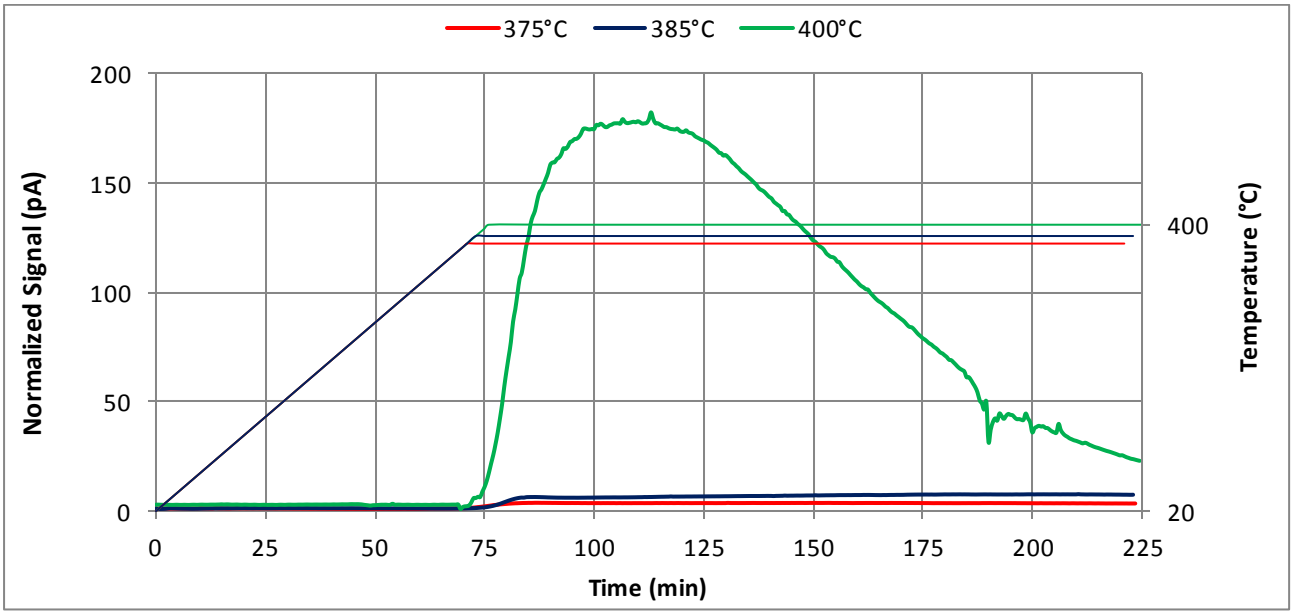

Figure 8.8 FID signals curves for three end temperatures (375-385-400°C) with 5°C/min heating rate.

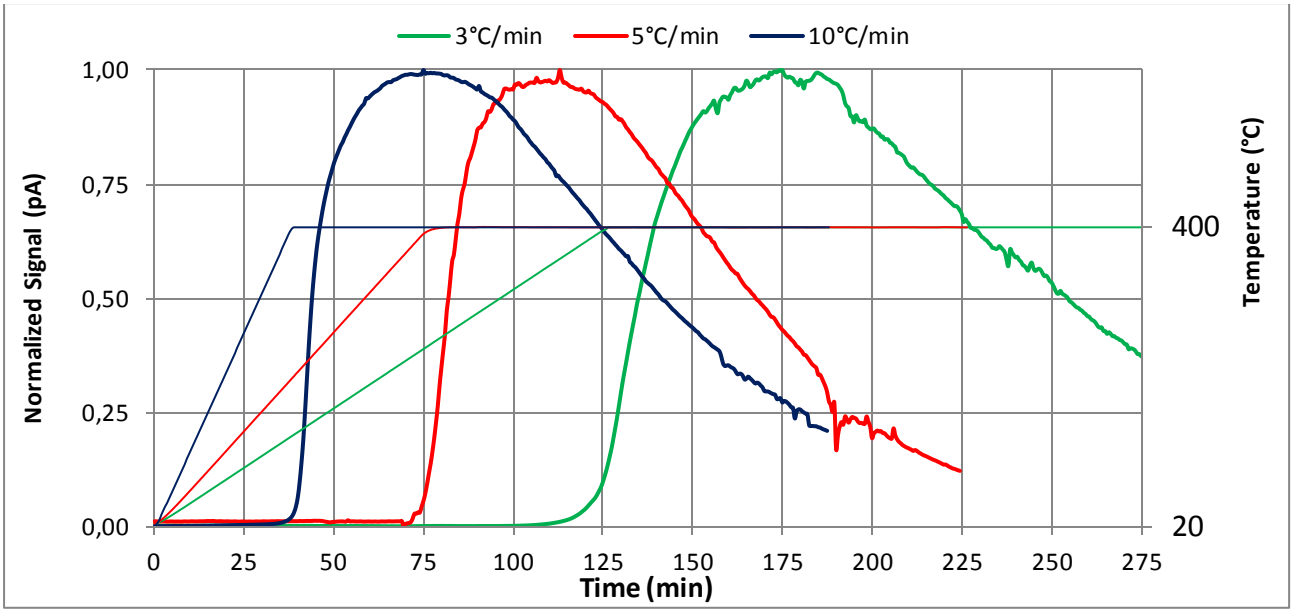

Figure 8.9 FID signals curves for three heating rates 3-5-10°C/min till 400°C for 150 minutes.

8.3. Oil analysis

8.3.1. Differential scanning calorimetry

The DSC analysis of the oils was carried out in 50 ml/min of Helium up to 300°C with a heating rate of 10°C/min. The result (figure 8.10) is clearly different from the initial polyethylene sample (paragraph § 2.1); in particular oils have no distinct fusion point as expected by a moisture of species. Above 200°C sample starts to volatilize and so the curve indicate and apparent exothermicity due to the loss of the 83% of the oil.

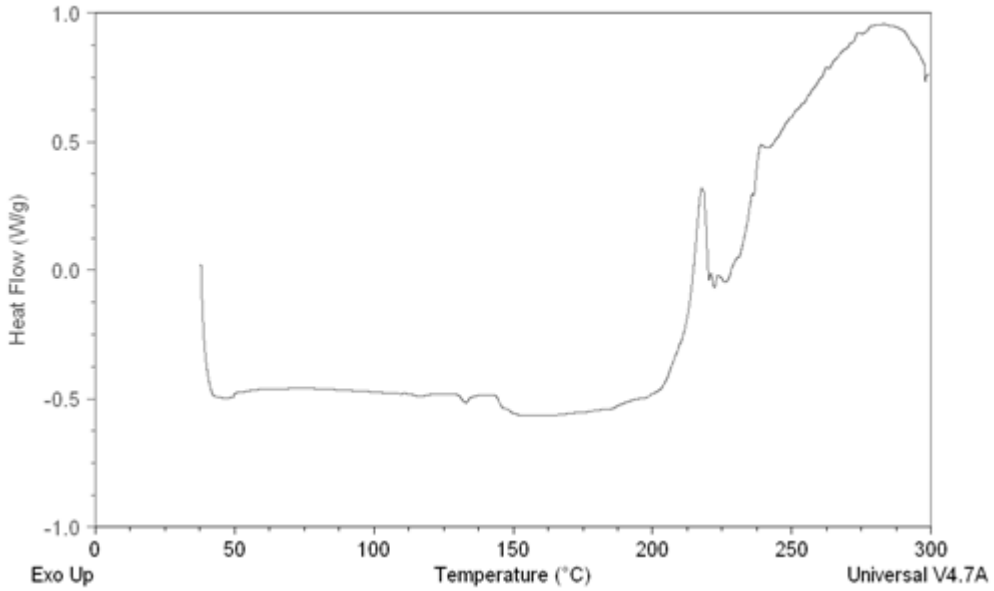

Figure 8.10 DSC analysis of the pyrolysis oil obtained after 60 minutes at 400°C with 5°C/min heating rate of and 20 ml/min flow rate.

8.3.2. Mass spectrometry

In order to perform GC-MS analysis, some parameters were preliminarly investigated such as: type of solvent, quantity of injected sample, oven program and degree of dilution.

The initial quantity of injected sample was 0.7 µl (using a 1 µl syringe); it was reduced down to 0.2 µl when the instrument was perfectly tuned. The injected amount does not seem to influence the output signal, so it was kept low not to overload the column. Oven temperature varies from 80°C to 280°C (table 8.4) and a ramp of 5°C/min seemed adapt to separate peaks well without prolonging too much the analysis. The mass scan is focused between 20 and 650 amu and the standard 30 cc/min split is maintained.

Table 8.4 Oven program for oils analysis in the GC-MS.

Temperature 1 (°C)	Time 1 (min)	Heating rate (°C/min)	Temperature 2 (°C)	Time 2 (min)
80°C	1	55°C/min	280°C	20

The ratio of dilution depends on the capacity of the solvent to dissolve the sample and does not affect the detector signal, as it is shown in figure 8.11, where the same amount of eicosane (0.02 g), used a s model species, was dissolved in increasing quantities of dichloromethane (from 2 to 8 ml). The first peak (1.66 min) is the solvent and the second is the solute (13.9 min). The oven ramp was different from the oils' one to shorten the analysis duration (15°C/min instead of 5°C/min), but isothermal times and temperature range were the same (80-280°C). It can be noticed that the TIC remains approximately the same.

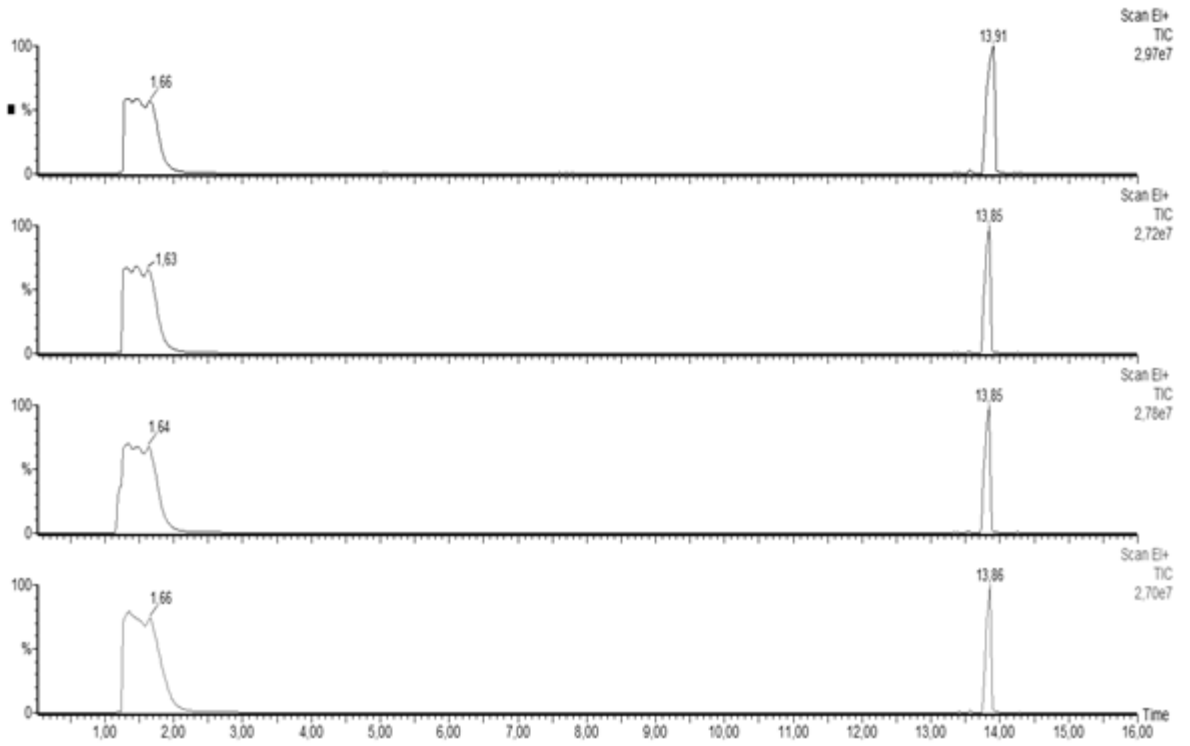

Figure 8.11 TIC signal's for different dilution ratio of eicosane in dichloromethane: 0.02 g eicosane were diluted in 2-4-6-8 ml dichloromethane from top to bottom, respectively.

In the choice of the solvent, dichloromethane was preferred to hexane and heptane, because it has a better capacity in dissolving the oil, as it is clear from figure 8.12, where the same quantity of oil (0.03 g) was diluted respectively in 3 ml of Dichloromethane, Esane and Heptane.

The three solvents are compared by means of a view that starts from 4 minutes onward, after that the solvent has been eluted from the column and they are displayed on the same TIC signal.

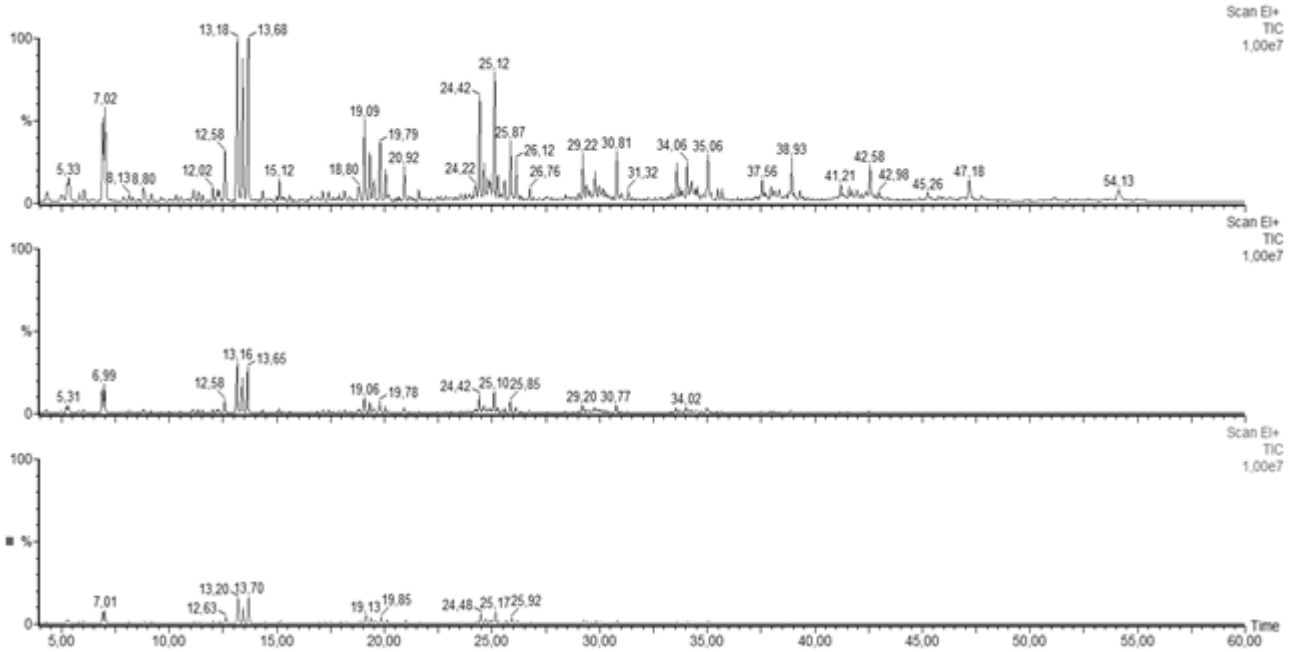

Figure 8.12 Chromatograms for 0.03 g oil diluted in 3 ml of Dichloromethane, Esane and Heptane, from top to bottom, respectively.

The minimum dilution ratio between grams of oil and ml of dichloromethane was found to be 0.01 g/ml. For lower ratios, the sample does not dissolve and only some peaks appear, as it can be seen in figure 8.13.

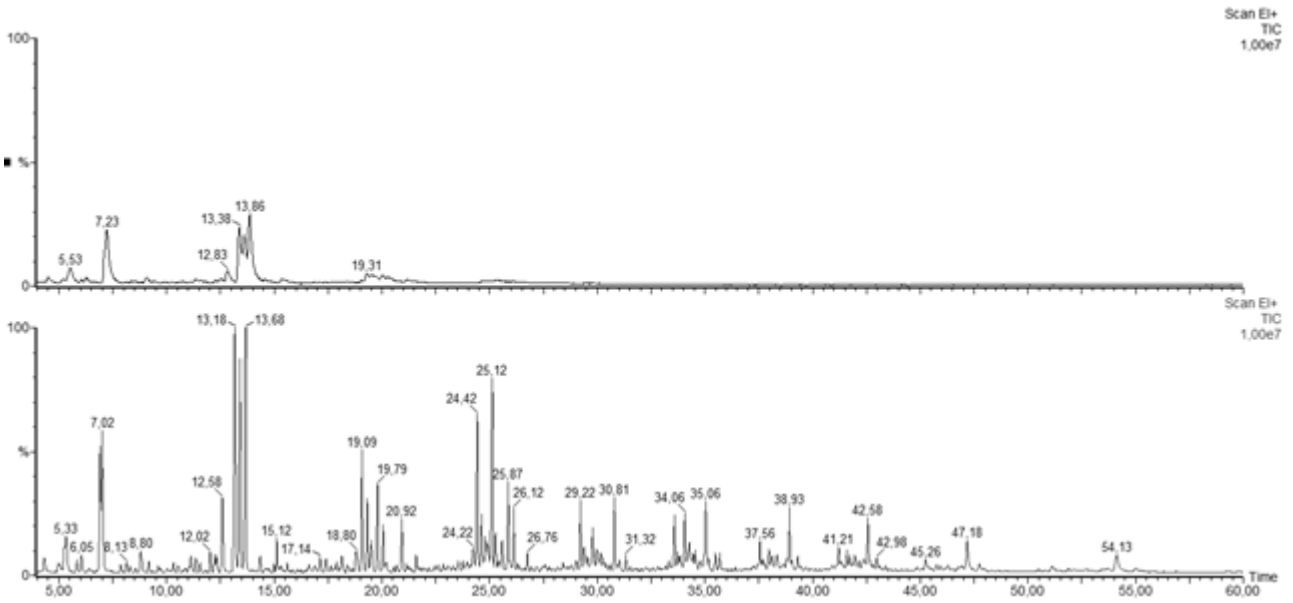

Figure 8.13 Chromatograms for 0.03g oil diluted in 2 (above) and 3 ml of Dichloromethane (below).

This is the starting point for a general oil characterization. It is clear that the first two group of peaks are branched otherwise they will not dissolve so easily in less solvent. The rest of the chromatogram presents a bell-shaped curve that starts at 15 minutes and ends at 54 and is characteristic of oils' analysis.

From the retention time of the eicosane with the same oven ramp (30.33 minutes), it can be deduced that the group of peaks that are eluted in about 30 minutes are C_{20}.

From the comparison with a traction fuel oil, which was constituted prevalently by linear alkanes, the retention times of the C_{10}-C_{20} can be deduced. This oil is used as fuel for agricultural machines and for other activities with agricultural purposes; technical details are reported in appendix A The traction fuel oil presents the oils' characteristic bell-shaped curve with the exception of two oxygenated compounds that were identified as additives and are of no interest for the identification purpose. In figure 11.6 the pyrolysis oil is compared with the traction fuel oil.

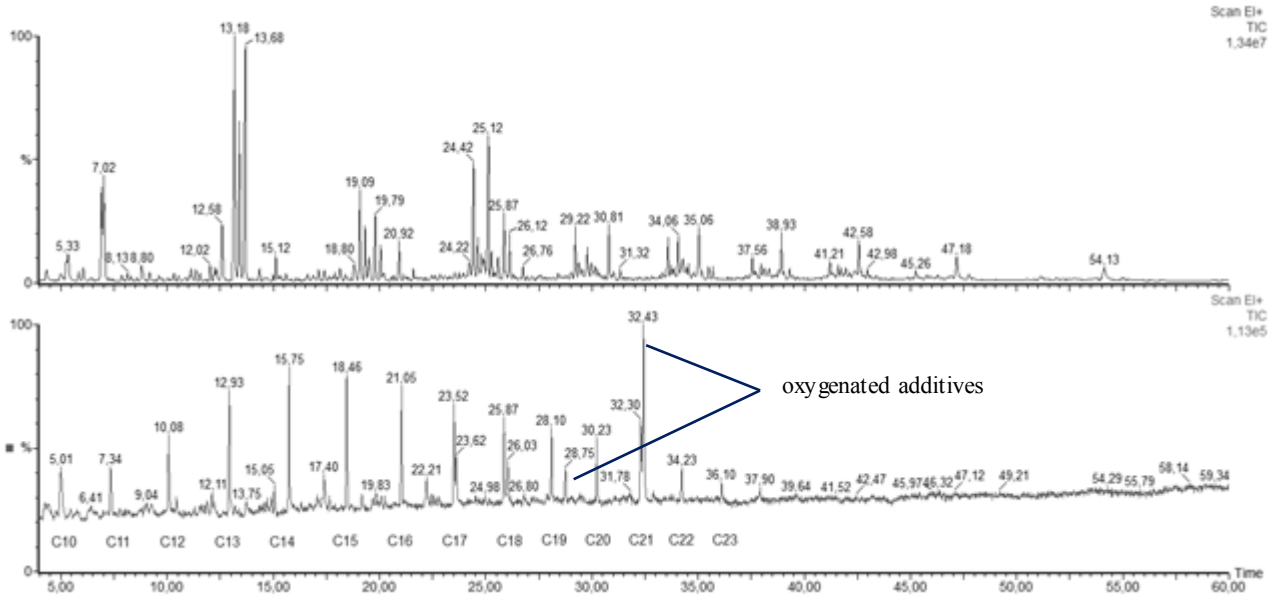

Figure 8.14 Polyethylene pyrolysis oil (up) and traction fuel oil with alkanes' retention times.

It is evident that the composition of the pyrolysis oil is far more complex that the traction fuel oil, because it presents different alkenes and isomers but to get a deep characterization was not the focus of this work; on the contrary it was important to define the heaviness of the oil through the number of carbon atoms of its species. Furthermore no cyclic aromatic compound were detected, so the problem of PAH pollution in the case of its reuse trough combustion is minimized. As far as the average molecular weight, the pyrolysis oil seems heavier than the traction one and more similar to a burning one, as it is clear from figure 8.15. This oil is used mainly for heating purposes and the final tail of its chromatogram presents a baseline drift that should not be considered as a curve second bell but a noise effect caused by an accumulation of heavier molecules released by the column. It was almost eliminated by dilution, but it still hinders the identification of compounds in the last part of the chromatogram.

It must be noticed that the dilution ratio with dichloromethane that was appropriate for the pyrolysis oil it is not for the traction oil and for the burning oil and it was lowered to 0.8 g/ml; otherwise the solute was too diluted and was not detected by the GC-MS.

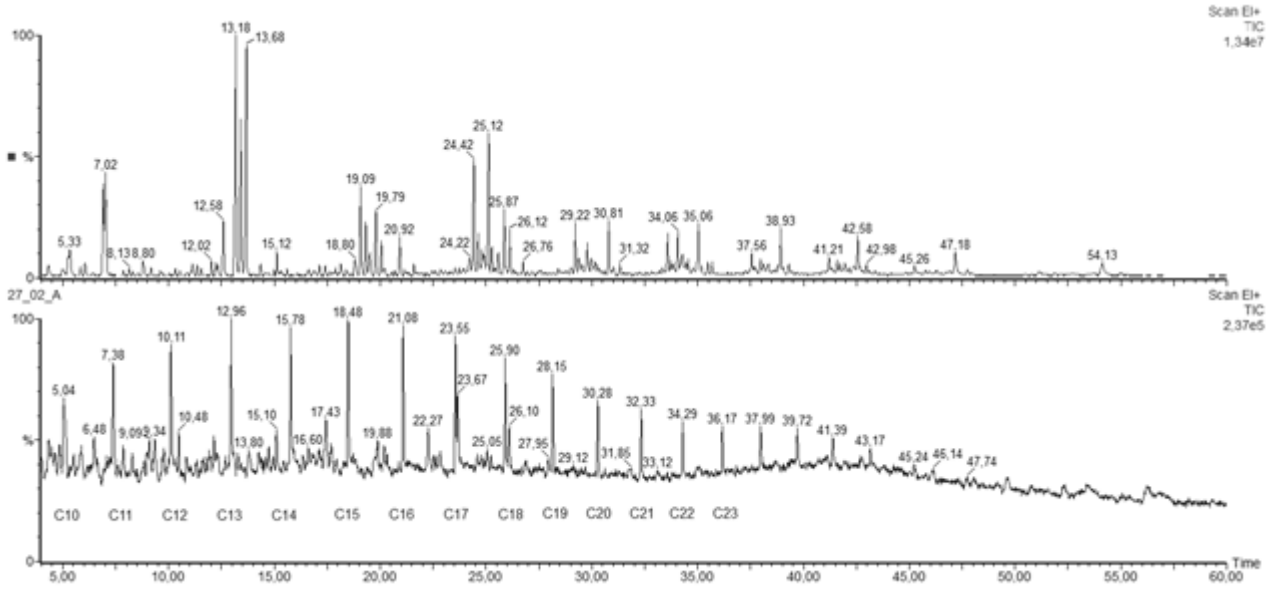

Figure 8.15 Polyethylene pyrolysis oil (up) and burning oil with alkenes retention times.

Finally, oil composition does not show remarkable variations with pyrolysis end temperature, final isotherm duration and inert flow rate. In figures 8.16-18 are reported comparative graphs for each of the parameter investigated. It is seems obvious that the flow rate shall have no influence on the oil composition, but determine its quantity and this is verified through the series of analysis presented in figure 8.16.

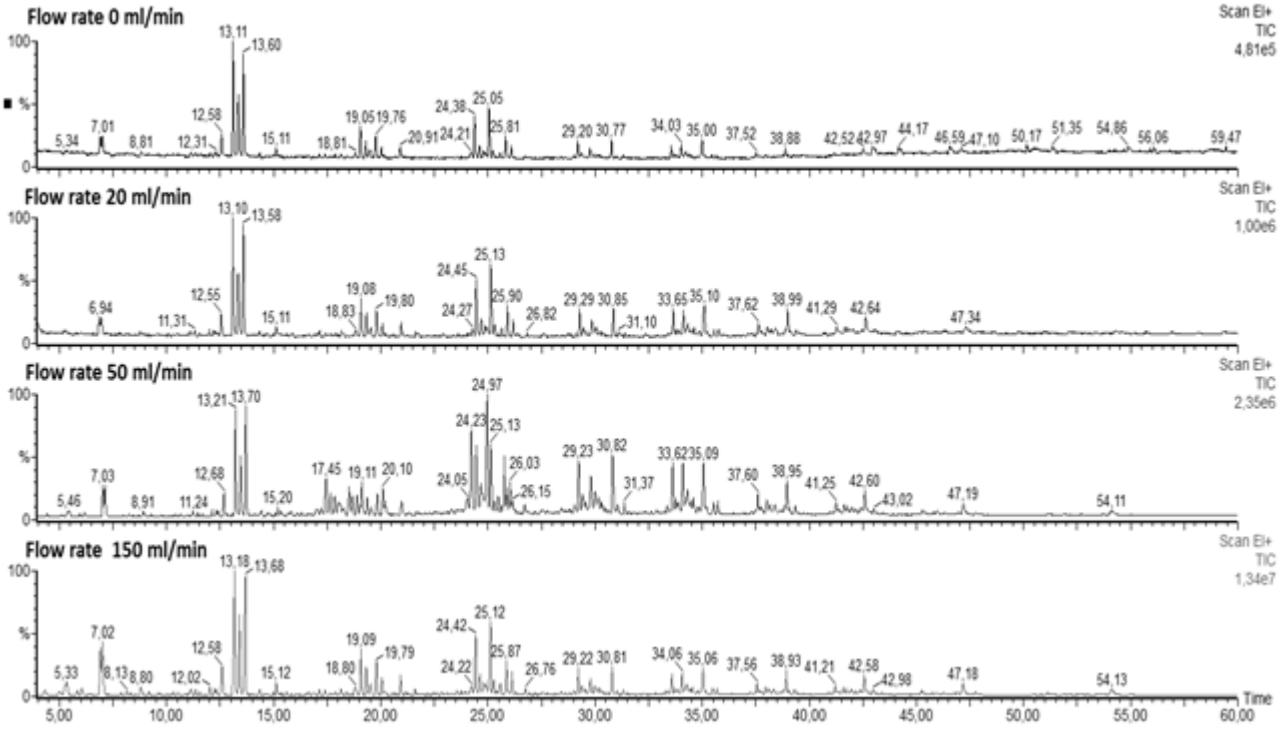

Figure 8.16 Polyethylene pyrolysis oil obtained at different flow rates with the same end temperature (400°C), heating rate (5°C/min) and isothermal time (60 min.).

As far as end temperature and heating rate, these have seems not to affect oils' composition too. Pyrolysis end temperature was lowered from 400°C to 385 and 375°C and the oils' spectra remains the same, as shown in figure 8.17; this is probably due to the fact that the temperature is too low to have any considerable effect.

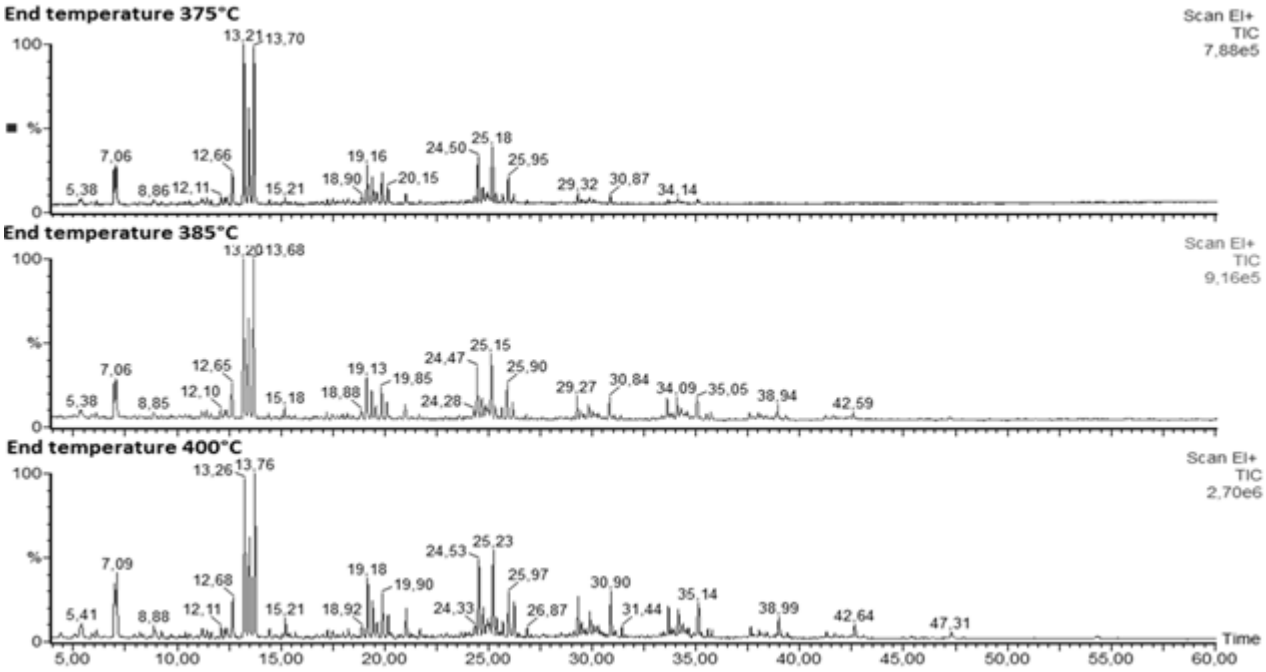

Figure 8.17 Polyethylene pyrolysis oil obtained at different end temperatures with the same heating rate (5°C/min), isothermal time (60 min.) and flow rate (50 ml/min).

The 5°C/min heating rate was both lowered to 3°C/min and increased to 10°C/min, but oils' chromatogram is always equal (figure 8.18). The 10°C/min spectrum seems to contain less species, but this is an effect of the background noise that is also present in the 3°C/min one, even if smaller. The 5°C/min and the 3-10°C/min analysis were run in different times, so with different tuning state of the instrument and the lack of the peak at 7.01 minutes in the last two is quite certainly due to the different sensibility of the GC-MS and not to a variation of composition.

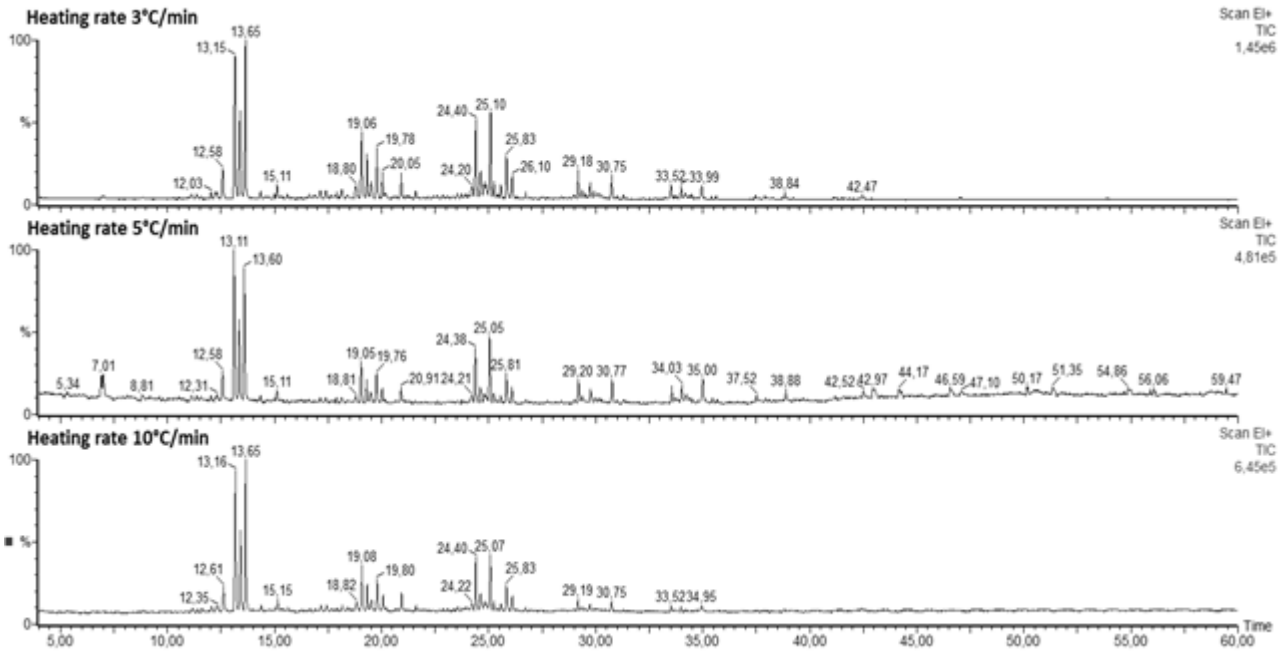

Figure 8.18 Polyethylene pyrolysis oil obtained at different heating rates with the same end temperature (400°C), isothermal time (60 min.) and flow rate (50 ml/min).

Conclusions

This master thesis work was aimed at experimentally investigating viable processes to extract useful products from waste polyethylene. This kind of plastic together with polypropylene is the mostly present in the municipal solid waste and pyrolysis is the way to get valuable oils and gases than can be used for energy purposes.

Preliminary tests investigated the physical behavior of plastics when heated; being a polymer it is a poor thermal conductor difficult to be uniformly heated. Melting occurs at 143°C and above this temperature, sample can became extremely fluid; decomposition causes some bubbling phenomena. Oxidation happens at 216°C and can lead the polymer to reticulate and increase its viscosity.

These considerations were taken into account in the design of the reactor; it was equipped with an upper filling of refractory material to improve gas pre-heating and with a crucible suited to retain the sample in the hot zone enhancing its degradation and its conversion into products.

Condensation happens at ambient temperature with water as cooling fluid; condensation was well satisfactory considering that the plant has a significant oil yield, between 60 and 70%wt of the initial sample, at the best conditions. These were identified by a series of tests, where parameters that are thought to influence oil production were investigated. It was found that oils yield can be maximized adjusting inert gas flow rate, maximum temperature, heating rate and permanence at the maximum temperature (isothermal time).

It was demonstrated with quite a good reproducibility that the best inert gas flow rate is 50 ml/min, allowing the best compromise between residence times in the reactor and in the condenser.

As known from literature (Williams et al, 1998), slow heating rates and low maximum temperatures favor oil production, but it was also proven that at lower temperature, such as 375 and 385°C an insufficient sample conversion is obtained within a reasonable reaction time. The remaining sample in the crucible raises to 60% and 39%, respectively; hence it is necessary to work at least at 400°C to maintain the residue quite low (9%).

Between the three values of heating rates investigated, 3-5-10°C/min, the one that provides the higher oil quantity is 3°C/min (73%); however the 5°C/min seems to be a good compromise to keep the tests short enough; its oil yield is 71%, much higher than at 10°C/min (66%).

Isothermal time at the chosen maximum temperature (400°C) has a slighter influence in oil production; in 80 minutes the maximum oil conversion can be reached (71%), but even doubling the time (150 minutes) oil yield remains fairly constant; the further sample conversion is into gases.

As regard to gas production, decomposition of PE begins at lower temperatures for slower heating rate, likewise happens for both PS and PP (Kim et al, 2003).

Gaseous products are a mixture of alkanes and alkenes up to C_6; traces of heavier compounds were detected by the mass spectrometer (up to C_9).

Oil composition was analyzed by GC-MS and linear hydrocarbons up to C_{26} were detected. Its composition is very complex; the mixture is clearly made by alkanes and alkenes with the double

bound in different position, but no aromatic compounds were found. This is particularly good for oil reuse as a fuel, due to the fact that they are identified as carcinogenic and thus banished.

Further suggested possible improvements are more elaborated heating programs, to uniformly heat and melt the sample; in this way the sample would degrade better and more extensively. Changing the heating program can also serve to manipulate oil composition, increasing the amount of linear hydrocarbons.

Appendix

Polyethylene technical sheets

Polyethylene 2 (PE2)

DOWLEX 2607G

Polyethylene Resin

Melt Index:	2.3
Density:	0.918

DOWLEX 2607G Polyethylene Resin is specifically designed for large/high output cast film lines to make high performance industrial stretch films.

Films made from DOWLEX 2607G Polyethylene Resin exhibit an excellent balance of processability, mechanical and stretchability performance properties.

DOWLEX 2607G Polyethylene Resin is to be used as a core resin in coextruded cast film structures together with a cling resin for films in the thickness range between 10 and 35 microns.

Note:
DOWLEX 2607G Polyethylene Resin should comply with FDA regulation 177.1520 and with most European food contact regulations when used unmodified and processed according to good manufacturing practices for food contact applications.

Please, contact your nearest Dow office for food contact compliance statements. The purchaser remains responsible for determining whether the use complies with all relevant regulations.

Applications:
- Cast Stretch Wrap Film.

Resin Properties[1]	Unit		Test Method	Values
Melt Index, 190 °C/2.16 kg	g/10 min		ISO 1133	2.3
Density	g/cm^3		ASTM D-792	0.918
Cast Film Properties, 23 µm[1,2]	**Unit**		**Test Method**	**Values**
Puncture Resistance				
Elongation	J		ASTM D-5748	160
Force	N			44
Dart Impact (Method A)	g		ISO 7765-1	150
Elmendorf Tear	g	MD	ASTM D-1922	190
		CD		420
Tensile Yield	MPa	MD	ASTM D-882	8
		CD		8
Ultimate Tensile	MPa	MD	ASTM D-882	35
		CD		29
Ultimate Elongation	%	MD	ASTM D-882	460
		CD		700
Stretch Performance[1,2]	**Unit**		**Test Method**	**Values**
Maximum Stretch	%		DOW METHOD	345
Maximum Stretch Force	kg		DOW METHOD	37

Fabrication Conditions For Cast Film Extrusion:
- Chill Roll Temperature: 20 to 40° C.
- Melt Temperature: 220 to 280° C.
- Recommended Gauge Range: 10 to 35 µm.

(1) Typical values; not to be construed as specification limits.
(2) Cast Film fabrication at 250 m/min.

Polyethylene 3 (PE 3)

A. Schulman Plastics S.p.A.
Via Baraggiola,6 – 21050 Gerla Maggiore- Varese - ITALIA
Tel +039 0331.60741 Fax +039 0331.366340

www.aschulman.com
www.polybatch.net

Gruppo Prodotto : **BREATHABLE**
Prodotto : **BTF 272 NP** Colore: **NATURALE**
Imballo : (sacchi pe)

Data Rilascio : 16/02/2005
Data revisione : 12/01/2005
Revisione # : 1

PROPRIETA'	UNITA' MISURA	METODO TEST	LIMITI
MFI 190°C – 2,16 Kg.	g /10 min	ASTM 1238 A	1,0 – 3,0
MVI 190°C – 2,16 Kg.	cc/ 10 min	ASTM 1238 B	0,7 – 2,5
PESO SPECIFICO	g / cm^3	ISO 1183	1,72 +- 0,04
DENSITA' APPARENTE	Kg/m3	ASTM D 1895-96	900,0 – 1100,0
CONTENUTO DI UMIDITA'	ppm	DIN 53715	MAX 300
CONTENUTO DI CENERI	%	SCHULMAN 435	68,0 – 72,0
RESINA BASE	---	---	PE
FORMA DEL GRANULO	---	---	SFERICO/CIL
IDONEITA' ALIMENTARE	---	---	APPROVATO
CONTENUTO TOTALE DI ADDITIVO	%	---	70 +- 2

Polyethylene 4 (PE 4)

TVK

TECHNICAL DATA SHEET

Polymer Marketing and Sales, Customer Service

TIPPLEN R 659

TIPPLEN R 659 is a random copolymer polypropylene for extrusion and injection moulding. **TIPPLEN R 659** is formulated with a nucleating agent. The product shows excellent transparency and gloss.

Typical application include the blow moulded bottles for detergent and toiletries and flat mineral water.

TIPPLEN R 659 is well suited for extruded sheet for stationery folder and thermoforming articles.

TIPPLEN R 659 is suitable for food contact. The product complies with FDA, BGA and EU norms.

Properties	Standard method	Unit	Value
MFI (2.16 kg/230 °C)	ISO 1133	g/10 min.	2
Tensile strength at yield	ISO 527	N/mm^2	30
Elongation at yield	ISO 527	%	13
HDT - 0.46 N/mm^2	ISO 75	°C	80
Rockwell hardness	ISO 2039/2	R scale	70
Flexural modulus of elasticity (drawn)	ISO 527	N/mm^2	950
Izod impact strength (notched, +23 °C)	ISO 180/1A	kJ/m^2	22

- MFI measured at 230 °C under a load of 2.16 kg with standard nozzle having a diameter of 2.095 mm.
- Average mechanical property values of several measurements carried out on standard injection moulded specimens (ISO 3167) conditioned at room temperature (ISO 291).

Polyethylene 6 (PE6)

A. Schulman Plastics S.p.A.
Via Baraggiola,6 – 21050 Gorla Maggiore- Varese -
ITALIA
Tel 0331.607401
Fax 0331.366340

Gruppo Prodotto : **BREATHABLE** Data Rilascio : 16/02/2005
Prodotto : **BTF 222** Colore: **NATUARLE** Data revisione : 05/01/2004
Imballo : (sacchi pe) Revisione # : 1

PROPRIETA'		UNITA'MISURA	METODO TEST	LIMITI
MFI 190°C – 2,16 Kg.		g /10 min	ASTM 1238 A	1,1 – 2,3
MVI 190°C – 2,16 Kg.		cc/ 10	ASTM 1238 B	0,7 – 1,5
PESO SPECIFICO	#	g / cm^3	ISO 1183	1,41 +- 0,04
DENSITA' APPARENTE		Kg/m3	ASTM D 1895-96	900,0 – 1100,0
CONTENUTO DI CENERI		%	SCHULMAN 435	68,0 – 72,0
Nr°GRANULI per GRAMMO	#	p/gr	SCHULMAN 465	35,0 – 50,0

Polyethylene 9 (PE 9)

Polyethylene
Borstar® FB4370
Bimodal PE film

Description
Borstar FB4370 a polyethylene grade combining excellent extrusion properties with high film stiffness and is well suited for blends and coex film applications. Borstar FB4370 gives as mono film a hazy matt surface. Good optical properties are achieved in a coex film with skin layers of PE's with good optical properties.

Applications
Borstar FB4370 is well suited for applications like:
- Core layer for lamination films
- Shrink films
- FFS automatic packaging
- Stiffness blending component

Additives
Borstar FB4370 contains antioxidant.

Physical Properties

		Typical Value*	Unit	Test Method
Density		937	kg/m^3	ISO 1183
Melt Flow Rate	(190°C/2.16 kg)	0.4	g/10 min	ISO 1133

* Data should not be used for specification work

Processing Guidelines
Borstar FB4370 is easily processed on conventional extruders. FB4370 is especially developed as an easy processing Borstar which gives low melt pressure also in blown coex film lines. Conventional LDPE die gaps 1,2-1,5 mm is recommended and this will give the best balance between extruder melt pressure and physical film properties.

Recommended melt temperature range is from 190°C to 210°C. Due to differences in screw and die head designs the optimum temperature adjustments are individual and should be sought for each production line.

With suitable equipment **Borstar FB4370** can be drawn down to 20 micron as mono film.

Film Properties**
The Film properties are strongly depending on the extrusion conditions.

		Typical Value*	Unit	Test Method
Tensile strength	MD/TD	56/39	MPa	ISO 527-3
Strain at break	MD/TD	530/830	%	ISO 527-3
Tensile modulus	MD/TD	450/540	MPa	ASTM D 882-A
Friction, COF		0,4	–	ISO 8295
Dart drop		130	G	ISO 7765/1
Tear resistance	MD/TD	1,5 / 10	N	ISO 6383/2

Storage and handling
Borstar FB4370 should be stored in dry conditions at temperatures below 50°C and protected from UV-light.

Oils technical sheets

Traction fuel oil

GASOLIO AGRICOLTURA

Scheda di dati di sicurezza
Conforme Regolamento (CE) n. 453/2010

Codice prodotto: GASOLIO motore (Tutti i tipi)
Data della revisione SDS: 27/09/2012
Versione della SDS: 1.1

Proprietà fisiche e chimiche

9.1. Informazioni sulle proprietà fisiche e chimiche fondamentali

Stato fisico	: Liquido
Aspetto	: Liquido limpido.
Massa molecolare	: Non applicabile (UVCB).
Colore	: Colore naturale: giallo pallido / ambra Nei casi previsti dalla legge il prodotto viene colorato artificialmente. GASOLIO AGRICOLTURA (Italia): Verde GASOLIO MOTOPESCA (Italia): Verde.
Odore	: Simile al petrolio.
Soglia olfattiva	: Dati non disponibili
pH	: Non applicabile
Punto di fusione	: (CFPP, EN 116) (a seconda dello specifico prodotto) °C
Punto di congelamento	: -20 - -2 °C (CFPP, EN 116) (a seconda dello specifico prodotto)
Punto di ebollizione	: 200 °C (ASTM D 86)
Punto d'infiammabilità	: ≥ 56 °C (ASTM D 93)
Velocità d'evaporaz. rel. All'acetato butilico	: Dati non disponibili
Infiammabilità (solidi, gas)	: Non applicabile
Limiti d'esplosività	: 0,6 - 7,5 vol %
Tensione di vapore	: ca 0,4 kPa (40 °C) (CONCAWE, 1996)
Densità relativa di vapore a 20 °C	: Dati non disponibili
Densità relativa	: Dati non disponibili
Densità	: 820 - 845 kg/m³ (EN ISO 3675 / EN ISO 12185)
Solubilità	: Il prodotto non è solubile in acqua. Acqua: Non miscibile e insolubile Solvente organico:completamente solubile.
Log Pow	: Non applicabile
Temperatura di autoaccensione	: ≥ 220 °C
Temperatura di decomposizione	: Dati non disponibili
Viscosità, cinematica	: 2 - 7,4 mm²/s (40 °C) (ASTM D 445) (a seconda dello specifico prodotto)
Viscosità, dinamica	: Non determinato
Proprietà esplosive	: Nessuno.
Proprietà ossidanti	: Nessuno.
Contenuto VOC	: = 100 % EU, CH

Burning oil

IPLOM
SOCIETA' PER AZIONI

ALLIBRAMENTO: 53

Rapporto di prova:	**96-14-C**	**Data emissione:**	**05/02/2014**
Protocollo Campione:	**2723-14**	**Data Ora Campione:**	**05/02/2014 00:04**
Descr. Campione:	**31**	**Origine:**	**serbatoio 31**
Tipo Prodotto:	**OC Denso BTZ Ecoden**	**Tipo Campione:**	**Presa Campioni**

Prove di laboratorio	Unità	Valore Analisi	Metodo
Massa volumica (a15°C)	kg/dmc	0.9499	UNI EN ISO3675/12185
Acqua per distillazione	% vol.	0.05	ASTM D 95 / ISO 3733
Viscosità a 50°C °E	øE	14.84	UNI EN ISO 3104
Viscosità a 80°C cSt	cSt	32.0	UNI EN ISO 3104
Residuo Carb. Conradson	% wt.	4.82	ASTM D 189/ISO 6615
Zolfo	% wt.	0.295	UNI EN ISO 8754
Punto di Infiammabilità	øC	77.0	UNI EN ISO 2719
Punto di scorrimento	øC	-12	ASTM D 97 / ISO 3016
Raccolto a 300°C	% vol.	< 60.0	UNI EN ISO 3405
Raccolto a 350°C	% vol.	< 85.0	UNI EN ISO 3405
Ceneri	% wt.	0.022	UNI EN ISO 6245
Vanadio	ppm	6.5	UNI EN 13131
Nichel	ppm	34.5	UNI EN 13131
Asfalteni	% wt.	0.6	IP 143
Sedimenti per estrazione	% wt.	0.01	ASTM D 473/ISO 3735
Potere Calorif. Inferiore	kcal/kg	9975	ASTM D 240

References

Websites

http://www.pslc.ws/italian/dsc.htm

http://europa.eu/legislation_summaries/environment/waste_management

www.ctechglass.com

Articles

Abatzogloua N., Barkerb N., Haslerc P., Knoefd H., The development of a draft protocol for the sampling and analysis of particulate and organic contaminants in the gas from small biomass gasifiers, Pergamon, 1999.

Al-Salem S.M., Lettieri P., Baeyens J., Recycling and recovery routes of plastic solid waste (PSW): A review, Waste Management, 2009.

Adrados A., de Marco I., Caballero B.M., López A., Laresgoiti M.F., Torres A., Pyrolysis of plastic packaging waste: A comparison of plastic residuals from material recovery facilities with simulated plastic waste, Waste Management, 2011.

Arabiourrutia A., Elordi G., Lopez G., Borsella E., Bilbao J., Olazar M., Characterization of the waxes obtained by the pyrolysis of polyolefin plastics in a conical spouted bed reactor, Journal of Analytical and Applied Pyrolysis, 2011.

Buekens A.G., Huang H., Catalytic plastics cracking for recovery of gasoline-range hydrocarbons from municipal plastic wastes, Resources, Conservation and Recycling, 1998.

Cozzani V., Nicolella C., Rovatti M., Tognotti L., Influence of Gas-Phase Reactions on the Product Yields Obtained in the Pyrolysis of Polyethylene, Ind. Eng. Chem. Res., 1997.

Della Zassa M., Favero M., Canu P., Two-steps selective depolymerization of polyethylene. Feasibility and devolatization heating policy, Journal of Analytical and Applied Pyrolysis, 2010.

Donaj J. Pawel, Kaminsky W., Buzeto F., Yang W., Pyrolysis of polyolefins for increasing the yield of monomers' recovery, Waste Management, 1999.

Greco A., Maffezzoli A., Correction of melting peaks of different PE grades accounting for heat transfer in DSC samples, Elsevier, 2007.

Islam M.R., Joardder M.U.H., Hasan S.M., Takai K., Haniu H., Feasibility study for thermal treatment of solid tire wastes in Bangladesh by using pyrolysis technology, Waste Management, 2011.

C. Li, Suzuki K., Tar property, analysis, reforming mechanism and model for biomass gasification-An overview, Elsevier, 2008.

Kaminsky W., Pyrolysis of polymers, Makromol. Chem., Macromol Symp., 1991.

Kaminsky W., Recycling of polymeric material by pyrolysis, Makromol. Chem., Macromol Symp., 1991.

Kaminsky W., Predel M., Sadiki A., Feedstock recycling of polymers by pyrolysis in a fluidised bed, Polymer Degradation and Stability, 2003.

Kaminsky W., Schlesselmann B., Simon C., Olefins from polyolefins and mixed plastics by pyrolysis, Journal of Analytical and Applied Pyrolysis, 1994.

Kim S.-S., Kim S., Pyrolysis characteristics of polystyrene and polypropylene in a stirred batch reactor, Chemical Engineering Journal, 2003.

Lam S. S., Russell A., Lee C. L., Chase H.A., Microwave-heated pyrolysis of waste automotive engine oil: Influence of operation parameters on the yield, composition, and fuel properties of pyrolysis oil, Fuel, 2011.

Mastellone M.L., Thermal treatments of plastic wastes by means of fluidized bed reactors, Ph.D. Thesis, Department of Chemical Engineering, University of Naples.

McCaffrey W. C., Kamal M. R., Cooper D. G., Tertiary recycling of polyethylene: mechanism of liquid production from polyethylene by thermolysis/reactive distillation, Polymer Degradation and Stability, 1997.

McCaffrey W. C., Kamal M. R., Cooper D. G., Thermolysis of polyethylene, Elsevier, 1994.

Moersch O., Splietho H.□, Hein K.R.G. Tar quantification with a new online analysing method, Pergamon, 1999.

Predel M., Kaminsky W., Pyrolysis of mixed polyolefins in a fuidised-bed reactor and on a pyro-GC/MS to yield aliphatic waxes, Polymer Degradation and Stability, 2000.

Siddiqui M. N., Redhwi H. H., Pyrolysis of mixed plastics for the recovery of useful products, Fuel Processing Technology, 2009.

Wang H., Chen D., Yuan G., Maa X., Dai X., Morphological characteristics of waste polyethylene/ polypropylene plastics during pyrolysis and representative morphological signal characterizing pyrolysis stages, Waste Management, 2012.

Williams Paul T., Williams Elizabeth A., Fluidised bed pyrolysis of low density polyethylene to produce petrochemical feedstock, Journal of Analytical and Applied Pyrolysis, 1998.

Yassin L., Lettierim P., Simons S.J.R., Germana A., Energy recovery from thermal processing of waste: a review, Engineering Sustainability, 2005.